Titre: Title:	Building on Existing District Energy Infrastructure to Decarbonize a Growing Urban Neighborhood
Auteur: Author:	Tasnim Alameddine
Date:	2022
Type:	Mémoire ou thèse / Dissertation or Thesis
Référence: Citation:	Alameddine, T. (2022). Building on Existing District Energy Infrastructure to Decarbonize a Growing Urban Neighborhood [Mémoire de maîtrise, Polytechnique Montréal]. PolyPublie. https://publications.polymtl.ca/10455/

URL de PolyPublie: PolyPublie URL:	https://publications.polymtl.ca/10455/
Directeurs de recherche: Advisors:	Michaël Kummert
Programme: Program:	Génie énergétique

POLYTECHNIQUE MONTRÉAL

affiliée à l'Université de Montréal

Building on Existing District Energy Infrastructure to Decarbonize a Growing Urban Neighborhood

TASNIM ALAMEDDINE

Département de génie mécanique

Mémoire présenté en vue de l'obtention du diplôme de *Maîtrise ès sciences appliquées*

Génie énergétique

Juin 2022

POLYTECHNIQUE MONTRÉAL

affiliée à l'Université de Montréal

Ce mémoire intitulé :

Building on Existing District Energy Infrastructure to Decarbonize a Growing Urban Neighborhood

présenté par **Tasnim ALAMEDDINE**

en vue de l'obtention du diplôme de *Maîtrise ès sciences appliquées*

a été dûment accepté par le jury d'examen constitué de :

Massimo CIMMINO, président
Michaël KUMMERT, membre et directeur de recherche
Gheorghe MIHALACHE, membre externe

ACKNOWLEDGEMENTS

First of all, I would like to express my appreciation to everyone at Énergir-CCU who collaborated to get through with this project. Also, thank you to everyone from the Louvain Est team, your expertise and your invaluable feedback have taught me so much.

Most of all, my deepest gratitude goes to my supervisor, Michël Kummert. Thank you. Thank you for being the kindest, most supportive, and most encouraging mentor and for constantly pushing us to do better. Particularly, thank you for teaching me how to execute beautiful reports and presentations and how to write using proper grammar!

I remain eternally grateful to my parents, Mohamad and Rakia, and to my brothers Firas and Youssef; I would have never become who I am today without your constant support and love.

A special thank you goes to my best friends, Mariam and Bashar. Thank you for always being here for me, even when you are 6000 km away; you have always supported me in a way no one else did. Thank you for always believing in me and for all the pep talks when I needed them the most!

I would like to thank my wonderful friends and family in Lebanon and Canada. You made my days much less lonely and kept my spirits and motivation high during this journey.

Lastly, to all the BeeLab members, it was a pleasure having the chance to know you and work with you. I learned a lot from you, and I wish you nothing but happiness and success in your future.

RÉSUMÉ

Les gouvernements et les villes ont déclaré l'urgence climatique et ont adopté des objectifs ambitieux pour réduire leurs émissions de gaz à effet de serre (GES). Étant donné que le secteur des bâtiments est responsable de plus d'un tiers des émissions de GES dans le monde, la décarbonation de l'environnement bâti est cruciale pour atteindre les objectifs fixés pour les prochaines décennies. L'électrification est au centre des stratégies de décarbonation des bâtiments, et les réseaux énergétiques de quartiers (REQ) offrent des avantages significatifs pour la transition des combustibles fossiles et l'intégration d'une part plus importante d'énergies renouvelables.

Ce mémoire évalue des scénarios pour décarboniser l'un des plus anciens et plus grands réseaux énergétiques du Canada tout en l'étendant à un quartier qui fait l'objet d'un redéveloppement majeur, ajoutant 1,2 million de mètres carrés de surface de plancher. Les scénarios sont basés sur des hypothèses réalistes – mais non confirmées – de phases de construction et aucune évaluation économique n'est effectuée. L'objectif est d'évaluer le potentiel technique de la conversion et de l'expansion de l'infrastructure REQ existante pour participer aux efforts de décarbonation de la ville.

Le système énergétique existant dans le centre-ville de Montréal, au Québec, est constitué de trois réseaux : vapeur, eau chaude et eau froide. Les 20 grands bâtiments connectés aux réseaux sont modélisés dans EnergyPlus à l'aide d'archétypes de bâtiments, qui sont calibrés à l'aide de données de consommation d'énergie mesurées fournies par la société qui exploite les réseaux. Ainsi, un profil dynamique de demande de chaleur et de froid a été obtenu pour chaque bâtiment. Les modèles EnergyPlus pour les nouveaux bâtiments sont tirés d'une étude précédente [1], et tous les bâtiments sont simulés avec le même fichier météo typique. Ensuite, chaque réseau thermique est modélisé séparément dans TRNSYS, et sa performance énergétique actuelle est évaluée.

Trois scénarios futurs sont définis : le scénario du *Business As Usual*, le scénario de l'*Électrification* et le scénario de la *Transition Énergétique du Secteur*. Le premier sert de base à la comparaison des deux autres scénarios. Dans le scénario *Business As Usual*, aucune modification n'est effectuée sur les REQ existants, et les nouveaux bâtiments sont supposés être équipés de systèmes de chauffage et de refroidissement typiques des nouveaux bâtiments respectant le code de l'énergie mais sans objectif de décarbonation. Le scénario *Électrification* représente un plan de décarbonation où des solutions d'électrification sont mises en œuvre séparément pour le réseau

énergétique et le nouveau quartier. Enfin, le plan de *Transition Énergétique du Secteur* applique différentes méthodes de décarbonation tout en connectant le nouveau quartier au réseau existant. Les résultats montrent que les scénarios d'*Électrification* et de *Transition Énergétique* atteignent tous deux des réductions très notables des émissions de GES sur une période de 25 ans, respectivement de 77% et 84%. La principale différence dans leur performance énergétique est que le scénario d'*Électrification* cause une demande électrique de pointe beaucoup plus importante, qui augmente de 70% par rapport au scénario *Business As Usual*. En comparaison, le scénario de *Transition Énergétique du Secteur* n'augmente la demande électrique de pointe que de 17%, après avoir imposé temporairement une pointe plus élevée pendant la transition énergétique progressive. Cela confirme que le REQ existant à Montréal, bien qu'il représente actuellement une source importante de GES, peut devenir un atout dans la transformation de la ville vers un avenir sans carbone. Ce mémoire ne tente pas de quantifier les aspects économiques des différents scénarios et n'évalue pas les autres avantages potentiels des REQ, tels que l’élimination du rejet de chaleur des refroidisseurs à air et de nombreux systèmes de climatisation individuels avec des réfrigérants ayant un fort potentiel de réchauffement global.

ABSTRACT

Governments and cities have declared a climate emergency and have adopted ambitious targets to reduce their greenhouse gas (GHG) emissions. As the building sector is responsible for more than a third of the GHG emissions globally, decarbonizing the built environment is crucial to meet the goals set for the next decades. Electrification is at the center of strategies to decarbonize buildings, and district energy systems (DES) offer significant advantages to transition from fossil fuels and integrate higher shares of renewables.

This thesis assesses scenarios to decarbonize one of Canada's oldest and largest district energy networks while expanding it to a neighborhood undergoing major redevelopment, adding 1.2 million square meters of floor area. The scenarios are based on realistic – but unconfirmed – construction phasing assumptions and no economic assessment is performed. The focus is to assess the technical potential of converting and expanding existing DES infrastructure to participate in the city's decarbonization efforts.

The existing district energy system in the downtown area of Montréal, Québec, consists of three networks: steam, hot water, and cold water. The 20 large buildings connected to the networks are modelled in EnergyPlus using building archetypes. The models are calibrated using measured energy consumption data provided by the company operating the networks. Thus, a dynamic heat and cold demand profile was obtained for each building. EnergyPlus models for the new buildings are taken from a previous study [1], and all buildings are simulated with a consistent typical weather file. Then, each thermal network is modelled separately in TRNSYS, and its current energy performance is assessed.

Three future scenarios are defined: the *Business as usual* scenario, the *Electrification* scenario, and the *District Energy Transition* scenario. The first one sets the base for comparing the two other scenarios. In the *Business as usual* scenario, no modifications are made to the existing DES, and the new buildings are assumed to be equipped with typical heating and cooling systems for new buildings. The *Electrification* scenario represents a decarbonization plan where electrification solutions are implemented separately for the district network and the new neighborhood. Finally, the *District Energy Transition* plan applies different decarbonization methods while connecting the new neighborhood to the existing network. Results show that both the *Electrification* and the *District Energy Transition* scenarios achieve very significant reductions in GHG emissions over a

25-year period, respectively 77% and 84%. The main difference in their energy performance is that the *Electrification* scenario results in a much larger electrical peak demand, which is increased by 70 % over the *Business as usual*. In comparison, the *District Energy Transition* scenario only increases the peak electrical demand by 17% after temporarily imposing a higher peak during the gradual energy transition. This confirms that the existing DES in Montréal, while currently representing a major GHG source, can become an asset in transforming the city towards a carbon-free future. This thesis does not attempt to quantify the economic aspects of different scenarios and does not assess other potential benefits of DES, such as avoiding heat rejection from air-source chillers and limiting distributed air-conditioning systems relying on refrigerants with a high global warming potential.

TABLE OF CONTENTS

LIST OF TABLES

LIST OF FIGURES

LIST OF SYMBOLS AND ABBREVIATIONS

ASHRAE American society of heating, refrigerating and air-conditioning engineers

BAU business as usual

BEM building energy modelling

BTAP building technology assessment platform

CCUM climatisation et chauffage urbains de Montréal

CEUD Comprehensive Energy Use Database

COP coefficient of performance

CV(RMSE) Coefficient of Variation of the Root Mean Square Error

CWEC Canadian weather for energy calculation

DC district cooling

DCN district cooling network

DES district energy systems

DH district heating

DHN district heating network

ÉCCU Énergir chauffage et climatisation urbaine

EUI energy use intensity

GHG greenhouse gas

GES gas à effet de serre

HHV higher heating value

HP heat pump

HVAC heating, ventilation, and air-conditioning

HWN hot water network

IECC international energy conservation code

LR_{75} Leakage Rate at 75 Pa

NMBE normalized mean bias error

NPS nominal pipe size

NRCan natural resources Canada

P steam pressure

Pr representative property of the buildings connected to the hot and cold water networks

P_{th} thermal power required from the river

REQ réseaux énergétiques de quartier

SN steam network

U-value thermal loss coefficient

UBC university of British Colombia

UBEM urban building energy modelling

UK United kingdoms

USA United States of America

US DOE united states department of energy

WSHP water-source heat pumps

Symbols

$Baselaod_{bld}$ monthly cold baseload added to each building

$Cold_{bld,month}$ monthly calibrated cold demand of the building

$CorrectiveFactor_{bld}$ corrective coefficient

Cp specific heat capacity of water

DIR design infiltration rate

$F_{schedule}$ schedule fraction of infiltration

$h_{condensate,100℃}$ enthalpy of condensate at P and a temperature of 100 ℃

$h_{saturated_{condensate}}$ enthalpy of saturated condensate at P

$Infil_{rate}$ infiltration rate

Q_{latent} latent heat

$Q_{sensible}$ sensible heat

Q_{steam} heat extracted from the steam network

$\dot{m}$ river's volumetric flow rate

$\dot{m_{steam}}$ mass flow rate of steam

$\overline{m}$ mean value of the measured values

$ModeledCold_{bld,month}$ simulated monthly cold demand of each building

n number of measured data points

p number of adjustable model parameters

P_{th} maximum cooling and heating power

s_i simulated value at the given timestep

T_{odb} outside dry-bulb temperature

T_{zone} zone's inside temperature

v_{wind} wind velocity

Δh_{vap} latent heat of vaporization of the steam

ΔP pressure difference

ΔT temperature difference

LIST OF APPENDICES

CHAPTER 1 INTRODUCTION

Governments worldwide have recognized the urge to reduce their Greenhouse gas (GHG) emissions to limit the damage already done to the environment. In Canada [2], the government has introduced the "Pan-Canadian framework on clean growth and climate change" plan, aiming to reduce GHG emissions by 30% below the 2005 levels by 2030. At the national level, the built environment alone accounts for 13% of the total GHG emissions due to the direct combustion of fossil fuels for heating. This contribution goes up to 17% taking into account indirect emissions from electricity used in buildings for heating, cooling, lighting, and appliances [3]. In Québec, buildings represent 30 % of the energy consumption. The share of fossil fuels in the residential energy consumption is low (14 %), but commercial buildings still rely on oil and gas for more than half of their energy use [4]. Thus, buildings play a major role in shaping the low-carbon pathways of the future.

Cities have taken a leadership role in fighting climate change, for example, through the "C40 Cities Climate Leadership Group" [5], which is focused on urban action to reduce greenhouse gas emissions and climate risks. Montréal is part of the C40 group, and the city has adopted ambitious targets in its 2020-2030 climate plan [6]. For the building sector, decarbonization through the reduction of gas and the elimination of oil for heating is at the center of proposed measures.

District energy systems (DES) have been identified as "the most effective approach for many cities to transition to sustainable heating and cooling," according to the United Nations Environment Programme [7]. DES can achieve large reductions in emitted GHGs due to lower primary energy consumption and fuel shifting. Some of the other benefits include better air quality, higher energy efficiencies, better use of locally available renewable sources, etc. However, DES can become highly emissive when fossil fuels are used at the production plant. For example, the DES at the University of British Colombia [8] is responsible for 78% of the total emissions of the site due to the combustion of natural gas.

Decarbonization requires introducing new energy systems relying primarily on renewable energy sources and waste heat recovery. In DES, these solutions can be more challenging to implement if high-temperature networks are used, which is the case in steam-based district heating systems. Steam networks generally operate by burning fossil fuels to produce high-temperature dry or superheated steam, leading to higher thermal losses in the distribution network. This is why recent research focuses on lower temperature operating DES, and existing steam networks are considering

an energy transition towards medium temperature hot water heating. Although this transition takes considerable time and investment, it presents a major advantage that should not be neglected. Rigorous work should prepare the piping network, the thermal production plant, and the consuming buildings to use hot water heating instead of steam. Across Canada, 40% to 80% of major equipment in buildings is estimated to undergo significant renovation, representing an opportunity to retrofit these buildings towards hot water heating [9].

In a decarbonized electricity sector, such as in Québec, using electricity to provide heat for heating and cooling can significantly reduce emissions related to energy production.

One of the leading technologies of electrification of heating encourages the implementation of heat pumps. Heat pumps are electricity-driven systems which operate by extracting heat from a cold medium, increasing its temperature via the compressor, and transferring it into a hot medium. It's a technology that has proven its efficiency worldwide in transferring heat from one medium to another. Heat pumps become especially important when simultaneous heat and cold demands are required or when a free heat source is available (waste heat, rivers, sewage water, etc.) [10]–[12]. Furthermore, electric boilers can be a great alternative to fossil fuel- and natural gas-fired boilers, especially when the electricity price is lower than that of fuels [11].

1.1 Case study

This thesis studies the decarbonization potential of a growing urban neighborhood in Montréal, Québec, through the use of an existing urban district energy network. The network, one of the oldest and largest in Canada, is operated by Énergir Chaleur et Climatisation Urbaines (ÉCCU). The district heating system was first designed and built to provide steam to the Canadian National operations in 1947. It has since then expanded to provide heat to over a third of the Montréal downtown core. In 2000, the urban energy network (then operated under the name of Climatisation et Chauffage Urbains de Montréal, CCUM) was expanded with two new networks providing hot and cold water to the Cité Multimédia district. The central energy plant has a total heating capacity of 145 MW provided by four gas boilers and a total cooling capacity of 18.4 MW provided by five chillers. The steam network serves 14 large customers, including Montréal's most outstanding commercial buildings, and the hot and cold water networks serve a total of six buildings. In total, Énergir-CCU provides heat and/or cold to 20 large buildings (17 commercial buildings and three

residential buildings). These buildings are represented in Figure 1.1 in dark blue and yellow, and the central heating and cooling plant is also shown in light blue.

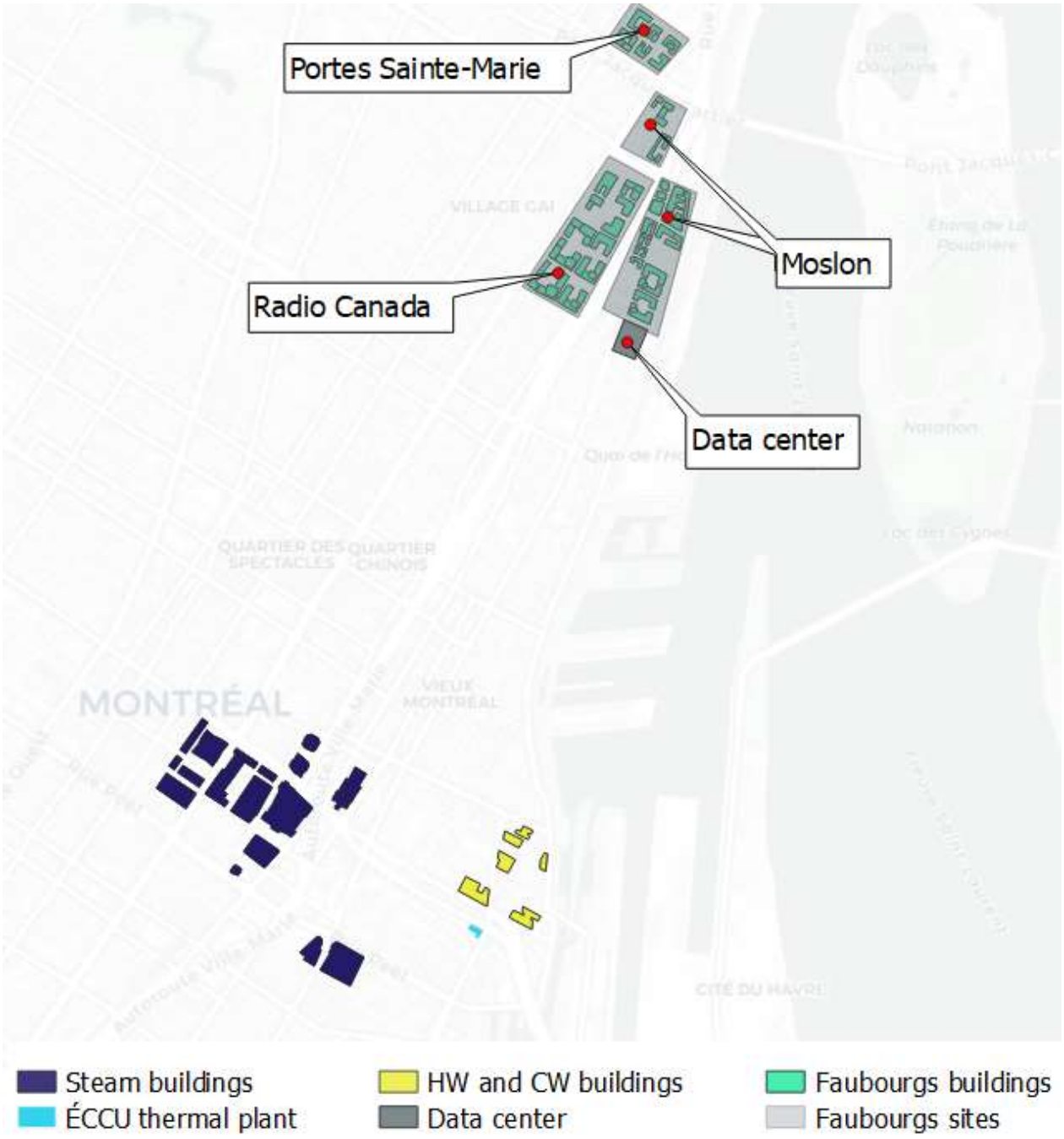

Figure 1.1: Buildings considered within the scope of the study, including buildings connected to the existing steam network (dark blue) and to the hot and cold water networks (yellow) and new buildings (green). The data center's location is for illustration only; its exact location within the sites has not been fixed.

In addition to the buildings already connected to the network, this study considers new buildings in the Faubourgs neighborhood. The neighborhood is located within 2 km of the existing district energy network and is currently undergoing major redevelopment, adding over 1.2 million square meters of floor area. The new built environment consists of 126 mixed-usage buildings spread over three main sites: Radio-Canada, Molson, and Portes Saintes-Marie, as shown in Figure 1.1. In addition, a 12 MW data center is predicted to be constructed, as mentioned in the study commissioned by the Ville-Marie borough [1]. The new build will pose some challenges in terms of energy supply as it will represent a peak heating demand of 30 MW and a peak cooling demand of 38 MW. However, the new neighborhood also represents a formidable opportunity to expand and decarbonize the thermal networks thanks to heating and cooling synergies.

In this study, the buildings are intended to be constructed gradually. The Molson site and the data center are supposed to be finished first in 2027. The other sites will be progressively completed in 2029 and 2030 for the Radio-Canada site and the Portes Sainte-Marie, respectively.

1.2 Research objectives

The work presented in this thesis looks into different decarbonization solutions for the growing urban neighborhood for the upcoming 20 years.

The sub-objectives of the research are as follows.

1. Build an hourly data set for the thermal and electric demands of the buildings currently connected to the networks by simulating and calibrating building archetypes modelled with the EnergyPlus software.
2. Implement a model of the existing district energy networks using the TRNSYS simulation program.
3. Quantify the current energy consumption for gas and electricity at the thermal plant level and the individual building level for the ÉCCU current and future possible clients.
4. Assess the decarbonization potential at the neighborhood level (existing buildings connected to the DES and future buildings in the Faubourgs neighborhood) through the implementation of different solutions, including electrification and heat sharing between networks.

1.3 Thesis organization

After this introduction, chapter 2 presents a literature review on district energy systems and their decarbonization, urban building energy modelling, and model calibration. Chapter 3 presents the methodology and results obtained to achieve objective 1 (building energy demand at the site level). Chapter 4 presents the modelling of the existing district energy networks (objectives 2 and 3), and chapter 5 presents the assessment of decarbonization scenarios. The thesis ends with a general discussion and conclusions in chapter 6.

CHAPTER 2 LITERATURE REVIEW

This chapter defines basic concepts related to district energy systems and decarbonization solutions and elaborates on different studies in the field. Additionally, as correctly estimating decarbonization potential requires an accurate estimate of community energy demands, this chapter will also investigate various building modelling tools and methods.

2.1 District energy systems

District energy systems (DES) are identified as the most effective approach to providing a cost- and energy-effective thermal energy supply in cities, according to the United Nations Environment Programme [7]. With multiple benefits, including GHG emissions reduction, air pollution reduction, energy efficiency improvements, and resiliency improvement, DES are considered the "cornerstone" in sustainable energy policies in many countries, including Denmark and China [7]. In DES, centrally produced heat and cold are delivered to customers through a piping network for use in space heating, domestic water, and space cooling [13].

District heating (DH) can be seen as a modern evolution of centralized heating systems such as the ones providing heat to hot-water baths and greenhouses in the Roman Empire, but "modern" district heating systems appeared at the end of the 19th century, with steam-based systems using coal-burning boilers. Early examples include the St. Petersburg network in Russia (1840) and the Annapolis, Maryland network in the USA (1853) [14]. Another famous network in the US is the Manhattan steam system [15], constructed in 1880 and still in operation today. It was considered the first commercially viable district system in the world. The first generation of district heating consisted of using high-temperature pressurized steam as the leading heat carrier [16]. Typical steam temperatures were up to 300 ℃, and pressures went up to 20 bar [17]. However, these systems were often associated with high piping distribution losses and severe accidents such as steam explosions. Major drawbacks also included high investment and operation costs and complex consumer connections in case of network expansion. Around the 1930s, the second-generation systems replaced steam as the main heat carrier with high-temperature water at 100 ℃ and above [18]. Using a colder fluid in district networks allowed higher systems efficiencies as it lowered the heat losses in piping systems and achieved important savings in fuel consumption. The third DH generation was introduced in the 1970s and has propagated quickly—it was implemented almost

in all the new district networks projects at the time. The use of medium temperature pressurized water, usually lower than 70 ℃, allowed for integrating alternative energy sources to oil. Recent research has shown increasing interest in using a carrier fluid of temperature lower than 70 ℃ (4th generation DH) or as low as 15 ℃ to 25 ℃ (5th generation DH).

District cooling (DC) has often been tied to district heating. In their most recent work, Østergaard et al. detailed the different generations of district cooling [19]. The first generation of DC was implemented in 1889 and used refrigerants like pressurized ammonia [20] as the main distribution fluid. Compared to using ice as the refrigerating agent, piped refrigeration systems offered convenience to clients at a favourable price. Second generation district cooling systems emerged in the 1960s when the central business district of Hartford, USA decided to test a higher proportion of large compression chillers in the supply instead of many small chillers [21]. These systems used cold water instead of the direct distribution of refrigerants in cold networks. DC soon started to expand to many countries, including France [22], Germany [19], Japan [23], and China [24]. Third generation cooling networks were established in the 1990s in France. These systems started using a more diversified cold supply, depending more on locally available cold sources rather than refrigerants. Natural heat sinks in rivers and deep seas were often used as a free source of cold [25]–[27].

New generations of DES involve meeting the challenge of low-temperature heating systems in more energy-efficient buildings [28] and integrated into smart energy systems (i.e. smart electricity, thermal and gas grids). The label “fourth generation district energy” was introduced in the late 2000s, describing transitioning paths for decarbonization of the DES. DH networks started using moderate supply and return temperatures between 60-55 ℃ and 20-30 ℃, respectively [29]. About 4th generation district cooling, Lund et al. [16] mention that “A future fourth generation of district cooling systems can be defined as new smart district cooling systems more interactive with the electricity, district heating, and gas grids.”. Recent research has mentioned “fifth generation district energy” [30]–[32]. Using a carrier fluid at ambient temperature and decentralized small heat pumps within each building, the fifth generation DES consists of a single collective water network to provide building heating and cooling loads [31]. This network plays the role of a heat source and a heat sink for local heat pumps simultaneously.

Researchers defined different operating temperatures of a 5th generation network. Buffa et al. mention that the networks supply water to decentralized heat at a temperature between 0 ℃ and 30 ℃ [32], Rhein et al. use a temperature range between 15 ℃ and 25 ℃ [33]. Such systems require a diversified client profile to balance the heat demand and rejection of the network instead of having clients absorbing/rejecting heat from the loop at the same time.

The full potential of DES could not be tapped without the integration of renewable energy sources in the supply system. In fact, the use of renewable energies in DES has been the subject of extensive focus within research as part of the future sustainable energy policy [34]. These sources include wind [35], solar [36], geothermal sources [37], etc. In their research about the potential of solar technology integration in district cooling systems [38], Ismaen et al. found that using integrated photovoltaic solar collectors in district cooling systems can lower the environmental impact of district cooling systems in the Middle East by 58 %. Using unrecovered waste heat from industrial plants, incineration, and district cooling networks can also significantly lower the energy supply sector's dependence on fossil fuels and natural gas. For example, in St. Paul, Minnesota (USA), the municipal wood waste fuelled district energy system has helped cut coal consumption by 275 kton annually [7].

2.1.1 Water-source district heating and cooling

Water from seas, lakes, or rivers can be used as a heat source or sink for DES. In the case of heating systems, the water temperature is usually insufficient to provide direct heating, but it is suitable for water-source heat pumps. For cooling systems, cold water (typically around 4 ℃) can be used to provide direct cooling, and warmer water can be used to reject heat from water-source chillers.

Water-source DC is regarded as a viable low emissive alternative to conventional air conditioning systems. It uses cold water naturally existing in seas, rivers, or lakes to fulfill cooling loads, drastically reducing the environmental impact of traditional cooling plants. This energy source especially becomes essential when a large cold water-source is located close to the production plant, limiting high piping costs and energy losses in the network. The world’s largest lake-powered cooling system is located in Toronto, Ontario. The system utilizes the near-freezing deep lake water to provide up to 140 MWh of cold to Toronto’s financial district [26], lowering carbon emissions by 13,500 tonnes yearly [39]. Similarly, the Lake Source Cooling facility at Cornell University,

USA, uses the deep cold water of Cayuga Lake to provide the cooling demands of the university and the neighboring Ithaca school [40]. Eliminating most of the existing chillers plant has helped reduce the electricity used for cooling by 85% [41]. In a recent study on the performance of the city of Gothenburg district cooling system [25], the river provided free cooling covering up to 22% of the annual chilled water production. The river's water provided 100% of the cooling loads when its temperature was lower than 5 ℃; otherwise, it was used to precool inlet chillers' water. In the Netherlands, three water-cooled chillers benefit from the cold water from the New-Meuse River to cool the large multi-function building De Rotterdam [42].

Water-source district heating also has enormous potential in decarbonizing cities and district networks. In Holland, the district heating network uses an open-loop sea water heat pump to provide the heating demands of the Duindorp district. The network maintained at a low temperature of 11 ℃ delivers 2.7 MW of heat and has helped cut the GHG emissions by half [43]. In the UK, the Thames River in London provides water of a temperature higher than 7 ℃ all year long to the 2.3 MW water heat pump installed nearby, providing heat 24/7 to the 56 homes in the neighborhood. The carbon emissions will be reduced by 500 tonnes a year and eventually reach zero as green electricity is supplied [44]. In his report about the viability of river source heat pumps (HP) for district heating in Glasgow, UK, Lyden found that his system configuration produces 60% lower GHG emissions in the long term than the traditional conventional systems [45]. The proposed system combines a 6.65 MW river source HP and gas-powered combined heat and power unit to provide 40 GWh of heat for the district. In a survey regarding available DES in Europe, the installed capacity of water-source heat pumps was estimated to be 390 MW, representing 24% of the total installed capacity [46].

Several ecological concerns have been raised when planning water-source DES. One of the biggest concerns of the deep lake cooling system of Cornell University was to possibly transport the phosphorus from the bottom of the lake in late summer [40]. Additionally, high solids level in rivers could cause problems when extracting water if a proper filtering system is not established [47]. Changing the temperature of the water source can affect the aquatic flora and fauna and mess with the ecological system. Additionally, variations in water temperature can change its chemical properties over the long term.

In the Montréal context, a new study on energy sources for a new neighborhood exploited the Des Prairies River as a potential heat and cold source [1]. Using the minimum flow of the river estimated to be 400 m^3/s, the maximum change in the river's temperature was calculated. Results showed that in order to provide 5 MW of cold, the heat dissipated in the river would only rise its temperature by 0.003 ℃. The report also stated that a thermal power of 1 GW, sufficient for the whole Montréal area, will affect the river's temperature by only 0.6 ℃.

2.1.2 Waste heat recovery between networks

Employing the heat in the return pipe of a district cooling network (DCN) to provide the heat required by the district heating network (DHN) is both cost- and energy-efficient. Instead of using chillers to cool down the water in the return pipes of the DCN, water-source heat pumps (WSHP) are used to extract the heat. The WSHP upgrades the extracted heat to a higher temperature and injects it into the DHN supply or return. A recent study performed in Sweden [48] investigates the potential of using WSHP to cover heat and cold demands at the same time. The heat pumps were sized to cover 51% of the peak load and 96% of the total heat demand. The peak heat demand, which only occurred 4% of the time in a year, was fulfilled by an immersion heater. The results showed that "free cooling" from the recovery between the networks accounted for 35% of the total cold and that the central production plant could be entirely replaced for approximately 140 days. Moghaddam et al. [49] used an electric heat pump with a COP equal to 2.5 in their optimization model for different energy source integration in an energy system of a building. The heat pump provided up to 72.7% of the building's heating loads on a typical cold day and 80% of its cooling loads on a typical hot day. Similarly, Ahmadisedigh [50] found that integrating a heat pump to cover the simultaneous demands on the heating and cooling networks can cover up to 45% of the annual heat demands. The optimal capacity of the heat pump was found to be 80% of the peak heat demand, and its coefficient of performance was between 3 and 5. According to the Heat Roadmap Survey about district energy in Europe [46], four heat recovery units from district cooling were installed. These systems rely solely on rejected heat from the district cooling networks to provide a total capacity of 30 MW in the heat for the heating networks. Additionally, four other units used district cooling heat recovery as a secondary heat source along with other sources, including sewage water. The water source temperature ranged between 0 ℃ and 9 ℃, with the system in Denmark having the lowest supply temperature of 0 ℃.

2.1.3 Hot water vs steam networks/Transition from steam to hot water

Steam was the only heat carrier used historically in DH networks. However, the conversion of these systems towards hot water has gained much popularity recently, especially with the many advantages that hot water has proven against steam networks. At first, using hot water systems can greatly increase the system's efficiency, thus, reducing the total energy consumption due to higher plant efficiency and reduced heat and mass losses in the distribution system [8], [51]. In a presentation about the conversion potential of a DES [52], the savings in the energy required from the central plant were estimated to be 5%. Most of the savings were achieved during winter, thanks to lower heat losses during winter. In addition, a study on the conversion capacity of the Jamestown Community College in the USA showed that the percentage of heat losses in the distribution system was 3-5% for hot water networks compared to 15-20% for steam networks [53]. The mass loss accompanying steam networks can also breed operational costs for the thermal plant. Charges related to pumping makeup water for lost condensate and its chemical treatment before being introduced to the system can all be avoided with a hot water system. Additionally, the new systems can deliver savings in annual operational and maintenance costs related to steam trap losses and steam maintenance reduction [8].

Converting the system to hot water promotes the integration of heat pumps and renewable energy sources such as solar, geothermal, and biomass energy. The University of British Colombia campus was able to integrate a 6 MW biomass gasification system providing 25% of the campus's space heating and hot water needs [54]. Equally, Stanford University DES and Illinois University [55] can benefit from heat recovery to provide 53% and 65% of the heat loads and 88% and 55% of the cooling loads, respectively. In the UC Davis DES [56], in California, the conversion allowed the system to use solar energy along with heat recovery technologies between the new hot water network and the cooling network. High temperature evacuated solar collectors can provide 40% of the heating load, whereas recovered heat can provide 30% of the heat load and 25% of the cooling load.

However, this conversion poses challenges mainly related to very significant investments [57]. Primarily, retrofitting the buildings' HVAC equipment to be adequate for hot water heating is costly, time-consuming and can lower the comfort of the building's tenants. The University of Rochester [58] studied the conversion economics for 22 buildings still connected to the steam

network towards hot water heating. The conversion project costs are approximately 15 million dollars related to construction fees, contingencies, and project commissioning. In the UBC project [8], the conversion of some old buildings was too pricey; they had to be taken off the DES. Other costs can be related to modifying the piping network, although some can be avoided if some of the existing pipes are re-allocated in the new network. In most of the cases, the piping network was replaced entirely as most of the steam pipes were too small [59], were unsafe to reuse because of damaged insulation, or were used with steam to water heat exchangers at the end of each building until all buildings were converted and the hot water network piping was installed [58].

In Canada, EQUANS recently described an ambitious conversion project for the government-owned district energy network in Ottawa [60]. The 7 km network delivers heat and cold to 82 federal buildings using high-pressure steam and cold water. The 30 years project intends to modernize the current system (five thermal plants) by renovating one thermal plant and building three new ones, putting four thermal plants out of service at the end of the project. Over the upcoming period, the heating network will be converted from steam-based heating to low-temperature water heating, and the transition will be performed gradually. The hot water piping network will be installed parallel to the steam network, but it won't be used until all the buildings are converted to hot water heating. Meanwhile, steam to hot water heat exchangers will be installed at each retrofitted building until the hot water network is in operation. At the end of the project, the GHG emissions savings are expected to be at least 40%.

2.2 Building energy modelling

With the increased urge to accurately forecast the energy performance of buildings for design, code compliance, or implementation of new control strategies [61], building energy modelling (BEM) has gained remarkable popularity amongst engineers and researchers. A building energy model predicts the heat and mass flows within a building due to changes in the environment of the space. Once these flows are assessed, changes in the space's conditions (temperature, humidity, etc.) and the required thermal loads to achieve a certain comfort level may all be determined. On a broader scale, these techniques can be used to evaluate the energy performance of buildings for neighborhoods, districts, or entire cities in what is called Urban Building Energy Modelling (UBEM). As represented in literature [62]–[65], UBEM can follow one of two main approaches:

top-down and bottom-up. “Top-down” models use statistical data to look at buildings' energy usage to a larger spatial extent. These models can deliver a holistic understanding of energy predictions as a consequence of a decision taken at a city or a country level. For example, Zhang [66] tested the sensitivity of energy consumption to climate variations in China. Nesbakken [67] used an econometric model to examine the relationship between a house’s energy use and the family’s income and energy prices in Norway.

“Bottom-up” models, on the other hand, incorporates detailed building models into the modelling procedure of a larger scale dataset. Modellers often select these models as they allow a more reliable assessment of the energy behavior based on the end-uses of buildings or groups of buildings. Mohammadiziazi et al. [64] have defined two methods to develop UBEMs using the “bottom-up” methodology: the prototype and archetypal methods. The prototype method utilizes building clusters with average values of geometric and non-geometric parameters (height, window-to-wall ratio, HVAC COP, etc.). The second method groups buildings of only similar non-geometric parameters into individual building models [61]. According to the study [64], the majority of the studies focused on creating archetypes for residential buildings due to their simpler envelope properties and energy systems. Shimoda et al. [68] developed a model which simulates different types of households and dwellings to determine the energy consumption at a city level. The model takes a large set of parameters of input data, including occupancy schedules by type of activity (sleeping, eating, working, etc.), hot water temperature and total consumption, set point temperatures for heating and cooling, meteorological data for the city, and energy efficiency of appliances. The total energy consumption at the city level simulated by the model was 18% less than the statistic value. The authors defined the reason for that error as the uncertainties in input values and assumptions and that the model did not consider “unreasonable” occupants’ behavior, such as leaving the lighting and the HVAC system on while the room was not occupied. Shimoda also studied the effect of different thermal insulation standards on the total heating and cooling energy consumption, emphasizing the importance of building models in decision-making regarding new energy policies.

Until recent times, only a few studies focused solely on commercial buildings in UBEM. For example, Chen et al. [69] used “CityBES” a toolkit which provides energy retrofit analysis in USA cities by looking into each commercial building (office and retail) individually. The authors used

the toolkit to evaluate the savings potential in energy consumption due to five energy conservation methods related to the HVAC systems, the lighting system, and the windows properties. One challenge to the use of such toolkits is the necessity to have a large dataset with information on each individual building which is scarcely available publicly.

2.2.1 Defining archetypes

Building energy models can be generated and simulated using different available software tools such as TRNSYS, EnergyPlus, ESP-r, or eQuest. These archetypes can be selected based on different criteria, including the building's main and secondary usages, its construction year, its primary heating system, and the climate zone to which it belongs within a country, as identified in the literature [70]–[72]. In their classification of Greek residential buildings, Theodoridou et al. [73] segmented the building stock into five categories depending on the year of construction. These categories were later refined based on the available statistical data for the number of floors, construction materials, socio-economic aspects, etc. The authors used EnergyPlus to simulate the energy behavior of the buildings under study. The results showed that the building models underestimated the heating energy consumption by 39.4%, primarily because of the lack of thermostatic control.

In Europe, the Intelligent Energy Europe TABULA project [74] elaborated residential building archetypes for 15 different European countries. Each building model represents a certain vintage and a specific building size. Similarly, the United States Department of Energy (US DOE) has produced three sets of archetypes: a Commercial Reference building archetypes set, a Commercial Prototype building Archetypes set, and a Residential Prototype building set. Commercial building models are intended to analyze the energy behavior of single-use commercial buildings, including office buildings, hotels, mid-rise and high-rise residential buildings, etc., whereas residential building archetypes represent single-family detached houses and multi-family low-rise apartment buildings. The Commercial Reference building archetypes represent typical commercial buildings with standard engineering practices for three vintages: “new construction” built after 2004, existing buildings constructed during or after 1980 (“Post-1980”), and existing buildings built before 1980 (“Pre-1980”) [75], [76]. These archetypes are further divided by 16 climate zones within America. Commercial Prototype building models [77], although derived from the Reference building archetypes, are more energy-efficient since they are adapted to the ASHRAE 90.1 standard. The

set of Prototype building models was also expanded with residential models matching different versions of the International Energy Conservation Code (IECC) [78]. The Residential Prototype building archetypes are differentiated into two base sets consisting of 32 models in total. Each base set consists of 16 models adapted to accommodate four different heating systems and four foundation types. On the Canadian level, CanmetEnergy has launched the Building Technology Assessment Platform (BTAP) [79], which comprises 16 building archetypes for 70 locations in all climate zones. These archetypes adapt the DOE archetypes to the National Energy Code of Canada for Buildings (2011) but use extremely simplified HVAC systems.

2.2.2 Calibrating building models

Building model calibration can be defined as the adjustment of the input parameters of a model to represent the measured data more accurately. Two main methods can be pursued in calibration: manual and automated model calibration. Manual calibration based on an iterative approach can be time-consuming when a large set of building models is to be calibrated. Still, it can be more time-effective if a smaller group is to be adjusted, given the lack of proven automated calibration methods. Liu et al. [80] defined a detailed strategy to manually calibrate building models based on two characteristic signatures: the calibration signature and the characteristic signature. The calibration signature consists of plotting the difference between measured and simulation-result data, function of outdoor dry-bulb temperature. The characteristic signature requires the modeller to plot the difference between simulation results when one input parameter is modified versus outdoor dry-bulb temperature. When assessing the disparity between the two signatures, the modeller is better-sighted on the errors in the simulation inputs [81]. Coakley et al. [82] denoted the several issues related to building energy performance calculations, such as the lack of explicit calibration standards and the lack of high-quality input data to create a detailed model.

On the other hand, automated calibration consists of implementing numerical and statistical methods into the calibration process. The increasing urge to use building models on an urban level in order to better predict energy demand at the community level has inspired many researchers to explore different large-scale calibration methodologies. According to Chong et al. [83], the number of papers using automated calibration methods has tripled between 2004 and 2021.

Yang et al. [84] proposed a fully automated calibration method based on mathematical optimization. The method was introduced to calibrate the electricity consumption per end-use of an office building in Shanghai. In the beginning, the authors completed a sensitivity analysis to reduce the number of input parameters to be tuned in the calibration process. For this matter, a typical office building model for the area of research was built using e-Quest simulation program. According to the analysis results, the electricity demand was the least sensitive to the envelope parameters. Lighting, equipment, occupant density, and the chiller's COP had the highest sensitivity coefficients. Given the direct effect of lighting and equipment density on the electricity consumption, these parameters were calibrated by rule estimation; thus, by tuning the densities based on a direct comparison between the simulated and the metered electricity consumption for lighting and equipment. The remaining parameters were optimized based on a numerical algorithm to lower the Coefficient of Variation of the Root Mean Square Error between simulated and measured data. The calibration results showed that the error by end-use was lower than 12%, and the error regarding the total electricity consumption was 6.1%.

Davila et al. [61] proposed a Bayesian approach to calibrating stochastic parameters in urban building energy modelling using a limited training sample of measured energy data. At first, the author gathered different types of data. Several data on the building's geometry, properties and measured demand were extracted from the available literature. Later, the buildings were divided into four categories: original villas built between the 1960s and the 1980s, retrofitted villas 1960s-1980s, villas 1990s-2000s, and villas after 2010. Later, a sensitivity analysis was performed on different input parameters such as envelope U-values, infiltration rates, etc., to determine whether to model them deterministically or probabilistically. Given the similar construction typologies and HVAC systems in the district under study, only the occupant-related parameters were modelled probabilistically. In the calibration procedure that followed, those parameters were adjusted based on metered energy consumption. The calibration process resulted in building models that accurately estimate the energy use intensity (EUI) distribution at the neighborhood level, with errors lower than 5% in the mean EUI.

2.2.3 Assessing the model accuracy

Determining the degree of confidence in the building model can be studied through the calculation of the Normalized Mean Bias Error (NMBE) and the Coefficient of Variation of the Root Mean Square Error (CV(RMSE)), according to the ASHRAE Guideline 14 [85]. Equations (1) and (2) demonstrate the calculation procedure of these two parameters.

$$NMBE = \frac{1}{\bar{m}} * \sum_{i=1}^{n} \frac{(m_i - s_i)}{n - p} \quad (1)$$

$$CV(RMSE) = \frac{1}{\bar{m}} * \sqrt{\sum_{i=1}^{n} \frac{(m_i - s_i)^2}{n - p}} \quad (2)$$

Where: $\bar{m}$ is the mean value of the measured values

n is the number of measured data points

m_i is the measured value at the given timestep

s_i is the simulated value at the given timestep

p is the number of adjustable model parameters, set to 1 [85]

For monthly data calibration, ASHRAE Guideline 14 [85] recommends that the $NMBE$ should not exceed 5% and that the $CV(RMSE)$ should be lower than 15%. Although the Guideline is not explicit about this, it is understood that the absolute value of the $NMBE$ should be used when assessing the criteria. Note that (1) is formulated with the opposite sign (i.e. $s_i - m_i$ instead of $m_i - s_i$) in the guideline, but this has no impact on assessing the 5% threshold in absolute value.

CHAPTER 3 BUILDING ENERGY MODELLING

This chapter lays the foundation for the rest of the thesis as it determines the hourly energy demands for all the buildings considered within the scope of this study. It details the methodology followed to obtain accurate estimations of the heating, cooling and electricity demands for a typical year. Building archetypes are selected based on several criteria and are then calibrated using actual measured data. The energy profiles are also discussed at the end of this chapter.

3.1 Buildings connected to the existing networks

3.1.1 Building data collection

Gathering the required data on each building is one of the most critical and time-consuming tasks in developing a portfolio model. Important data include the year of construction, type of use, total floor area, and floor area per type of use. Although the latter is hard to acquire for most buildings, some methods can account for different types of services in each building. First, the total floor area of each building was determined using information available on each client's official webpage or their owner's official web pages when available [86]–[91]. If not, other sources such as the ÉCCU clients profile website [92] were used. This information was then compared to data gathered from several different sources, including Property Assessment Roll (*Unités d'évaluation foncières* [93]), the Google maps distance estimator tool [94], and Emporis [95]. Emporis collects structural and technical information (structural material, types of usage, height, number of floors, etc.) about buildings worldwide, especially in North America and northern Europe. Using Google maps, an estimation of the total floor area and the floor area by end-use was obtained by multiplying the footprint of the building by the corresponding number of floors.

The company provided energy use data for 2019 for each client. These data included:

- Monthly steam consumption (in lbs) of all buildings connected to the steam network
- Monthly heat consumption (in Btu) of all buildings connected to the hot water network
- Cold consumption (in Btu) of all buildings connected to the cold water network
- Monthly electricity use (in kWh) and billed power (in kW) for selected buildings
- Monthly natural gas use (for cooking) of one educational building

The breakdown of the clients' profiles and the type of measured data provided by the company is represented in Table 3.1. The buildings were sorted by decreasing order of heating demand fraction according to 2019 measured data.

Table 3.1: Overview of all buildings connected to the ÉCCU networks and available data.

				Available data			
Building #id	**Year built**	**Building use type**	**Heat demand fraction (*)**	**Steam**	**Hot/Cold water**	**Electricity**	**Gas**
1	1962	Office, retail	22%	●		●	
2	1967	Office, hotel, retail, exhibition	15%	●		●	
3	1958	Hotel	12%	●			
4	1960	Office, retail	10%	●			
5	1977	Residential	8%	●			
6	1967	Hotel	6%	●		●	
7	1964	Office, retail	5%	●			
8	1974	Education	5%	●		●	●
9	1967	Office	5%	●			
10	1983	Office	2%	●			
11	1990	Office	2%		●	●	
12	1918	Office, retail	2%	●			
13	1990	Office	1%		●		
14	1990	Office	1%		●		
15	N/A	Residential	1%		●		
16	N/A	Residential	1%		●		
17	2002	Residential	1%		●		
18	1992	Office, retail (**)	0.4%	●		●	
19	1957	Office, retail	0.3%	●			
20	1950	Office, retail	0.2%	●			

(*) Percentage of the total heat demand for ÉCCU according to monthly energy use values for 2019.

(**) This building contains an ice skating rink which will be considered later.

The company also provided the steam pressure at the outlet of the thermal plant (Figure 3.1). The steam pressure varies in a year between 2618 kPa and 1101 kPa, depending on the month.

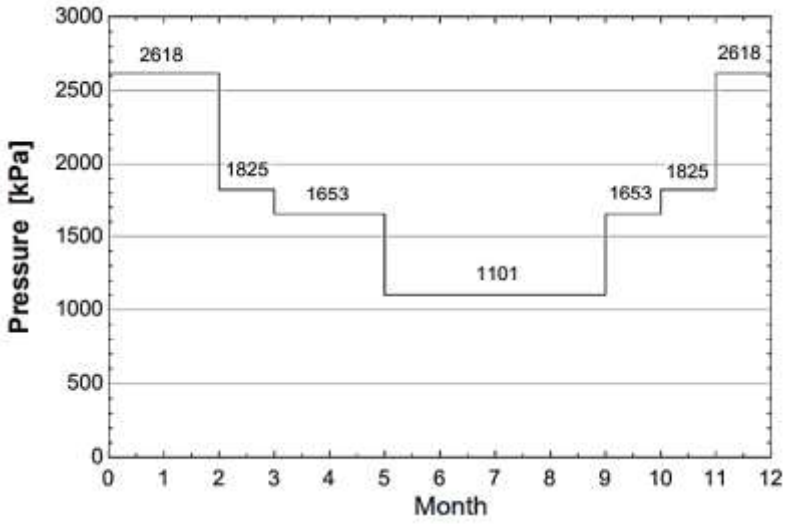

Figure 3.1: Estimated seasonal variation of steam pressure (in kPa) in the steam network. The estimation is used to convert the measured steam amount into a heating load.

This information was used to determine the monthly thermal loads for each building. The heating load is estimated for buildings connected to the steam network by assuming that steam reaches them at saturation conditions at the provided pressure P. At this point of the study, the pressure drop along the distribution system was neglected but is studied later in section 4.4.3. According to the plant manager, the temperature of condensate leaving the buildings is approximately 100 ℃, meaning that the heat consumption is equal to the latent of the steam at P added to the sensible heat for the condensate lowering its temperature from the saturation temperature at P to 100 ℃. The latent heat was calculated by multiplying the mass of steam required for each building by the latent heat of vaporization of the steam (Δh_{vap}) at P, and the sensible heat was calculated by subtracting the enthalpy of condensate at 100 ℃ from the enthalpy of saturated condensate at P multiplied by the steam mass. Equations (3) and (4) demonstrate the calculation method of the heat demand on the steam network.

$$Q_{steam} = Q_{latent} + Q_{sensible} \quad [kJ] \tag{3}$$

$$Q_{steam} = \dot{m_{steam}} \cdot \Delta h_{vap} + \dot{m_{steam}} \cdot \left(h_{saturated_{condensate}} - h_{condensate,100°C}\right) \quad \text{[kJ]} \tag{4}$$

Q_{steam} represents the amount of heat extracted from the steam network. It does not necessarily represent the total heat demand, as some buildings can use electric heating or heat recovery on chillers.

Information about the newly developed Faubourgs sector was extracted from a previous study commissioned by the Ville-Marie borough, Montréal [1], to assess the heat-sharing opportunities in the neighborhood. According to the study, each new building will contain a commercial floor (ground floor), two office floors (floors 1 and 2), and a variable number of high residential floors (floor three and up). The authors also considered constructing a 12 MW data center. According to Hydro-Québec's Strategic Plan, setting up data centers in Québec is one of its decisions to increase its revenue [96], especially in Montréal, which was announced the world's best place to host data centers in a press release in 2019 [97].

3.1.2 Selecting the building archetypes

Modelling buildings connected to the existing thermal networks was performed using the building archetypes developed by the US DOE mentioned in section 2.2.1. Given the type of use of these buildings, certain commercial archetypes were selected from the commercial reference and prototype sets. A simple method for using the archetypes to model actual buildings is to normalize simulated energy profiles per floor area of the model and then multiply it by the floor area of the building. For example, if an office building of 2000 m^2 in floor area is simulated using an office archetype of 1000 m^2, the simulation results are multiplied by two. Also, if a multi-usage building is to be modelled, a combination of several single-use models is used. A total of nine different archetypes were considered in this study. The office buildings were modelled using the Large Office, the Medium Office and the Small Office archetypes. The hotels were modelled using the Large Hotel and the Small Hotel archetypes. The retail space was simulated using the Strip mall archetype, the residential buildings using the Midrise Apartment archetype, and the educational institution and the exhibition space using the Secondary School and the Warehouse archetypes, respectively. The archetype combination giving the closest thermal demands to the measured thermal data of each building was selected (Figure 3.2).

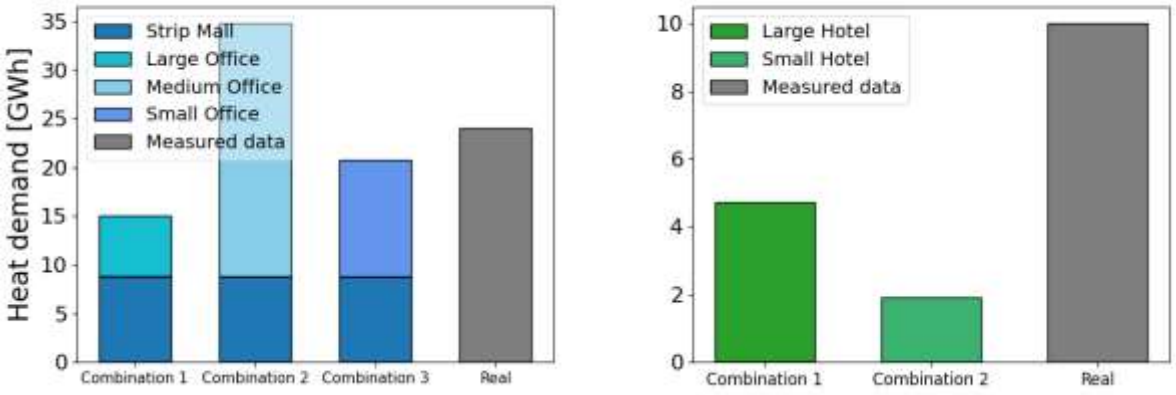

Figure 3.2: Different archetype combinations used to model an office/retail building and a hotel. The figure on the left shows three different combinations simulated for the office building: 1. Large Office + Strip Mall, 2. Medium Office + Strip Mall, 3. Small Office + Strip Mall. For this building, the Small Office and Strip Mall combination was chosen. The figure on the right represents two different approaches to model the hotel building in question. The Large Hotel archetype was used to estimate the energy demands of this hotel.

The archetypes were selected based on the location of the represented buildings. According to ASHRAE Standard 169 [98], Montréal belongs to climate zone 6A and is classified as Dfb (warm summer humid continental climate) according to Köppen climate classification [99]; therefore, building archetypes representing climate zone 6A were used. Minneapolis, Minnesota and Rochester, Minnesota are selected as representative cities for commercial reference and prototype archetypes. As this research focuses mainly on old buildings, commercial reference building models were primarily studied. Using Commercial prototype building models was considered optimistic in predicting the energy performance of the buildings since they are adopted to energy codes dating after 2004. Then, the archetype's vintage was selected based on the building's year of construction, unless some buildings underwent recent renovations; in this case, a more recent vintage was selected. These building models were simulated in the EnergyPlus simulation program using the 2019 weather file for the McTavish meteorological station obtained from the Simeb website [100]. The results of the first simulation (Figure 3.3) indicate that the models overestimated the heat demand during winter (30% in January) and underestimated the heat demand during summer (39% in June). These results demonstrate the need for calibration to reduce the discrepancies between simulated and measured data.

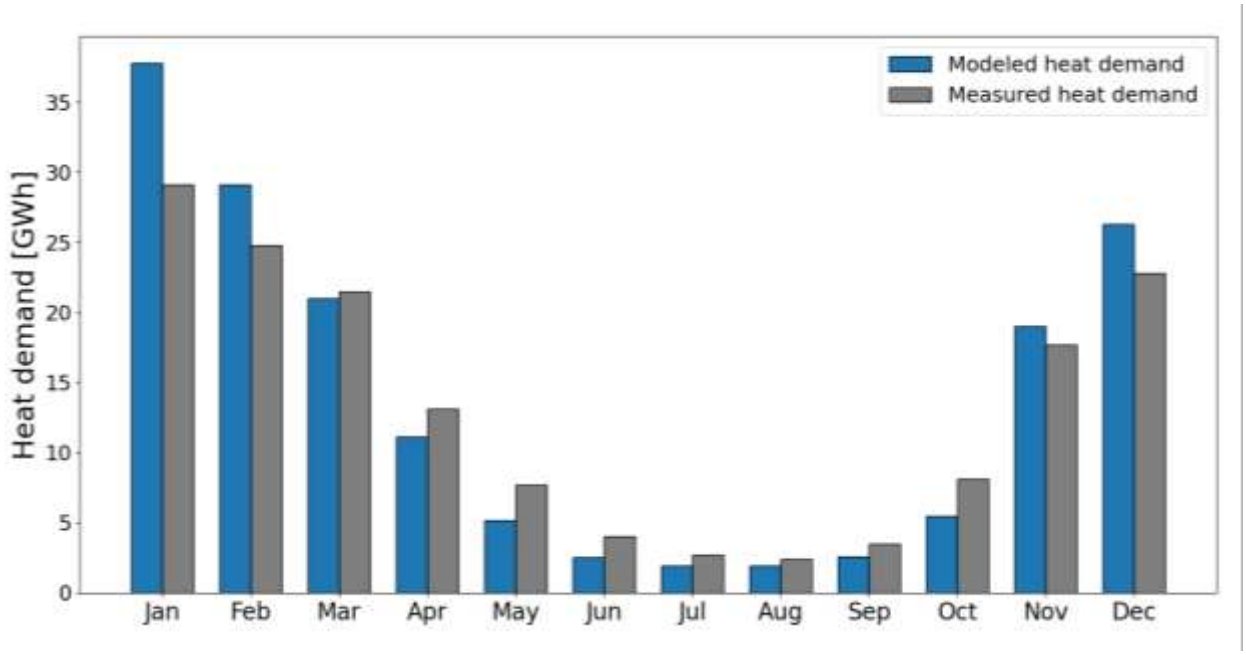

Figure 3.3: Monthly measured vs simulated heat and cold demand before calibration for all the buildings connected to the ÉCCU networks. The results show a significant disparity between the two datasets, especially in extreme cold and hot months when the models tend to overestimate the heat demand of the buildings in colder months and underestimate it during the hotter month.

3.1.3 Meteorological data

Choosing the correct weather data file is crucial in building simulation practices. Energy systems performance depends largely on external weather conditions such as the dry-bulb temperature, humidity ratio, incident solar ratio, etc. [101]. For calibration purposes and comparison with measured data, the archetypes were simulated using measured hourly meteorological data for the McTavish station for 2019. After the calibration, the building models were simulated again, using a statistically typical weather data file also for the McTavish station. These weather files contain hourly measured meteorological variables, such as dry-bulb temperature and solar radiation, that best represents median weather conditions over a multiyear period. The “Canadian Weather for Energy Calculation” (CWEC, updated in 2020) weather file obtained from Environment Canada [102] was selected for the second simulation.

3.1.4 Calibration

The calibration of the building models was performed manually in EnergyPlus by modifying seven input parameters. These input parameters included the infiltration rate [$m^3/s.m^2$] and the infiltration calculation method, the heating and cooling setpoint temperatures [°C], the domestic water peak [$m^3/s\text{-}m^2$], and the equipment and lights intensity [W/m^2]. Along with changing direct input parameters in EnergyPlus, several other modifications were considered, including the type of energy source for space heating. The modelled cold demand of each building was also calibrated using a linear equation. Finally, the heat, the cold, and the electric loads were modified for one building featuring an ice-skating rink to account for the additional loads imposed on the system. The detailed calibration practices performed on the models are presented below.

3.1.4.1 Design infiltration rate and infiltration calculation method

The envelope infiltration rate is among the most influencing parameters in the correspondence between simulated and metered energy consumption [103]. Infiltration implemented in the commercial reference buildings in EnergyPlus [104] depends on the design infiltration rate (DIR) [$m^3/s.m^2$], the schedule fraction if the infiltration rate is to be adjusted throughout the year $F_{schedule}$, the temperature difference between the zone's inside temperature T_{zone} and outside dry bulb temperature T_{odb} and the wind speed v_{wind}. The resulting infiltration is given by equation (5).

$$Infil_{rate} = DIR * F_{schedule} * (A + B * (T_{zone} - T_{odb}) + C * v_{wind} + D * v_{wind}^2) \quad (5)$$

In the commercial reference archetypes, the default DIR is set to 0.001133 [$m^3/s\text{-}m^2$], and the infiltration coefficients A, B, C and D are set to 1, 0, 0, 0 for commercial reference buildings, respectively. The value of the DIR was modified to a value between the default value and 0.00023 [$m^3/s\text{-}m^2$]. The latter corresponds to the recommended value of the IECC [78]. The infiltration coefficients were set to 0, 0, 0.224, 0 [105] for some buildings.

3.1.4.2 Heating and cooling setpoint temperatures

The heating setpoint temperature was increased for buildings with higher measured heating demand during warm months than simulation result demands (usually during April, May, June, and October). For example, increasing the heating setpoint temperature from 21 to 22 means activating

the heating system when the room temperature decreases to 20℃ instead of 21℃. The cooling setpoint temperature was also modified for some buildings for which measured electricity demand was available. For example, if measured electric demand during summer is much lower than that modelled by the archetypes, the cooling setpoint temperature was increased to lower the cooling demand since it's responsible for the electricity peak consumption in hotter weather.

3.1.4.3 Space heating heat source

The data collected from ÉCCU allows to determine the heating demand provided by the networks but does not necessarily represent the total heat demand of the buildings, as some clients may use supplementary heating sources. Figure 3.4 shows the measured and modelled electricity demand intensity of two office buildings versus the outside dry bulb temperature. Measured data show that the electricity demand increases with decreasing temperatures when the temperatures drop below 7 ℃, whereas the models predicted a constant consumption intensity during winter. This increase in electricity demand can be linked to heating practices as the dry bulb temperature drops, which justifies the assumption of electric heating.

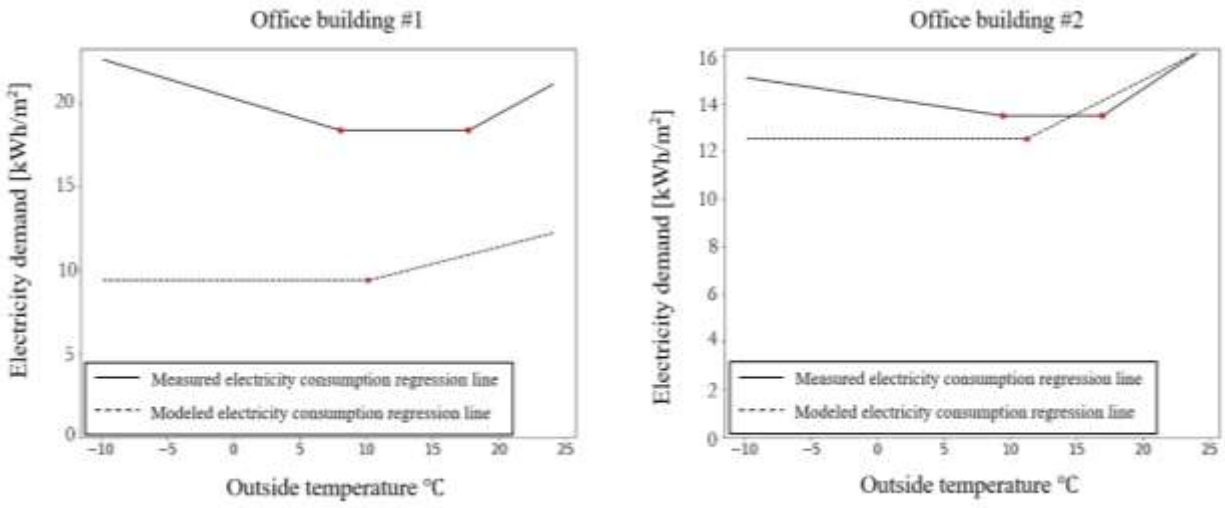

Figure 3.4: Electricity consumption vs outside dry-bulb temperature

3.1.4.4 Equipment and lighting intensity

According to the Comprehensive Energy Use Database (CEUD) statistics [106] produced for Québec by the office of Energy Efficiency at Natural Resources Canada (NRCan), energy use for auxiliary equipment in offices has increased by over 70% from its 2000 baseline. Lighting intensity has also seen a slight increase over the past few years, with a growth of 8% from its 2000 baseline. This rise in installed equipment power and lighting intensity in offices indirectly affects the thermal energy balance as additional internal gains are being neglected. The simulation results showed that the electric power simulated by the models was underestimated for several office buildings.

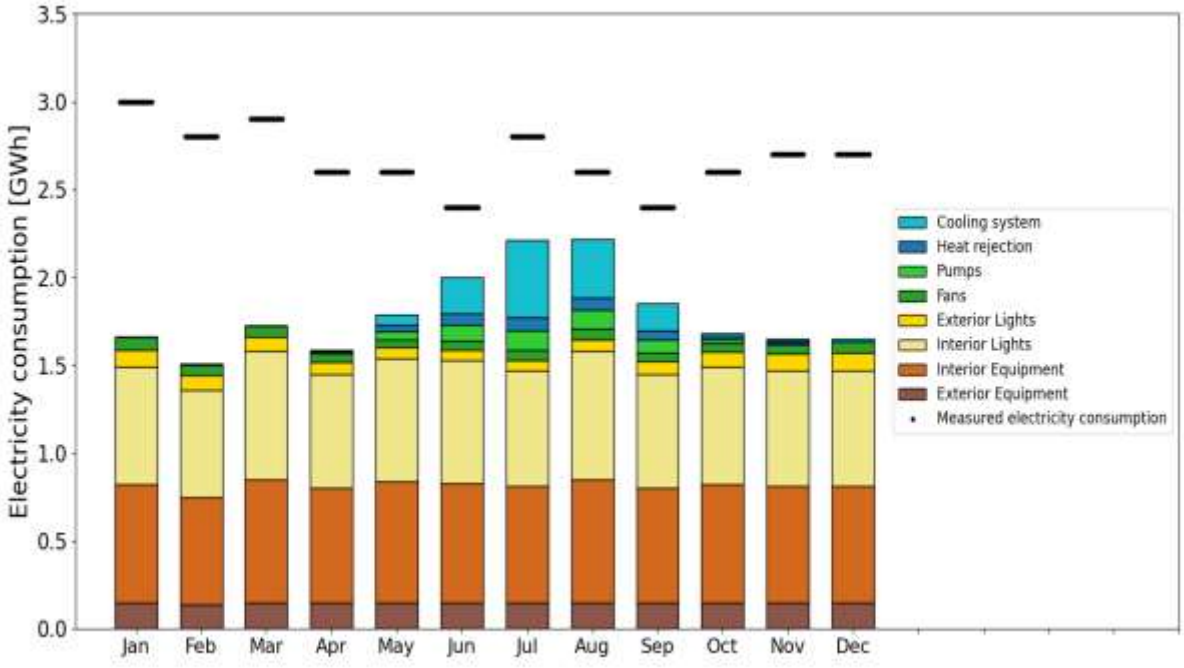

Figure 3.5: Office building electric demand. The bars represent the electric energy consumed by the building each month as per the building model, while the black lines above represent the total measured electric consumption in kWh.

Figure 3.5 represents the simulated monthly electric consumption of an office building compared to measured data. Over the course of a year, the model estimated a yearly electricity consumption of 22 GWh, 33% less than the annual measured data, which was determined at 32 GWh. A key observation from this graph is that an almost constant load is missing all year long, which justifies the increase in equipment and light intensity performed for some buildings.

3.1.4.5 Domestic hot water consumption

In summer, steam can be used in buildings for terminal reheat and for domestic hot water. Unfortunately, building models did not always accurately estimate this baseload, so the calibration was performed by editing the 'water peak' input parameter in EnergyPlus. That parameter represents the maximum water flowrate usage (in m^3/s, for each building zone), modified by a schedule to define the use hours.

3.1.4.6 Ice-skating rink

As mentioned in Table 3.1, one of the buildings includes an ice-skating rink. This causes a significant cooling load, and provides an opportunity to heat the building with recovery from the chillers, so this particularity should be implemented in our model. According to Rogstam [107], typical energy consumption shares by energy usage are shown in Figure 3.6. The primary energy-demanding end-use is refrigeration required to maintain the ice surface in good conditions (43% of the total energy demand of the rink). Heating and electric energy come next with 26% and 25% respective shares. Dehumidification consumes almost 6% of the total energy demand.

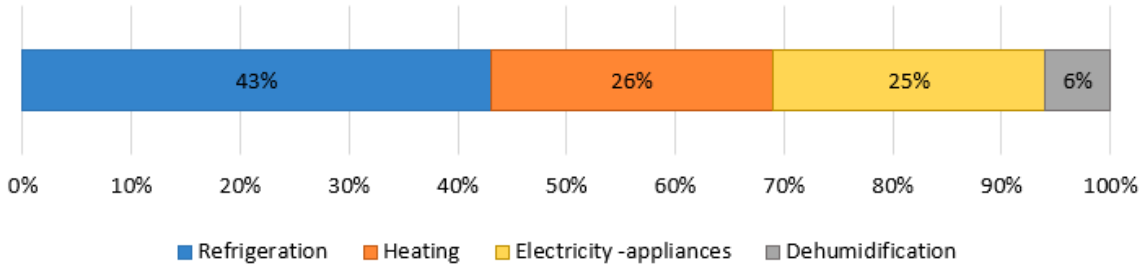

Figure 3.6: Shares of energy consumption per end-use of a typical indoor skating rink.

Given that the models do not account for the skating rink in the building, supplementary heat, cold and electricity demands were added to the modelled loads of the building. According to the ASHRAE code for refrigeration [108], daily refrigeration loads for indoor skating rinks in cities belonging to climate zone 6 are estimated to be 2.743 [kWh/m^2 of skating rink area] during spring 3.253 [kWh/m^2 of skating rink area] during summer. The 2.743 [kWh/m^2 of skating rink area] is considered an average daily refrigeration load value all year long.

3.1.4.7 Cold demand

The building models assumed that no cooling load was imposed during colder months, contrary to the measured data (Figure 3.7).

In order to have a better prediction of the actual cooling loads for these buildings, calibration was performed using the linear equation (6) presented below.

$$Cold_{bld,month} = (Baseload_{bld} + ModeledCold_{bld,month} * CorrectiveFactor_{bld}) \quad (6)$$

Where bld represents the id of the building $bld \in \{1,..,20\}$

$month$ represents the month of the year $month \in \{1,..,12\}$

$Cold_{bld,month}$: monthly calibrated cold demand of the building [kWh]

$ModeledCold_{bld,month}$: simulated monthly cold demand of each building [kWh]

$Baseload_{bld}$: monthly cold baseload added to each building [kWh]

$CorrectiveFactor_{bld}$: corrective coefficient

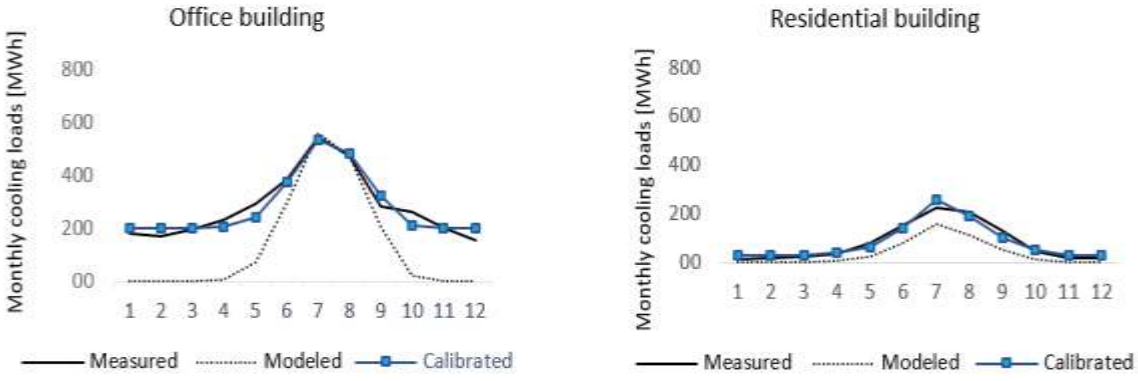

Figure 3.7: Monthly cold demand in [kWh] for an office and a residential building before and after calibration. The black line represents the measured cold demand of the building, the black dotted line represents the modelled cold before calibration, and the blue line represents the modelled cold after calibration. After calibration, the office and residential buildings' resulting CV(RMSE) went down from 0.62 and 0.65 to 0.11 and 0.2, respectively.

The optimization was performed using the Lingo optimization modelling software [109] to achieve a minimum CV(RMSE) for each building. This calibration was also performed for other facilities where measured cold data was not available. The Equation's variables for the remaining buildings were chosen equal to the minimum baseload and the corresponding corrective factor obtained after optimization. Figure 3.7 illustrates the result of the calibration equation for two of the buildings connected to the cold water network.

3.2 Faubourgs buildings

The Faubourgs buildings were modelled using archetypes derived from the Commercial Prototype building archetypes [77] and adapted to the Canadian context by Natural Resources Canada [79], meeting the 2011 National Energy Code for Buildings [78]. The archetypes were selected by the study's authors, who further modified these models to account for the Québec regulations. The commercial, office and residential parts were modelled using three different archetypes: the Retail Standalone, the Large Office, and the Midrise Apartment, respectively.

The modelers of the Faubourgs neighborhood [11][25] performed several calibrations to the selected NECB building archetypes mentioned above to account for the Québec regulations. The assumptions made by the team are as follows:

- The Window-to-Wall Ratio was set at 40 % for each building orientation (North, East, South, West).
- The thermal loss coefficient (U-value) of the glazing was set to 1.53 W/m²-K, according to the 2019 EnergyStar standards [26].
- The infiltration rate was calculated by a model taking into account wind speed, and the Leakage Rate at 75 Pa (LR_{75}) was set at 2.2 L/s-m2.
- The thermal resistance values of the exterior walls and the roof were chosen respectively at 3.4 m²-K/W and 5.46 m²-K/W, according to the "Règlement sur l'Économie de l'Énergie dans les Nouveaux Bâtiments" of Québec [111].

3.3 Results

3.3.1 Calibration results for the ÉCCU buildings

Figure 3.8 shows the monthly heat demands of all the buildings of the ÉCCU network. The CV(RMSE) decreased from 25% before calibration to 6% after.

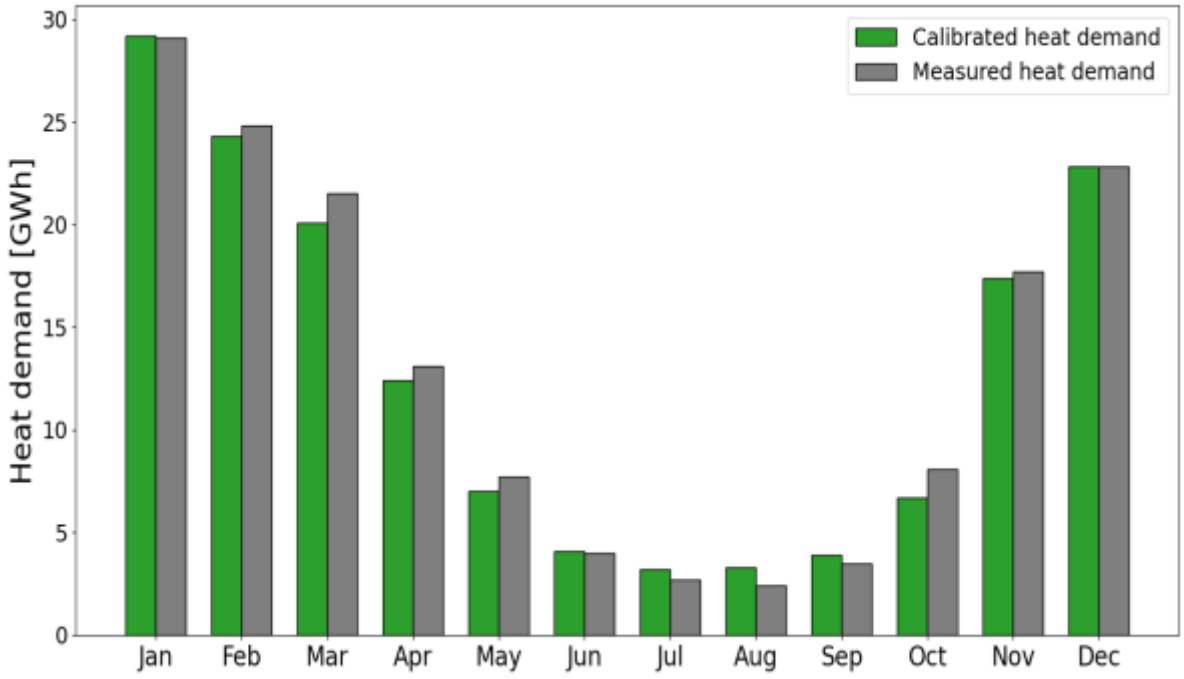

Figure 3.8: Monthly measured vs simulated heat demand after calibration for the total of the buildings connected to the ÉCCU networks.

On the individual building level, the heat, the cold, and the electricity demands were accurately estimated. Table 3.2 breaks down the NMBE and CV(RMSE) after calibration for all the clients. Although the obtained heating CV(RMSE) was higher than 15% for some buildings, it was only for some buildings for which the heating demand was less or equal to 5% of the total heat demand. On the other hand, the cold CV(RMSE) was kept between 11% and 48%, and the electricity CV(RMSE) was held below 19%.

The main objective of the modelling process was to determine a precise approximation of the heat demand since the heat network is the most GHG-intensive, being gas-fired.

Table 3.2: NMBE and CV(RMSE) results for all the clients after calibration.

	Building	NMBE	CVRMSE	Building	NMBE	CVRMSE
Heat demand	**1**	5%	13%	**11**	2%	10%
	2	5%	10%	**12**	-1%	19%
	3	2%	6%	**13**	1%	12%
	4	-1%	13%	**14**	3%	14%
	5	0%	8%	**15**	5%	14%
	6	-3%	11%	**16**	2%	26%
	7	3%	11%	**17**	4%	19%
	8	-3%	23%	**18**	0%	0%
	9	0%	20%	**19**	5%	28%
	10	0%	0%	**20**	4%	21%
Cold demand	**11**	0%	11%	**15**	0%	44%
	13	0%	32%	**16**	0%	48%
	14	0%	28%	**17**	-3%	20%
Electricity demand	**1**	-7%	8%	**10**	-4%	11%
	2	-1%	8%	**13**	-17%	17%
	6	-2%	8%	**18**	-7%	8%
	8	-15%	22%	-	-	-

3.3.2 Annual consumption and peak demand

3.3.2.1 ÉCCU buildings

Figure 3.9 shows the daily average thermal loads for the clients of the ÉCCU. Throughout a typical year, the heating load of all client buildings is equal to 145.5 GWh, of which 94% is attributed to the buildings connected to the steam network. Buildings connected to the hot water and the cold water networks present a total heating load of 8 GWh and a cooling load of 12.2 GWh. These

numbers represent only the loads fulfilled by the ÉCCU networks and not the total loads of the buildings, as some clients adopt additional heating and cooling sources such as electric heating equipment or chillers.

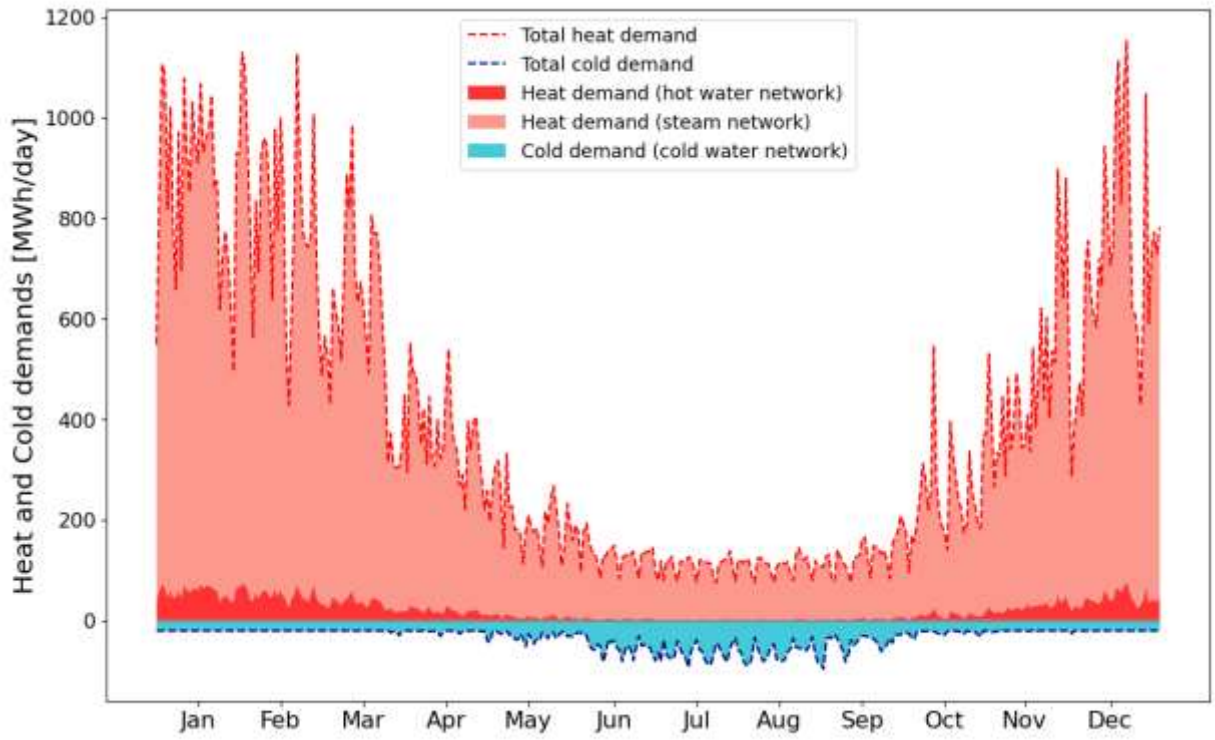

Figure 3.9: Average daily heating and cooling loads for buildings connected to the steam, hot water, and cold water networks.

Table 3.3 summarizes the total consumption and peak demands for the buildings connected to each thermal network. It also contains information regarding the cold demand for the buildings not connected to the cold water network. This information will be used further in the next chapter. The winter peak corresponds to the hour of the maximum heat demand of the steam network for the period between October and April (inclusive), and the summer peak corresponds to the hour of the maximum cooling demand of the cold water network for the period between May and September (inclusive). It is to notice that the cold demand is higher in both networks; this is due to the fact that most buildings contain small data centers that require constant cooling all year long.

Table 3.3: Consumption and peak demand for the buildings connected to the networks.

	Consumption [GWh]	**Winter peak [MW]**	**Summer Peak [MW]**
Heat demand from the steam network	137.5	73.3	4.3
Heat demand from the hot water network	8	5	0.1
Cold demand from the cold water network	12.2	0.9	6
Cold demand for buildings not connected	153.4	8.5	84.5

3.3.2.2 Faubourgs buildings

Table 3.4 shows the annual total thermal loads for the three sites of the Faubourgs neighborhood. The yearly heat demand for the whole neighborhood is 75 GWh, with a peak heat load of 29.3 MW. The cold demand is estimated at 17.6 GW and a peak demand of 25.8 MW; adding to that, the cold load from the data center is approximated to 105.1 GWh a year, and its peak demand is 12 MW all year long. According to Table 3.4, the Molson site requires the most energy for both heating and cooling, with 54% and 51% respective percentages of the total thermal demands of the neighborhood. The Radio Canada and the Portes Sainte Marie sites contribute each to 30% and 16% of the total heating load and 32% and 17% of the total cooling load. The electricity consumption for appliances of all the buildings in the neighborhood is of the same order as the electricity demand for the data center alone (112.8 GWh vs 105.1 GWh, respectively

Table 3.4: Consumption and peak demand for the three sites of the Faubourgs neighborhood and the data center to be constructed.

		Consumption [GWh]	**Winter peak [MW]**	**Summer Peak [MW]**
Heat	Molson	40.5	15.6	2.2
	Radio Canada	22.7	9	1.3
	Portes Sainte-Marie	11.8	4.7	0.7
Total heat	**-**	**75**	**29.4**	**4.1**

		Consumption [GWh]	Winter peak [MW]	Summer Peak [MW]
Cold	Molson	8.9	0	13.2
	Radio Canada	5.7	0	8.3
	Portes Sainte-Marie	3	0	4.3
	Data center	105.1	12	12
Total cold	**-**	**122.7**	**12**	**37.8**

Electricity – appliances	Molson	34.1	12.4	11.3
	Radio Canada	20.2	9.1	3.7
	Portes Sainte-Marie	10.6	4.7	7.1
	Data center	105.1	12	12
Total Electricity	**-**	**217.9**	**41.4**	**24.3**

3.4 Conclusion

This chapter has presented a detailed methodology for determining the thermal energy profile of the two building sets under study. The ÉCCU buildings were modelled using the US DOE building archetypes and calibrated using measured data for 2019. The total heat load is estimated at 145.5 GWh for a typical year, with a maximum heat load of 78.8 MW. The cold demand for buildings connected to the cold water network equals 12.2 GWh a year with a maximum cold load of 6 MW.

The Faubourgs sector buildings were modelled using archetypes selected by the project team, using a typical weather file. The neighborhood's total heat demand is 75 GWh, and the peak demand is almost 30 MW. The neighborhood's cooling load, including the data center, is equal to 172.7 GWh a year, and the peak load is 38 MW.

CHAPTER 4 EXISTING DISTRICT ENERGY SYSTEM MODELLING

The buildings' energy demands determined in the previous chapter are used to model the existing steam, hot water and cold water networks. The methodology followed to model each network in TRNSYS is described thoroughly. The models estimate the thermal plant's total energy demand, taking into consideration the thermal and mass losses of the networks. This chapter serves as the first step to modelling long-term decarbonization scenarios as it sets the base scenario to which solutions will be compared.

4.1 Steam network

In the absence of detailed data on the existing network, we created a simplified piping layout and estimated the design parameters of the pipes based on the literature. The steam network clients are distributed on six main roads in Montréal. To make the modelling process less complicated, six building blocks were configured, where each block encompasses all the buildings located on the same street. Nine pipe branches were also configured to deliver steam from the thermal plant to all the steam clients (Figure 4.1). First, each block's hourly energy profile (heat, cold and electricity) was determined by summing up the heat demands of all the buildings enclosed within that block. Then, main distribution pipes and sub-branches connecting the blocks to the main pipes were routed along the main roads. Maximum flow rates in the sub-branches were determined using the peak demand for each block, and the upstream flow was calculated by summing the outgoing flows.

Table 4.1: building blocks' peak loads and maximum flowrates

Block	**Peak heat load [MW]**	**Maximum flowrate [kg/s]**
a	7.1	3
b	15	6.4
c	10	4.3
d	11.3	4.8
e	4	1.7
f	31.3	13.3
Total	**73.3**	**31.1**

Table 4.1 presents the peak load of each block and the corresponding required flow rate. Given that the peak loads do not occur simultaneously, the total peak demand of the network is not equal to the sum of the peak demands of each block. Note that the individual pipes connecting each building to the sub-branch were not modelled. This network configuration may not represent the exact current network, but it does give an idea of the thermal losses expected by the distribution system.

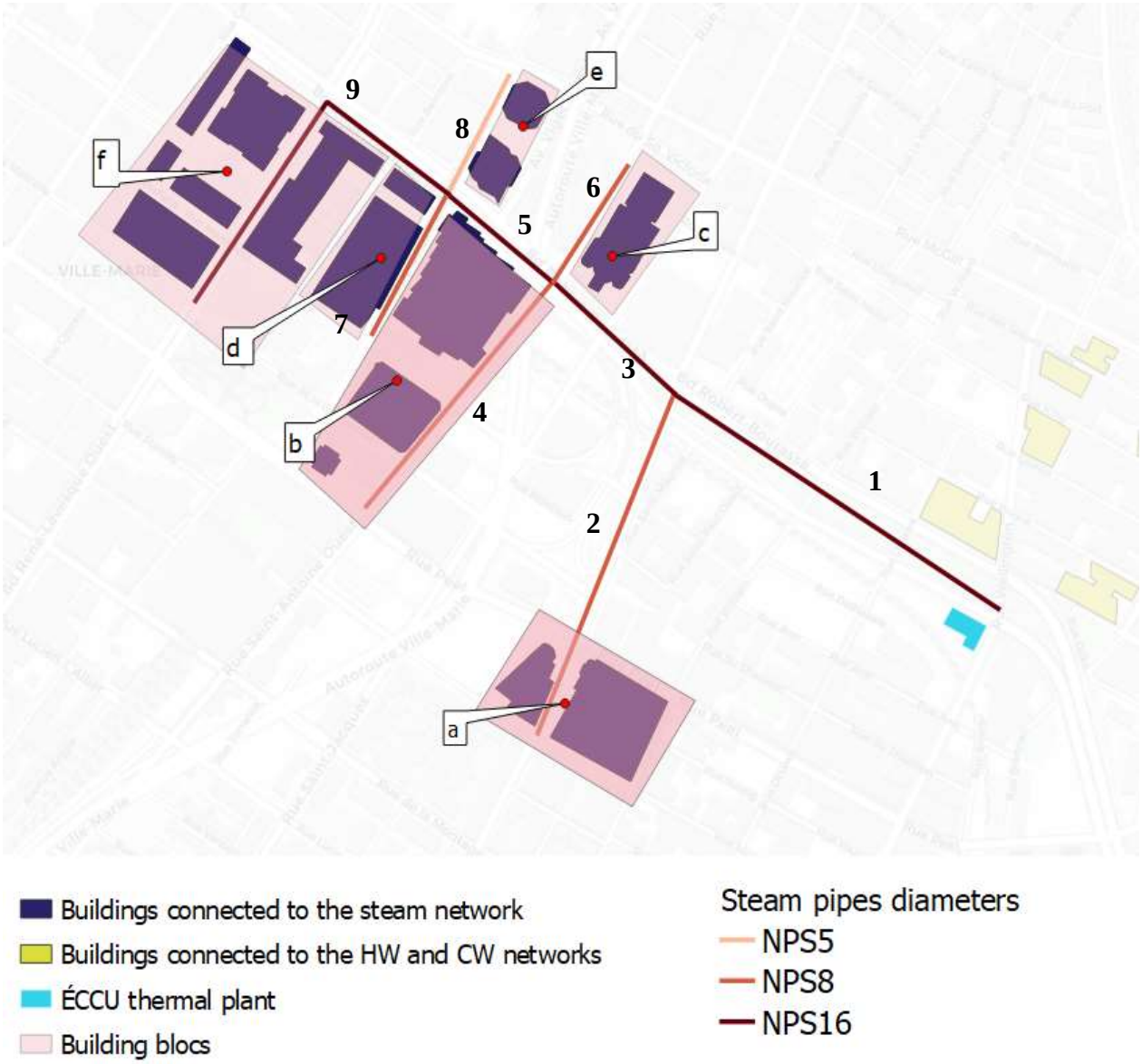

Figure 4.1: Building blocks and pipes details of the steam network

The pipe diameters were approximated in three successive steps. The first step was to estimate each pipe diameter based on its peak flow rate, considering a maximum steam velocity of 45 m/s [112].

Next, the diameters were adjusted according to the total pressure drop at the end of each sub-branch. The pressure drop was calculated for each of the four initial pressures at the outlet of the thermal plant using the AioFlo pipe sizing software [113], which performs calculations based on the Darcy-Weisbach pipe head loss [112]. Finally, the results were refined in order to keep the total pressure drop from the thermal plant to each block lower than half of the initial gage pressure. The design pipe length used was 50% longer than the actual network length to account for fitting losses [112]. Table 4.2 details the final pipe diameters, the design pipe lengths and the maximum resulting pressure drop. Insulation material and thickness were determined in line with the 2012 International Energy Conservation Code [78].

Table 4.2: Pipes diameters, design pipe lengths and maximum pressure drop

Pipe #id	**Nominal diameter [cm]**	**Design pipe length [m]**	**Maximum pressure drop [kPa]**
Pipe 1	38.1	690	350
Pipe 2	20.3	510	91
Pipe 3	38.1	360	190
Pipe 4	20.27	525	305
Pipe 5	38.1	270	77
Pipe 6	20.27	300	79
Pipe 7	20.27	300	113
Pipe 8	12.82	225	156
Pipe 9	38.1	720	123

The Steam network was modelled in TRNSYS simulation software. The piping model consisted of six loads served by nine supply pipes, representing the above distribution. Due to the steam's thermal losses, steam traps were placed to remove condensate forming in pipes. Six return pipes were also configured to collect the condensate forming at each building's end. Condensate pipe diameters are much smaller than those of the steam pipes due to the lower specific volume of water compared to high-pressure steam. Schedule 80 steel piping was used for condensate lines because

of the extra allowance for corrosion [114]. The pipes are contained in a pipe tunnel kept at 17.5 ℃. Using a high-pressure boiler feed pump, condensate is electrically pumped to the thermal plant.

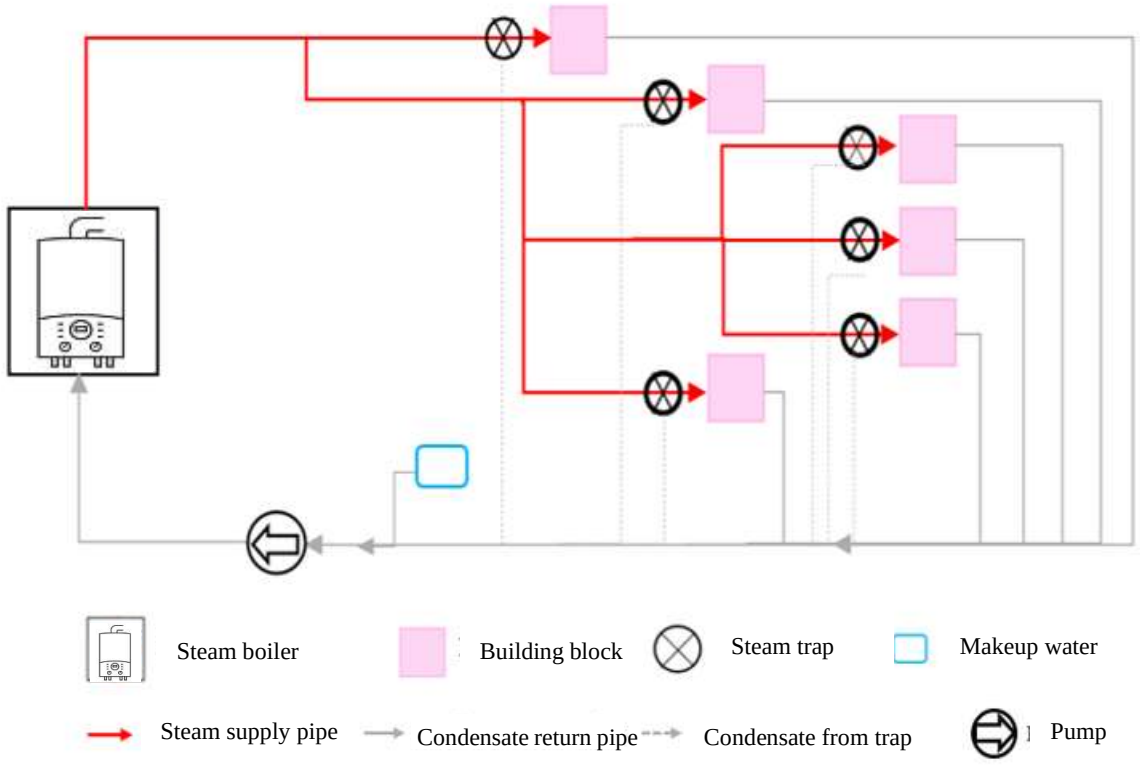

Figure 4.2: Steam network graphical representation.

Figure 4.2 gives a graphical representation of the steam network model used in TRNSYS. The steam leaves the thermal plant at the specified pressure (Figure 3.1) at saturation conditions and is delivered to the clients through supply steam pipes. The buildings use the heat from the high-pressure steam and liberate the condensate at 100 ℃ at full load. The return condensate is later transported to the thermal plant through condensate pipes with condensate collected from the steam traps and is finally pumped to the boiler using a boiler feed pump. Makeup water is also used to compensate for mass losses in the network. According to the company's site [115], the total mass loss of the network is estimated to be 3%. In addition to the steam required by buildings for space heating and domestic water heating, ÉCCU indicates that 12% of its total steam demand is used for humidification purposes. This load was taken into consideration in the TRNSYS model of the steam network by counting an additional heat demand for humidification. ÉCCU also indicates that the piping network is responsible for a mass loss of 3% of the total steam mass injected into the network. This indication was also taken into consideration while building the model.

4.2 Hot water and cold water networks

The networks deliver heat and cold to six buildings located in the Cité multimédias area. The centralized hot water network delivers hot water at 82.2 ℃, which directly satisfies the heating demands of each property. The buildings consume heat to fulfill their demand and leave the water at 54.4 ℃, resulting in a total ΔT of 27.8 ℃ on full load. The centralized cold water network delivers chilled water at 4℃, which absorbs the heat rejected from the buildings and returns to the thermal plant at 15.6 ℃ on full load. The detailed piping network was not modelled for the hot water and cold water networks; instead, all the buildings were seen as one big property "Pr" with a heating and a cooling load equal to the sum of the heating and cooling loads of all the buildings, respectively (Figure 4.3). A minimum pump turndown ratio of 15% is considered.

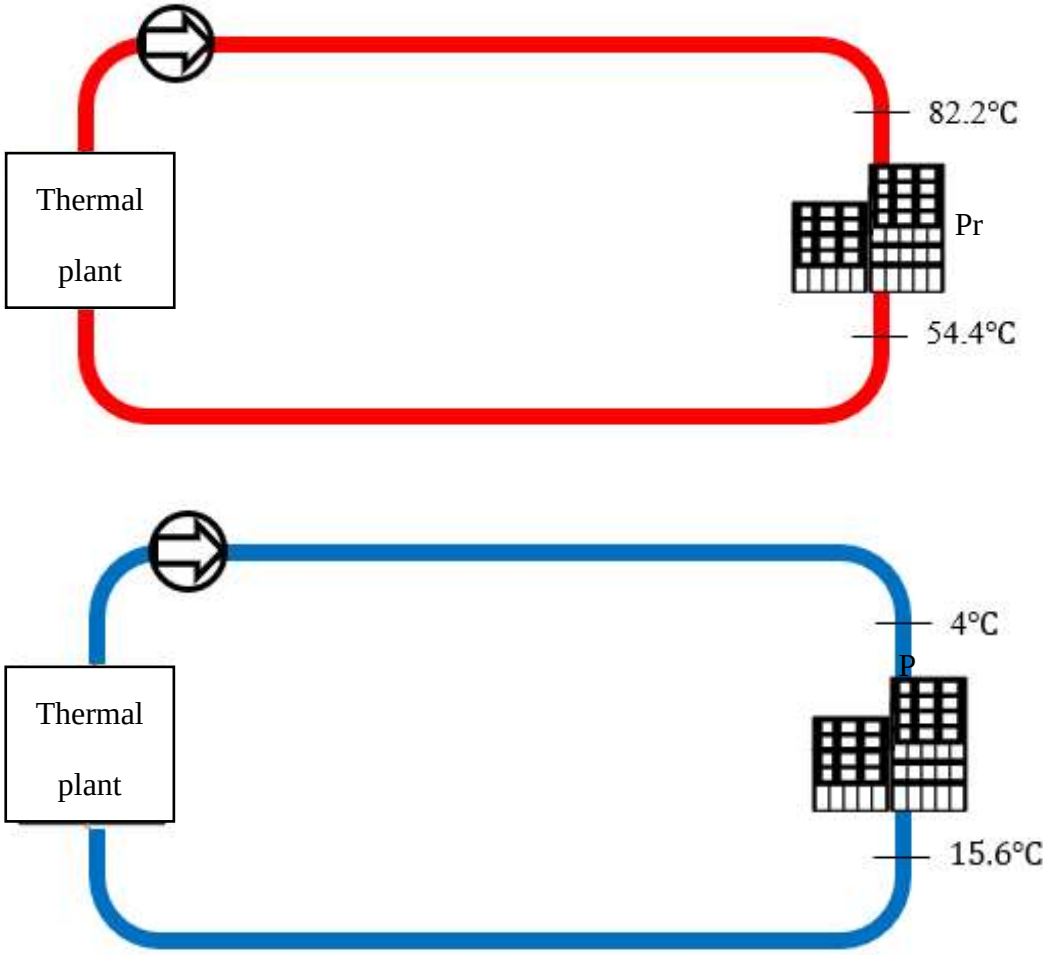

Figure 4.3: Hot water and cold water network graphical representation

Figure 4.4 represents the hourly temperatures of the hot and cold water networks. The boiler outlet temperature is set to 82.4 ℃ and reaches the building block "Pr" slightly lower due to piping losses (81.45 ℃ at the lowest flow rate). The heating network's return temperature ranges vastly between 54.4 ℃ and 80.1℃ depending on the heating load. During summer, when the heat demand is lower than 15% of the peak load, the pump still forces the water at a minimum turndown ratio of 15%, which leads to an increased DH return temperature. This increase is caused by a required heat load lower than that actually carried by the hot water.

On the cold network side, the chiller's outlet temperature is fixed at 4 ℃. Due to heat gain from the piping network, the water reaches the buildings at a temperature slightly higher than 4 ℃ (maximum 4.2 at the slowest flow rate). The return temperature from the cold water loop varies between 11.2 ℃ (winter) and 14 ℃ (summer) for a similar reason to that of the hot water network.

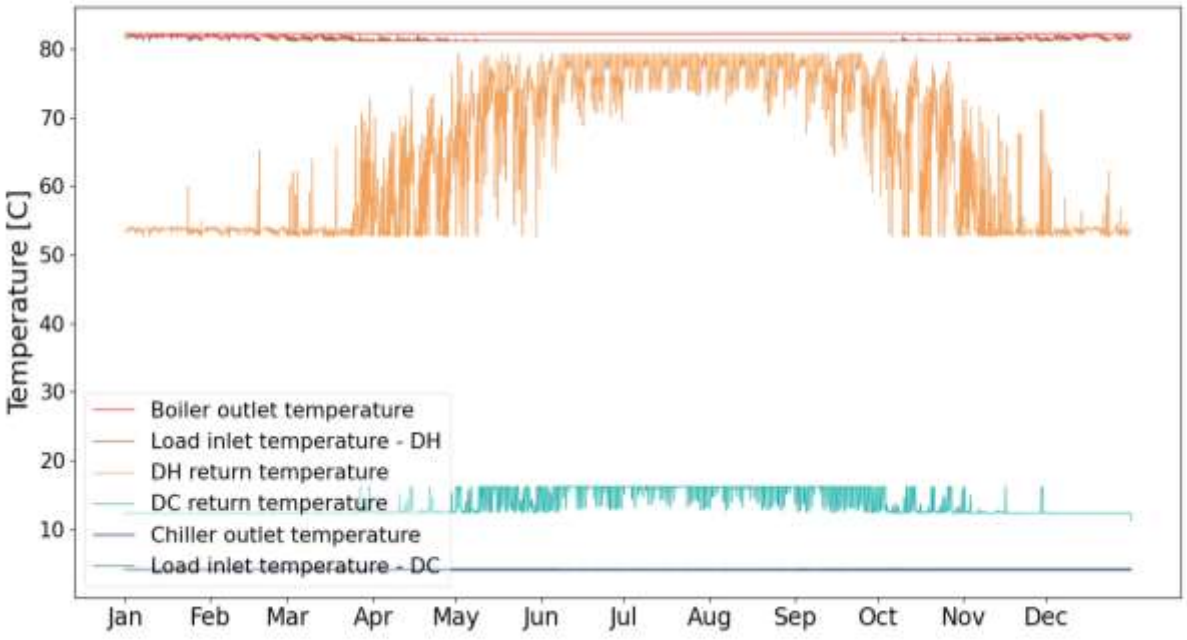

Figure 4.4: Hourly operational temperatures of the hot and cold water networks.

Table 4.3 shows the peak demands and corresponding flow rates for the hot and cold water networks. The pipe diameters were determined based on the maximum flow rates and peak loads of "P" and the maximum temperature differences. The pipes sizes were conceived to permit a maximum pressure drop of 200 Pa/m as recommended by ASHRAE [112].

Table 4.3: Total peak loads and flow rates for the hot and cold water networks.

Network	**Peak demand [MW]**	**Peak flow rate [kg/s]**	**Pipe diameter [cm]**	**Maximum ΔP [Pa/m]**
Hot water	5.1	42.6	19.36 (NPS8)	125.8
Cold water	6	124	28.89 (NPS12)	127.5

4.3 Heat production efficiency

The energy efficiencies of heat production at the thermal plant are detailed in Table 4.4. In the absence of actual data from the existing system, these numbers were chosen based on average values used in the industry. Gas boiler efficiency is provided as a percentage of the fuel's Higher Heating Value (HHV).

Table 4.4: Energy indicators of the systems at the thermal plant.

Steam boiler efficiency	**Hot water boiler efficiency**	**Chiller COP**
80%	85%	3

4.4 Results

This section represents the current energy demands, heat peaks and GHG emissions according to the simulation. These results will be used in the next chapter to build the Business As Usual scenario to which the decarbonization scenarios will be compared.

4.4.1 Annual energy consumption

Table 4.5 summarizes the main energy indicators of the existing thermal plant and its clients. The gas consumption was calculated by dividing the heat load accounting for pipe losses by the boilers' overall efficiency. It should be mentioned that the required gas for the steam network includes that required for additional steam for humidification.

Both the total electricity demand and that for the thermal plant alone were also represented. The electricity demand for the networks was calculated by summing the demands of its electric equipment (water pumps, condensate pumps, and chiller). On the other hand, the total electricity demand was determined by summing the electricity consumption of the thermal plant and that of the clients.

The Greenhouse gas emissions are measured by an equivalent quantity of CO_2 resulting from primary energy use. The emission factors used correspond to the values recommended by *Transition Énergétique Québec* (2019) [116], which indicates that the combustion of natural gas releases 179.4 g of CO_2 per kWh of gas consumed by gas-fired boilers. Electricity consumption releases 2 g of CO_2 per kWh of electricity used on site.

Table 4.5: Summary of the main energy indicators of the thermal plant and the ÉCCU clients.

	Consumption [GWh]	**Winter peak [MW]**	**Summer peak [MW]**	**Emissions [kt $CO_{2,equiv}$]**
Gas	232.8	117.4	10.8	41.8
Electricity (Central plant)	4.1	0.5	2.1	0
Electricity (Total)	265.3	47	43.9	0.5
Total	498	164.9	56.8	41.8

Table 4.6 breaks down the contribution of each network to the total energy consumption. In this table, the yearly consumptions, energy peaks and GHG emissions of the whole site (thermal plant + clients) are represented separately by end-use. The electricity demand for buildings connected to the steam network was divided into electricity for appliances, cooling, and heating. Whereas buildings connected to the hot water and cold water networks only consume electricity to run their appliances as the networks are assumed to fulfill 100% of their thermal loads.

As noticed, the gas consumption for the steam network accounts for 95% of the total gas of the thermal plant, with a yearly value of 222.6 GWh. The gas consumed for hot water production is estimated to be 10.2 GWh per year. Although most gas is consumed during colder times, the numbers show that heating is also required during summer. The hot water and cold water networks and their clients contribute to only 7% of the total electricity demand. Almost 50% of the electricity demand (179.2 [GWh]) is attributed to the buildings connected to the steam network in order to run their appliances. This observation reinforces the previous hypothesis explaining the excessive

cooling demands all year long because of the electric equipment (primarily computers) installed in most buildings.

Table 4.6: Annual consumption, peak demands and GHG emissions of the thermal plant of ÉCCU.

		Consumption [GWh]	**Winter peak [MW]**	**Summer peak [MW]**	**Emissions [ktCO^2$_{equiv}$]**
Hot water and cold water networks	Gaz	10.2	5.1	0.3	1.8
	Electricity – plant	4.5	0.4	2.1	0
	Electricity – appliances	12.1	2.9	1.1	0.02
Steam network	Gaz – heating	195.9	92	8.6	3595
	Gaz – humification	26.7	12.5	1.2	5990
	Electricity – plant	0.3	0.2	0	0
	Electricity – appliances	179.2	28.1	7.6	0.4
	Electricity – heating	8.5	12.1	0	0.1
	Electricity – cooling	61.4	3.4	33.1	0

The total GHG emissions of the central plant are approximated to **41780** tonnes of equivalent CO_2, mainly caused by gas consumption. These emissions are compared to the average yearly emissions declared by ÉCCU for the past 10 years [117]. The average was determined from 2012 till 2019, excluding 2020 since many buildings were closed due to covid 19, and thus, the energy consumption at the thermal plant was much lower. The annual average of the reported CO_2 emissions is equal to 41130 tonnes of equivalent CO_2, resulting in an error of only 1.5% between the simulated and measured data. This shows that our calibrated models of the networks and connected buildings provide a good estimation of the yearly performance, while allowing us to estimate the dynamic energy profile and resulting peak demands.

4.4.2 Dynamic energy profile (with peak weeks)

This section presents the dynamic energy demand profiles per end-use. The end uses for gas consumption are divided into heating for the Hot Water Network (HWN), heating for the Steam Network (SN), and gas for the production of steam used for humidification. The electric energy consumption is divided into four end uses: electricity for appliances, electricity for the electric equipment of the thermal plant, electricity for heating purposes, and finally, electricity for cooling purposes. Figure 4.5 shows the total daily energy consumption for gas and electricity. The stacked areas represent the different contributions of end uses to energy consumption.

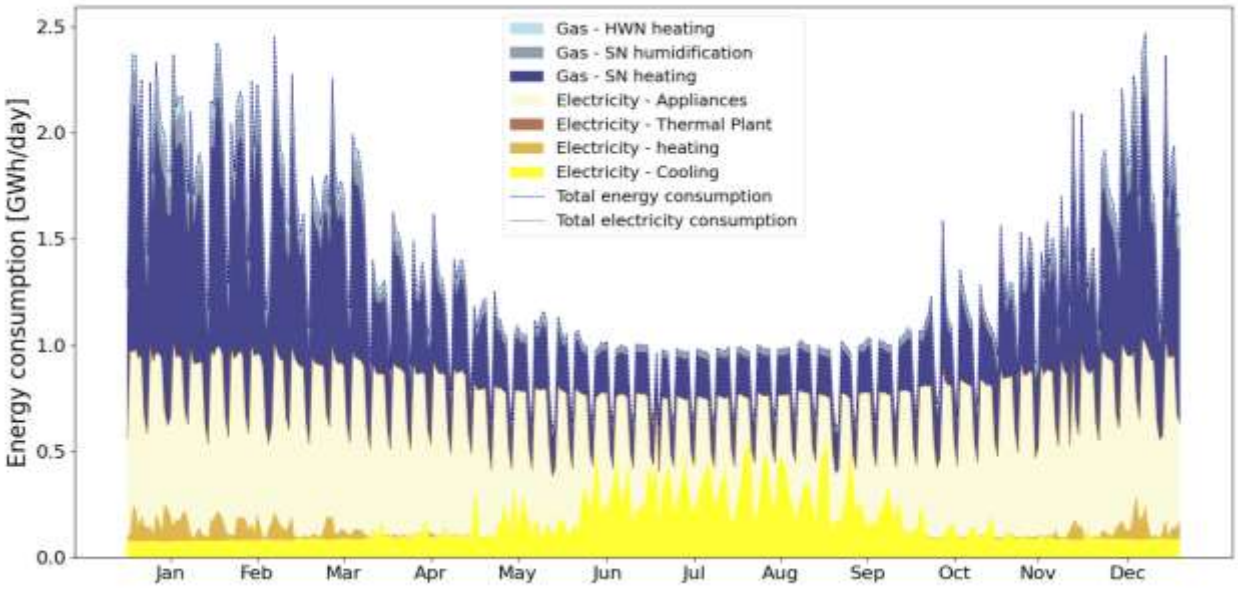

Figure 4.5: Daily energy consumption for gas and electricity per end-use for thermal plant.

Figure 4.6 shows the dynamic energy consumption of gas and electricity per end-use for the week of the 19th of February (Feb. 19 being a Saturday). This represents the coldest week in the selected typical year weather file, corresponding to the yearly peak heat demand. During this week, the gas demand for heating dominates, mainly due to the cold outside temperatures. In order to achieve a higher level of comfort, the clients use additional electric heating, which is shown in the increased electricity consumption for space heating as the temperature reaches lower values. Having cooling loads even during winter results in electricity consumption for cooling all year long and not only during summer. Inversely, Figure 4.7 shows the dynamic energy consumption for the peak summer week (the week of the 26th of August). Again, the 26th of the month represents a Saturday. This

week denotes the hottest week of the year, when the cold load on the thermal plant reaches its peak. Throughout this week, electricity consumption is the governing energy demand, primarily due to air conditioning and running the electric appliances in offices.

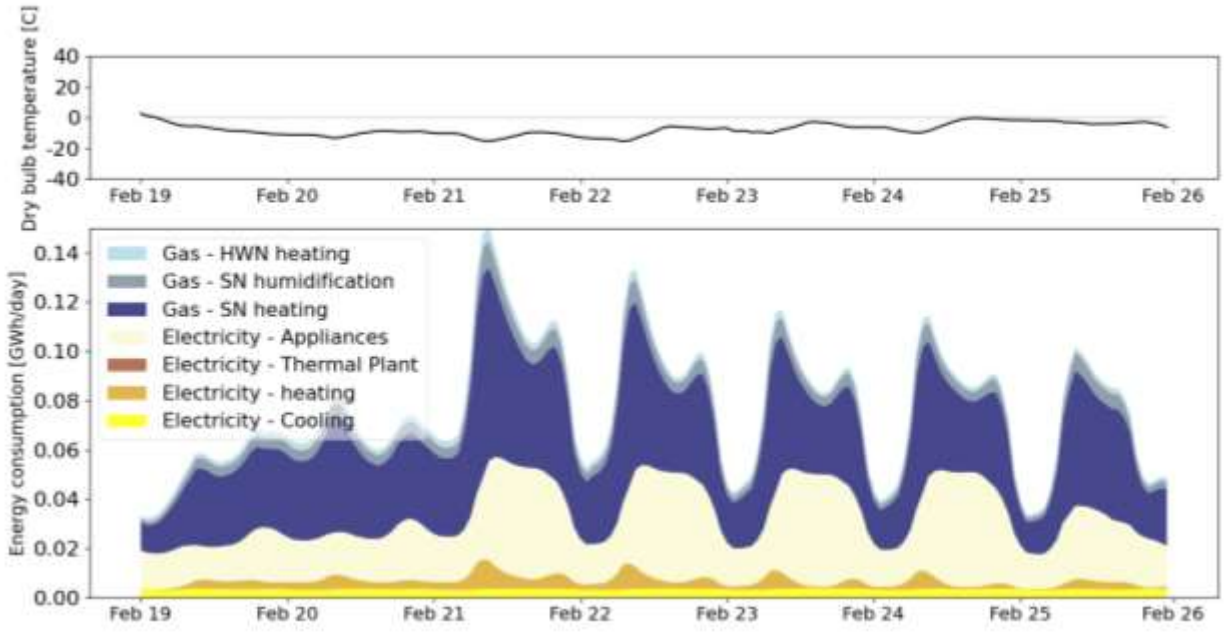

Figure 4.6: Dynamic energy profiles for a cold winter week.

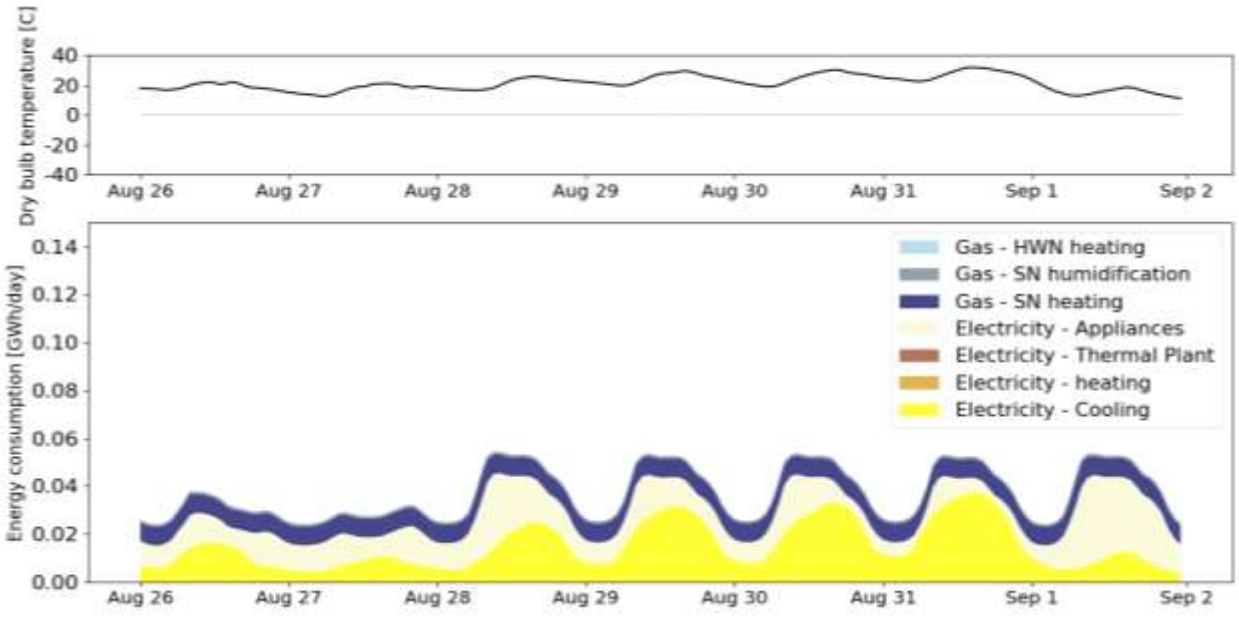

Figure 4.7: Dynamic energy profile for a hot summer week.

4.4.3 Results of pressure drop

This section investigates the consequence of steam pressure drop on the energy delivered to each facility. In Chapter 3, the heat demand of buildings connected to the steam network was determined based on the steam mass flow required and the available heat in steam, considering that the pressure drop in pipes is zero. Using the same methodology followed before with the maximum pressure drop in pipes mentioned in Table 4.2, the heat content in arriving steam was again calculated.

The maximum pressure drop occurs between November and March, when the pressure at the exit of the thermal plant is between 2816 and 1825 kPa, and the required mass flow rate of steam is at its highest. The steam arrives at each building block at a different pressure depending on its position and required mass flowrate. Table 4.7 details the maximum pressure drop at the end of each building block and the maximum percentage of variation in monthly thermal loads for buildings within this block. Note that these pressure drops are the maximum drops in the chosen piping system and were taken into account for the extreme operating conditions that could happen.

Table 4.7: Maximum pressure drop and corresponding variation in steam energy for each building block.

Block #id	**Maximum pressure drop [kPa]**	**Maximum rate of monthly thermal loads variation (%)**
a	441	0.3%
b	845	0.8%
c	619	0.5%
d	730	0.6%
e	773	0.5%
f	740	0.8%

Results show that the maximum variation in the thermal loads was always lower than 1%. This minimal variation is due to the fact that the calculated latent and sensible heat transfers vary inversely when the pressure varies. As pressure drops, the evaporation enthalpy increases, but the latent heat decreases. In fact, the enthalpy of saturated water decreases, which lowers the latent heat obtained after lowering the water temperature to 100 ℃ for condensate leaving the building. The two variations are mostly of the same order, leading to minor variations in total heat in the arriving steam.

Based on this observation, the thermal loads used to calibrate the building models were not modified from their values in Chapter 3.

4.5 Conclusion

The existing thermal networks were modelled using the hourly thermal load profiles determined in Chapter 3. Buildings connected to the steam network were divided into six blocks to simplify the modelling process of the network. On the other hand, buildings connected to the hot and cold water networks were modelled as one whole block. Then, the thermal loads and electricity consumption for each block were determined by summing the energy demands of buildings within that block. These blocks were then connected to the thermal plant via distribution piping networks. The energy consumption at the thermal plant was then calculated. The yearly gas consumption was approximately 233 GWh, and the total electricity consumption was estimated at 170 GWh for the whole site. The electricity demand was divided into several parts, including electricity consumed at the thermal plant, electricity consumed for appliances at the building's level, and electricity consumed for heating and cooling by each building’s induvial system.

The electricity consumed at the thermal plant is much higher in winter because of the need to pump more fluid into the system. Additionally, as expected, the gas and electricity consumption for heating purposes during the summer is negligible compared to winter. On the other hand, electricity for cooling is much higher during the hotter months.

The next chapter will use these results to set the base to which different decarbonization scenarios will be compared.

CHAPTER 5 DECARBONIZATION SCENARIOS

Three possible future scenarios are represented in this chapter. Each scenario studies the energy performance of the urban neighborhood as a whole (buildings connected to the current networks + new buildings in the Faubourgs neighborhood). The first scenario is the "Business As Usual" (BAU) scenario, which represents the future state of the city if no decarbonization actions are taken. The second scenario is the "Electrification" scenario, in which electric boilers and heat pumps are installed without expanding the existing district energy networks. The "District Energy Transition" scenario combines several solutions, including electrification, expanding the district energy networks, and transitioning buildings from steam to hot water heating.

5.1 Evolution of the Building stock

As discussed previously, this thesis looks at the buildings connected to the existing network, but it also considers the new buildings in the Faubourgs neighborhood. The additional floor area added to the current building stock is approximately 1.2 million square meters. In the absence of publicly confirmed dates for construction on the different sites, assumptions were made about the phasing of new building construction. Figure 5.1 shows the assumed building stock evolution over the 25 years period. Year 0 represents the base year of the study (2022). Years five, seven, and eight represent the beginning of the years in which the construction of the Faubourgs buildings will be completed and thus, they will be considered part of the study. All the buildings will be constructed from year nine, and no further change in the building stock will be made.

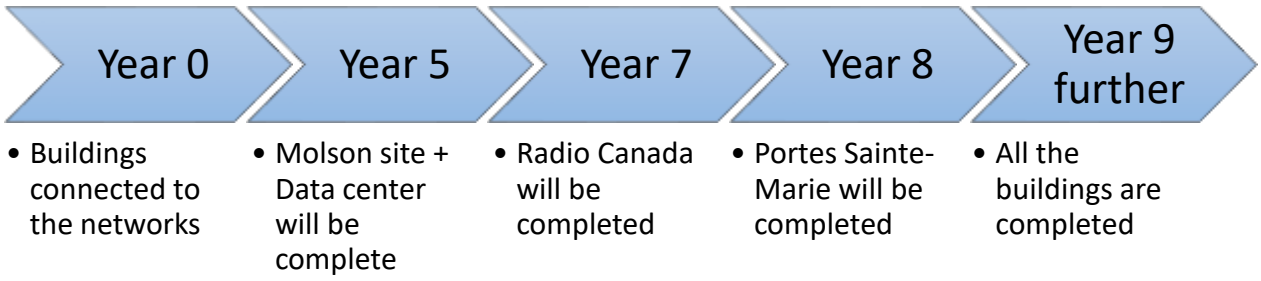

Figure 5.1: Building stock evolution.

5.2 BAU scenario

This scenario serves as the base case where no modification to the operational conditions of the thermal plant is made. This means that the required heating is provided mainly through the steam and hot water networks, using natural gas-fired boilers. Electric heating also contributes to approximately 6% of the total heat demand. Moreover, cooling demands are provided through the cold water network for six clients, whereas the remaining clients use individual cooling systems to fulfill their needs.

The newly constructed buildings in the Faubourgs neighborhood have their individual energy system, corresponding to a “non-decarbonized” Business As Usual scenario. According to the study on the neighborhood [1], a central gas system ensures hot water heating in each building with an overall efficiency of 80%. On the other hand, space heating is met by both electric and gas systems. Electric baseboards with 100% efficiency provide 30% of the total space heating demand of the buildings. The remaining 70% are ensured by a hybrid electric and gas system. Electric resistances provide up to 8.8 MW (30% of the peak heat demand), and a natural gas system provides the rest with an efficiency of 90%. This assumption corresponds to the traditional sizing in large Montréal buildings to limit power demand costs. Space cooling is assumed to be met using individual chillers with an average seasonal COP of 2.5 for the buildings and a COP of 4 for the data center. The data center has 12 MW of constant electric power for computer equipment and accessories and consumes 3 MW for cooling.

5.3 Electrification scenario

This second scenario combines partial electrification of the existing district energy system (without expanding it) with the electrification of the new buildings in the Faubourg neighborhood. In the central plant, several electric heat sources were used to reduce the use of gas-fired boilers. This transition is foreseen over three years. A heat pump “HP” is first employed to use the waste heat rejected by the cold water network and inject it into the hot water network. Then, two years later, an electric steam boiler of 35 MW is installed. No additional modifications will be made to the system from the fourth year forward.

The heat pump is sized only to provide the maximum heat recovered from the cold water network in order to limit the need for additional heat sources (such as sewage water, river, etc.). In case of

simultaneous demands on the hot and cold water networks, the HP extracts heat from the low-temperature return flow of the cold water network (at 15.6 ℃) and injects its output heat into the hot water network. The heat pump has a maximum power of 1.8 MW with an average yearly COP of 3.5 in heating [118]. In this study, the COP of the HP was assumed constant for simulation simplification even though it varies slightly over a year.

The electric steam boiler is intended to reduce gas use further. The load duration curve for clients connected to the steam network is represented in Figure 5.2. This graph shows the period when the heat demand exceeds a specific value. For example, although the peak demand reaches 88.8 MW, it barely occurs for a few hours a year; even a power above 60 MW is only required for 313 hours over the year: less than 4% of the time. Therefore, using an electric steam boiler with enough power to deliver 100% of the heat demand would be inefficient, especially since electricity consumed during peak demand is more expensive and carbon-intensive, as fossil backup generators are required.

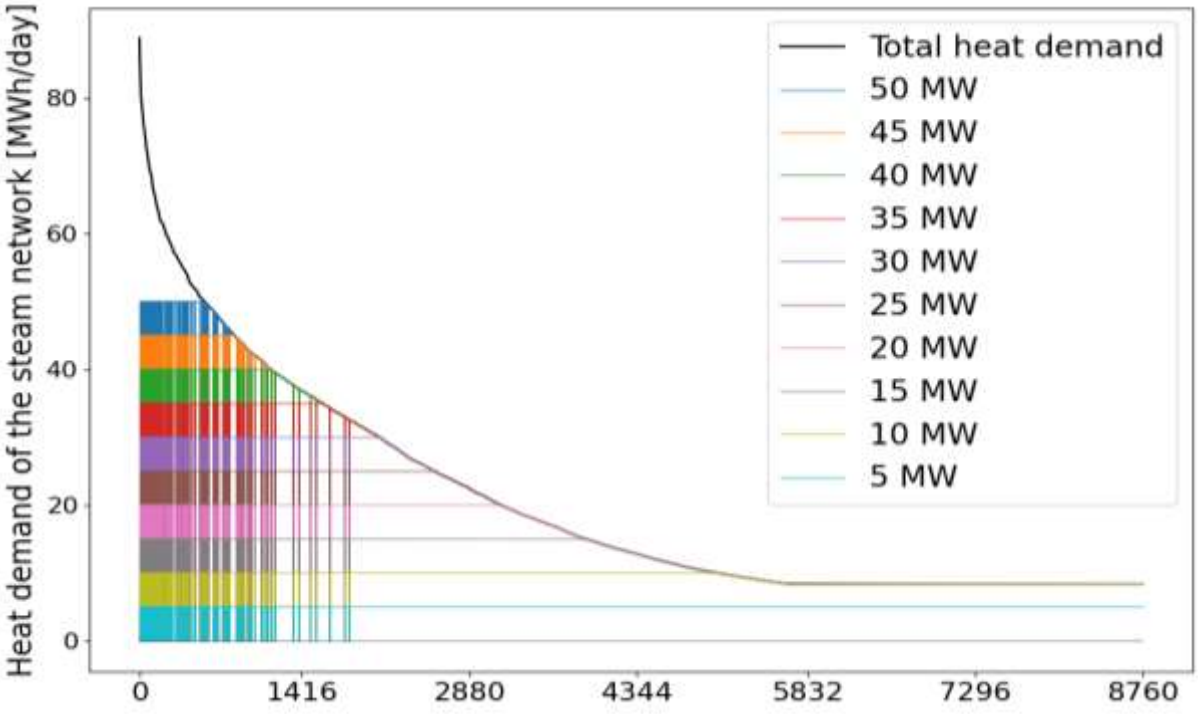

Figure 5.2: Different electric boiler integration possibilities.

Figure 5.2 also investigates the potential of installing a high-pressure electric steam boiler. Different boiler power ranging from 5 MW to 50 MW were studied. The boiler is intended to work only outside the peak electric demand hours. Hydro-Québec defines the peak hours as somewhere

between [6 AM, 9 AM] and [4 PM, 8 PM] from the 1st of December till the 31st of March. After analyzing the peak demand events registered by Hydro-Québec for 2020-2021, Bafrouei [119] found that the occurrence of these events can be approximated by selecting the periods when the outside temperature reached less than -12 ℃ during the specified peak hours. This method was used here to define "peak events" which are unknown for a typical weather year. The electric boiler was assumed to be switched off during peak events. The results of this policy are shown in Figure 5.2, as the produced heat from the electric boiler is set to zero when the conditions for peak events are met.

Table 5.1 details the contribution to heat demand for different boiler sizing. For example, a 5 MW boiler, even if it covers only 6% of the peak demand on the steam network, covers up to 24% of the total heat demand. The heat coverage from the electric boiler increases with the increase of the boiler power. Still, its contribution becomes less significant after a specific power since the peak demands occur only for a few hours a year. It is then inefficient and costly to install an electric boiler capable of delivering heat up to the maximum load. Therefore, a 35 MW electric steam boiler was introduced in year "3". Although the electric boiler can significantly lower the total heat demand required from the gas-fired boiler, the peak demand for the latter remains at 88.8 MW since the highest heat demand occurred during the peak hours on the electricity grid.

Table 5.1: Result of different HP power integration.

Electric boiler power MW	**Percentage of total heat demand**	**Percentage of peak heat demand**
5	24%	6%
10	45%	11%
15	57%	17%
20	67%	23%
25	74%	28%
30	80%	34%
35	85%	39%
40	88%	45%
45	91%	51%
50	92%	56%

The Faubourgs sector was also modelled to eliminate the gas heating system. All the heat demand for hot water production and space heating is provided using all-electric systems. Electric baseboards ensure the entire space heating with 100% efficiency, and hot water heating is provided through electric water heaters. The cooling equipment was not modified in this scenario since they are already electrified. A chiller of COP equal to 2.5 fulfills the space cooling demand of the neighborhood's buildings, and a chiller of COP equal to 4 satisfies the cooling load of the data center.

5.4 District Energy Transition scenario

The third scenario investigates the energy transition of the whole site relying on an expanded district energy system. First, the solutions mentioned in the Electrification scenario are also implemented for this plan. Later, starting in year 5, the Faubourgs' buildings and data center are connected to the hot and cold water networks as the construction is completed progressively. The steam buildings are transitioned towards hot water heating in several steps. These buildings are also connected to the cold water network to fulfill their cold demands instead of the current conventional cooling equipment.

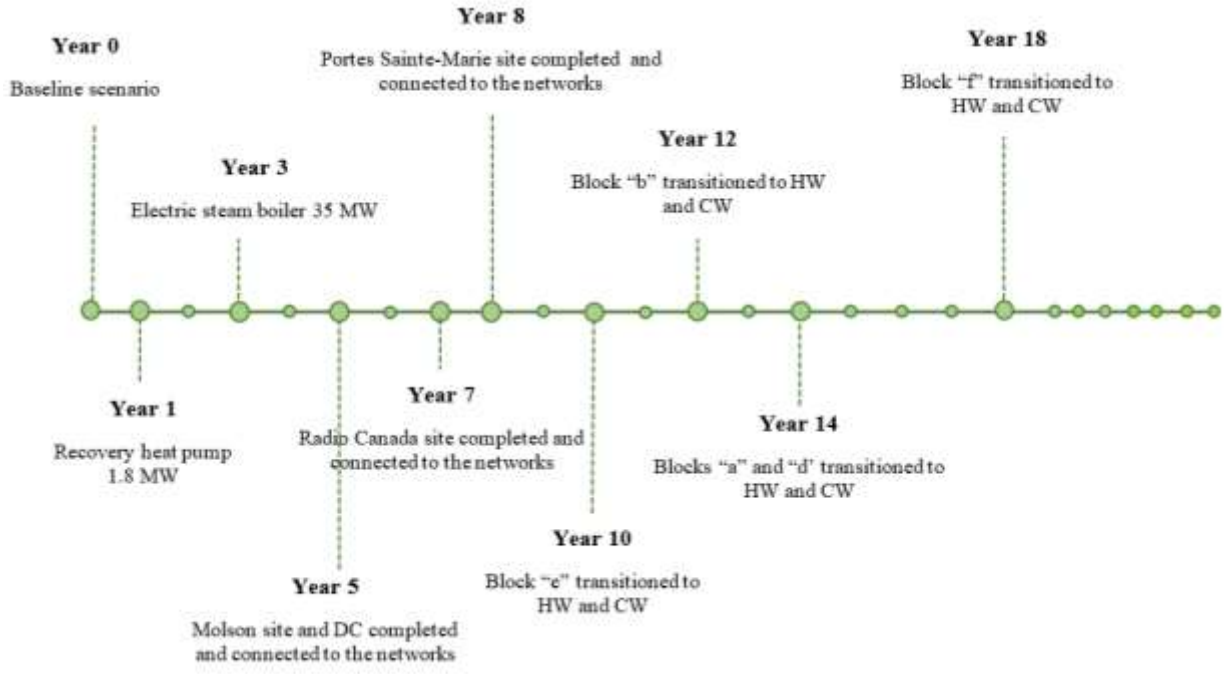

Figure 5.3: Decarbonization solutions over a 25-year timeline for the District Energy Transition scenario.

As shown in Figure 5.3, the scenario was simulated over a 25 year period. The Faubourgs buildings and data center connection is divided into three phases from the year “5” till the year “8”. Similarly, the transition of the steam buildings is performed over several years as buildings are gradually retrofitted, starting in the eighth year. As the buildings are transitioned from steam, their humidification needs are fulfilled by electric steam generators.

Starting the fifth year, the heat and cold loads of the hot and cold water networks are provided primarily by a water-source HP sized to meet 100% of the heating loads. The HP first collects rejected heat from the cooling network and then injects it into the hot water network. When the required heat demand is higher than that rejected, the HP extracts heat from the Saint-Laurent river. During summer, when the heat network requires smaller loads, the river is used as a heat sink to absorb the heat rejected from the cold network instead of liberating it into the ambient air. If the cold demand is higher than the HP capacity, the HP operates at full load, and the remaining cold is provided by high-efficiency chillers of COP equal to 4.

The river is a very suitable energy source, unfortunately still untapped despite an exceptional potential for the decarbonization of the Québec energy system. The large volume of water in the river enables extracting and rejecting heat without significantly changing the water temperature as relatively small amounts of heat are being used. According to the center of hydronic expertise of Québec [120], the minimum water flow in the river is approximately 5500 m^3/s. This flow rate was used to determine the maximum river’s temperature difference which is determined to be 0.003℃ [Appendix A].

5.4.1 Piping network evolution

Four new centralized hot and cold water loops are implemented to provide the heating and cooling loads. Two loops are defined for each site (Faubourgs and existing steam buildings). The new loops will be denoted by the Faubourgs, and the steam transition networks, respectively.

5.4.1.1 Faubourgs networks

The Faubourgs networks’ supply and return pipes are routed in the existing tunnel of the ÉCCU till Saint-Antoine Street W. The pipes are then directed along the street to reach the sites. Figure 5.4 represents the Faubourgs buildings and building blocks by site. It should be noted that the

piping network is not intended to represent the optimal DH and DC systems; instead, it provides an approximation of the network parameters and heat losses.

The maximum flow rates in the sub-branches connecting the main distribution pipes to the building blocks are determined using the peak loads of each block and the same ΔT used in section 4.2 (27.8 ℃ for heating and 15.6 ℃ for cooling).

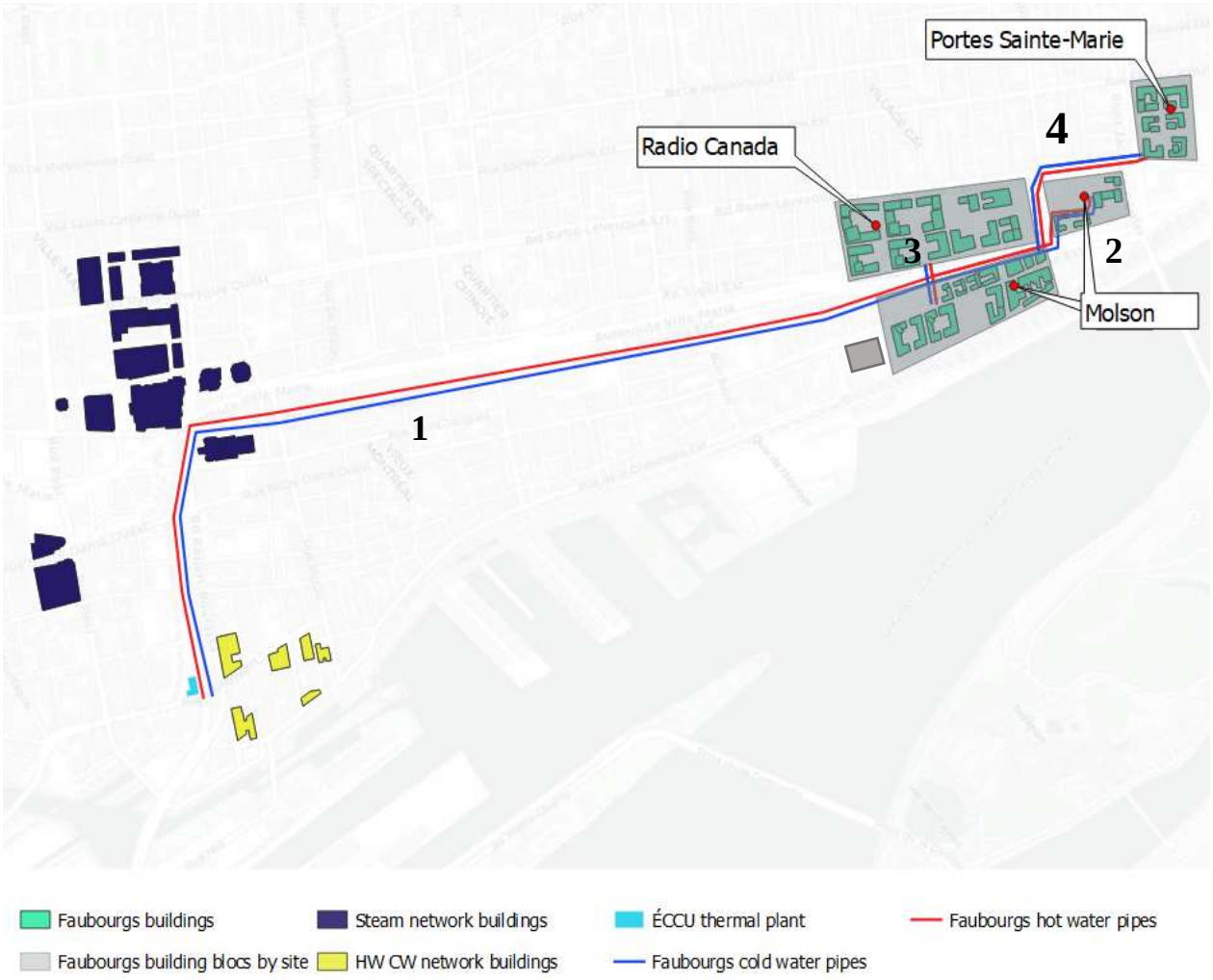

Figure 5.4: The Faubourgs sector connection to the hot and cold water networks. The map is rotated at a 50 degrees angle for display purposes.

The pipe diameters and the corresponding maximum pressure drops are represented in Table 5.2 for both networks. Given that the water delivers less energy per kg than steam, relatively large pipes were required to provide the same amount of heating loads. However, the large pipes might be problematic as the existing tunnel has limited space, and thus some enlargement projects might

be required. Again, the pipe sizes presented here are not meant to represent an actual optimized design but to provide a reasonable estimate of the piping losses and the dynamic behavior of the networks.

Table 5.2: Maximum heating and cooling loads for the three sites of the Faubourgs neighborhood and the data center and the corresponding selected pipes.

Pipe #id	**Pipe diameter DH [cm]**	**Maximum ΔP DH [Pa/m]**	**Pipe diameter DC [cm]**	**Maximum ΔP DC [Pa/m]**
1	54.2	166	71.0	163
2	45.6	199	71.0	100
3	41.0	145	45.6	191
4	36.4	137	45.6	191

5.4.1.2 Steam transition networks

The five transitional stages of the ÉCCU steam clients are distributed over ten years. At first, a new hot water piping network is installed parallel with the existing steam network. The steam buildings are then gradually retrofitted to hot water and connected to the water distribution system. Each other year, one building block is fully converted to hot water, and its steam equipment is removed. At the same time, each converted block is connected to the cold water network to provide its cooling needs. At the end of the transitional phase, the hot and cold water networks meet 100% of the heating and cooling loads (including those previously supplied by electric equipment). The steam network remains in operation until all the buildings are fully converted to hot water systems. This gradual transition of existing buildings from steam to hot water is similar to what is currently being planned for the Ottawa network serving 82 federal buildings [60].

Using the previous assumptions for ΔT and ΔP in both the hot and the cold water networks, the required diameters and corresponding ΔP are estimated. The extremely large pipes required do not account for possible mitigation measures such as building envelope retrofits that could happen at the same time or local storage to reduce peak demands. Again, they are intended to provide an estimate of piping losses for our model.

Table 5.3: The building blocks' maximum heating and cooling loads, corresponding pipes diameter, and maximum pressure drop.

Pipe #id	Pipe diameter DH [cm]	Maximum ΔP DH [Pa/m]	Pipe diameter DC [cm]	Maximum ΔP DC [Pa/m]
1	71.0	146	81.0	224
2	41.0	207	54.8	122
3	71.0	137	81.0	199
4	45.6	177	31.8	111
5	71.0	91	71.0	180
6	41.0	182	54.8	129
7	31.8	133	36.4	168
8	24.3	201	54.8	125
9	54.8	177	71.0	124

5.4.2 Thermal plant equipment

As more heat and cold demands are required from the hot and cold water networks at each phase, new equipment should be installed to fulfill all the thermal demands. The following section details the evolution in heat pump power and chiller power required.

Figure 5.5 details the HP and chiller thermal loads and their corresponding peak demands at each phase. The green bars represent the annual heat provided by the recovery from the cold water network, and the orange bars represent the remaining heat ensured by the river. The maximum heat loads of the HP are characterized by the green line. On the other hand, the cold demands are represented in negative values; the stacked bars represent the different cold sources: the heat pump

for recovery, the heat pump to/from the river, and the chiller. The negative lines represent the maximum cold demand provided by the heat pump and the chiller.

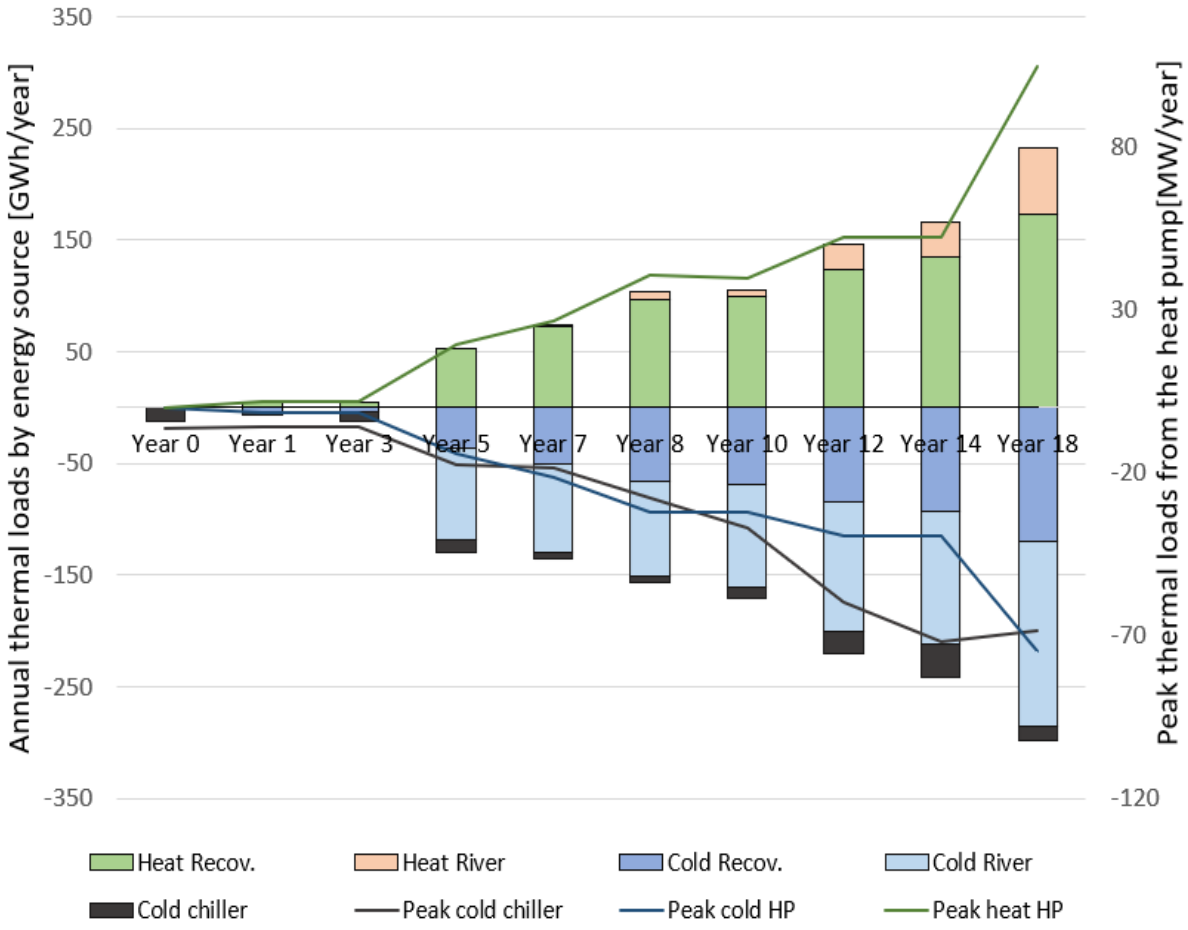

Figure 5.5: Evolution of the total thermal loads of the HP and chiller and corresponding peak demands.

A detailed look at the peak demands by each source is represented in Table 5.4. The base year ("year 0") comprises no heat pump; only the chiller provides 6.1 MW of cold to the six buildings connected to the cooling network. During the second year, denoted as "year 1", a heat pump of 1.8 MW power in heating recovers heat between the networks. The chiller's power remained at 6 MW as the peak demand occurred when the heating load on the hot water network was relatively small. No modifications to the hot and cold water network happened in the third year; the main change was performed to the steam network by adding the electric steam boiler.

The connection of the Molson site and the data center at the beginning of the fifth year allowed a very significant recovery potential between the networks. The 20 MW heat pump also provides

14.3 MW of cold, and the chiller ensures 17.4 MW of the cooling load. For similar reasons, the heat pump's heating capacity increases to 26.8 MW and 40.6 MW for years seven and eight, respectively. It should be noted that the eighth year also witnesses the transition of the block "c" to hot water heating. The chiller's power also increases to 18.5 and 27.6, respectively. Following the same pattern, the HP's and chiller's powers increase progressively at each phase of the plan as the remaining blocks are connected to the hot and cold water networks.

Table 5.4: Peak demands [MW] provided by the heat pump and the chiller.

Starting year	**Heat pump (heating)**	**Heat pump (cooling)**	**Chiller**
Year 0	0.0	0.0	6.1
Year 1	1.8	1.3	6.0
Year 3	1.8	1.3	6.0
Year 5	19.2	14.3	17.4
Year 7	26.8	21.4	18.5
Year 8	40.6	32.1	27.6
Year 10	40.6	32.1	37.0
Year 12	52.5	39.3	59.6
Year 14	52.5	39.3	72.0
Year 18	104.7	75.0	68.5

5.5 Results

5.5.1 Thermal load evolution of the hot and cold water networks

Figure 5.6 shows the evolution of the thermal loads of the hot and cold water networks over the 25 years. The stacked areas represent the progressive heating (positive) and cooling (negative) loads added at each phase; each phase is characterized by one color for both heating and cooling. The first five years represent the current network's demand without adding new clients. Then, the Faubourgs buildings and the ÉCCU steam buildings will be gradually added. The most prominent addition to the network is in the year "5" as it accounts for the most important cooling load due to the introduction of the data center to the cold water network. This addition greatly increases the potential of heat recovery between the two networks and thus results in a more efficient system.

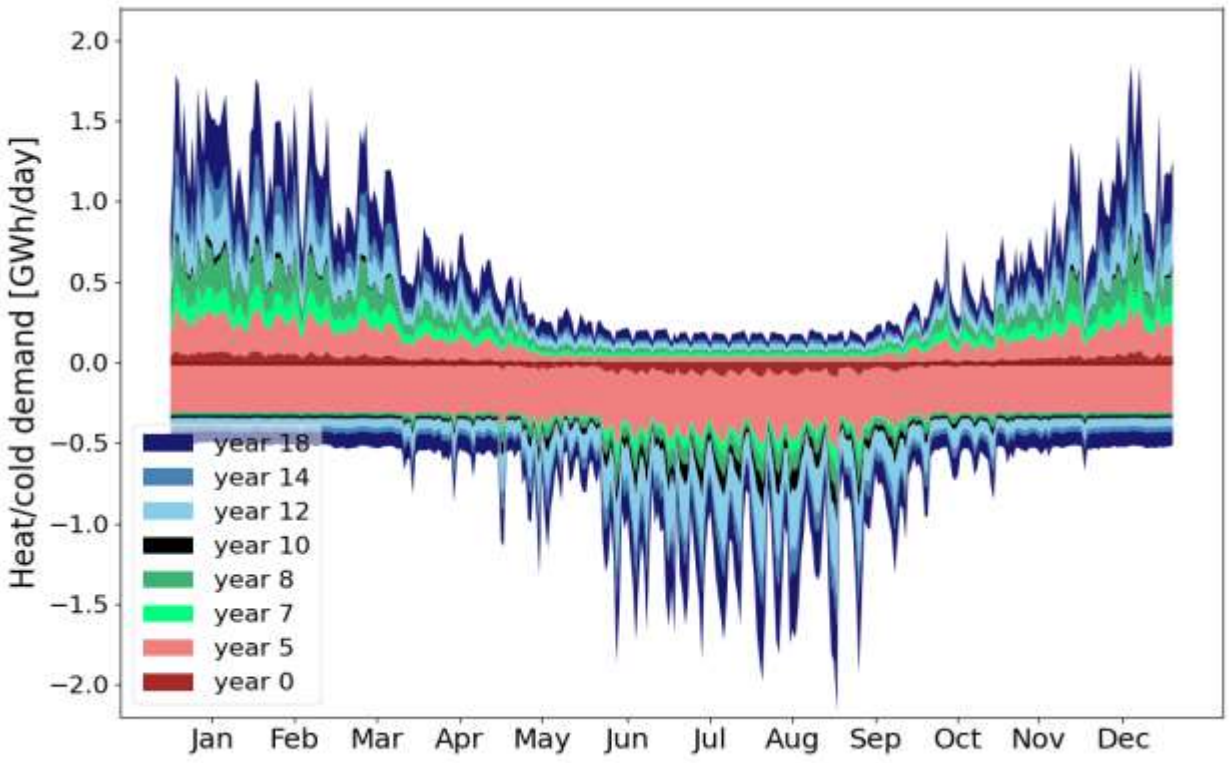

Figure 5.6: Thermal demand evolution for the hot and cold water networks – scenario #2.

5.5.2 Energy consumption

5.5.2.1 BAU scenario

The energy consumption over 25 years is determined by assuming that the energy demand is constant for the thermal plant and its buildings over the years. However, as the new Faubourgs buildings are completed in years 5, 7, and 8, the thermal and electric demands for the whole site (Existing thermal plant and its buildings + Faubourgs) increase consequently. The electricity consumed at the building level accounts for the electricity consumed for appliances, heating, and cooling within the buildings. The total energy consumption by the whole site over 25 years is represented in Figure 5.7.

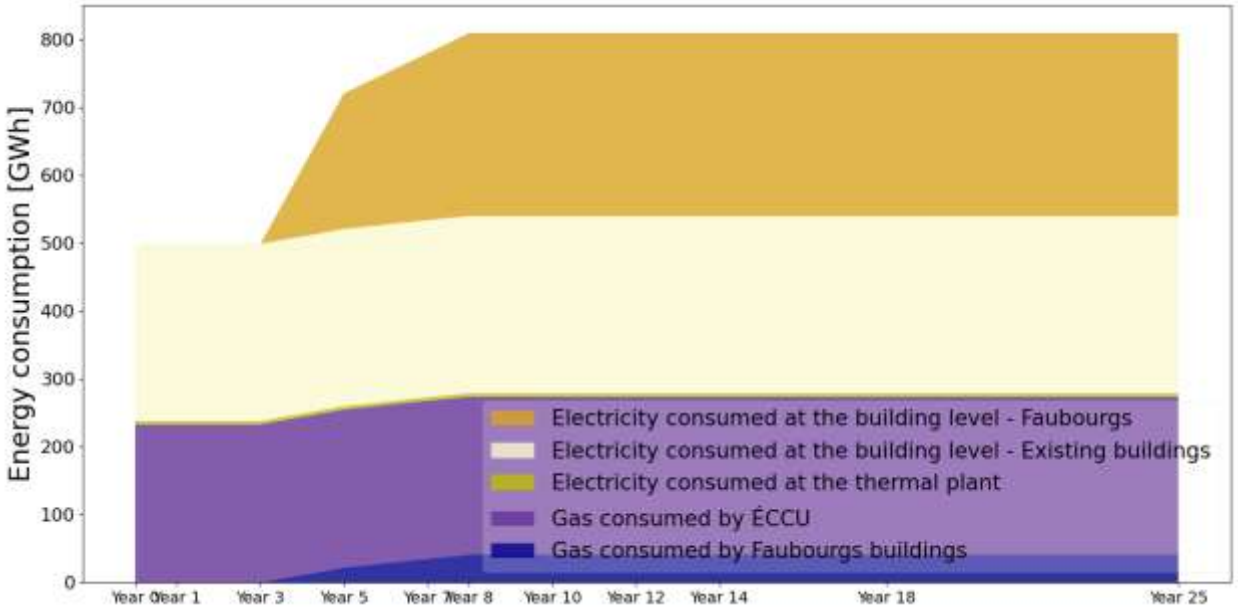

Figure 5.7: Energy demand for the whole site - BAU scenario.

5.5.2.2 Electrification scenario

The energy consumption over 25 years for the Electrification plan is represented in Figure 5.8. The gas consumption by the thermal plant decreases slightly in year 1, as the heat pump covers a fraction of the heating loads. Later, in year 3, this consumption decreases dramatically with the introduction of the electric steam boiler, which also explains the significant increase in electricity consumption at the thermal plant. The electricity consumption at the building level remains

constant over the period. On the other hand, the gas consumption for the Faubourgs buildings is zero as the electric system fulfills 100% of the heating demands.

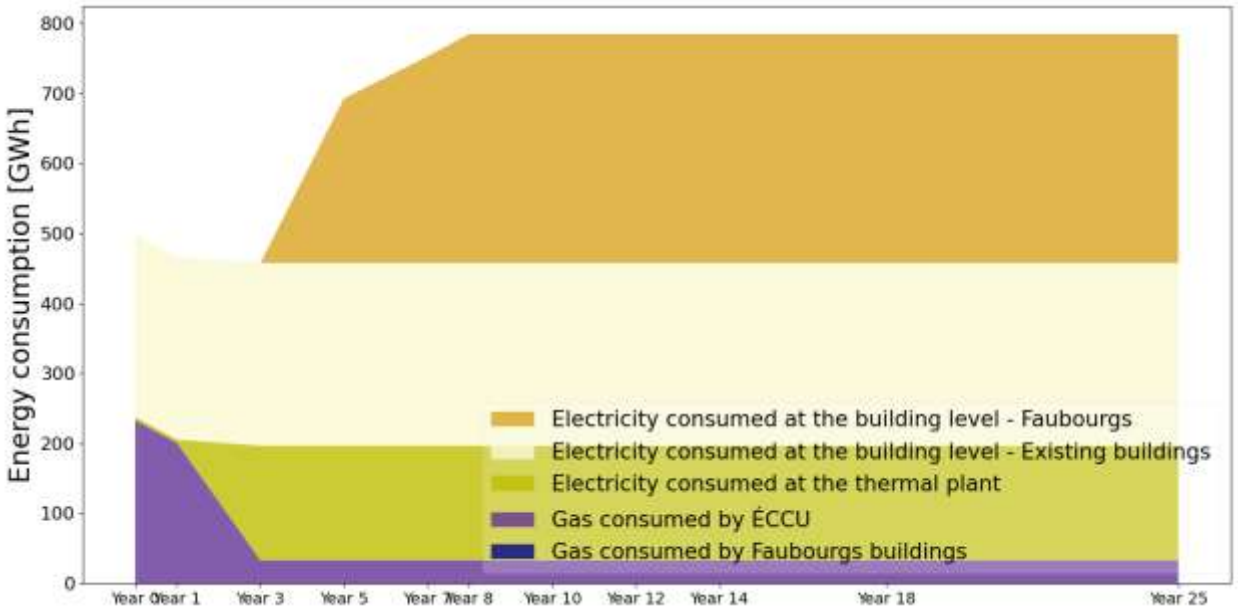

Figure 5.8: Energy demand for the whole site – Electrification scenario.

Details regarding the thermal loads per energy source will be presented Figure 5.9. As mentioned in section 5.3, the heat pump is installed to recover the heat between the hot and cold water networks; thus, the heat demand from the steam network is not affected by the HP. Areas in green represent the heat (positive) and cold (negative) that the HP can provide during simultaneous demands on both networks. Although the recovered heat does not fulfill 100% of the heat demand of the hot and cold water networks, it can provide up to 70% of the hot water network heat load and 35% of the cold water network cooling loads. At the thermal plant level, the HP covers only 3% of the heat loads. The blue area represents the cold demand covered by the existing chillers. On the other hand, the areas in orange and red represent the heat demands provided by the electric steam boiler and the gas-fired steam boiler, respectively.

The electric steam boiler plays the most significant role in decarbonizing the networks as it reduces the heat required from the gas-fired boiler by 81%. The electric boiler can fully replace the gas-fired steam boiler for 298 days, reducing the use period of the boiler by 82%. The proposed solutions in years “1” and “3” can replace the thermal plant for 166 days each year, resulting in over nine years of eliminating gas use over the 25 years period.

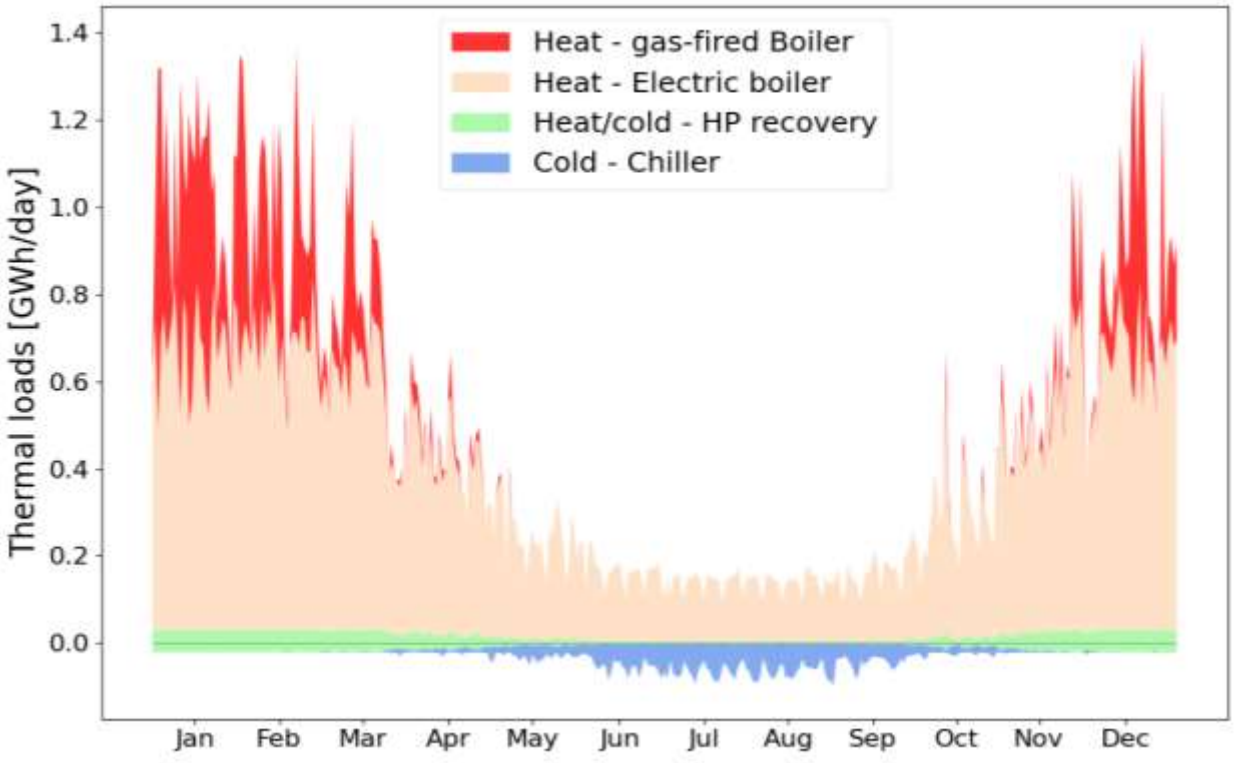

Figure 5.9: Total thermal energy by heat source in the first decarbonization scenario.

5.5.2.3 District Energy Transition scenario

The total energy consumption and thermal loads of the urban neighborhood are shown in Figure 5.10. The stacked blue and gray areas represent the yearly gas consumption for heating purposes for the Faubourgs area and the ÉCCU plant, respectively. The green area represents the electricity consumed at the thermal plant level. In the third year, the massive rise in electricity consumption results from installing the electric boiler, which plays a significant role in reducing gas consumption. An increase in electricity demand is noticed in the fifth year due to installing the 19.2 MW heat pump. The yellow area represents the electricity consumed at the building level for the existing buildings, including the electricity demand for supplementary heating and cooling purposes. This consumption decreases at each phase due to the drop in the total electricity consumed locally for heating and cooling.

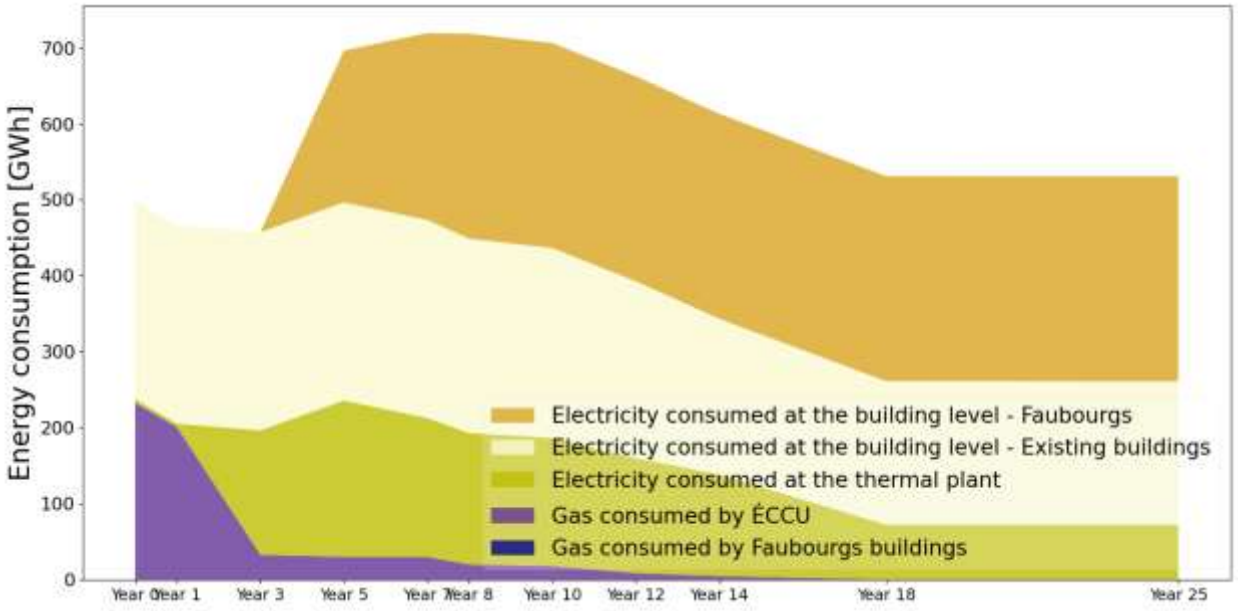

Figure 5.10: Energy demand for the whole site – District Energy Transition scenario.

5.5.2.4 Comparison between the three scenarios

Figure 5.11 compares the energy consumed by gas and electricity for the three scenarios over 25 years. Compared to the BAU scenario, the "Electrification" scenario consumes 80% less gas over the 25 years but uses 40% more electricity. When it comes to the total energy consumption, the "energy transition" scenario scored the lowest consumption, showing a decrease of 86% in gas demand and only a 17% increase in total electricity demand.

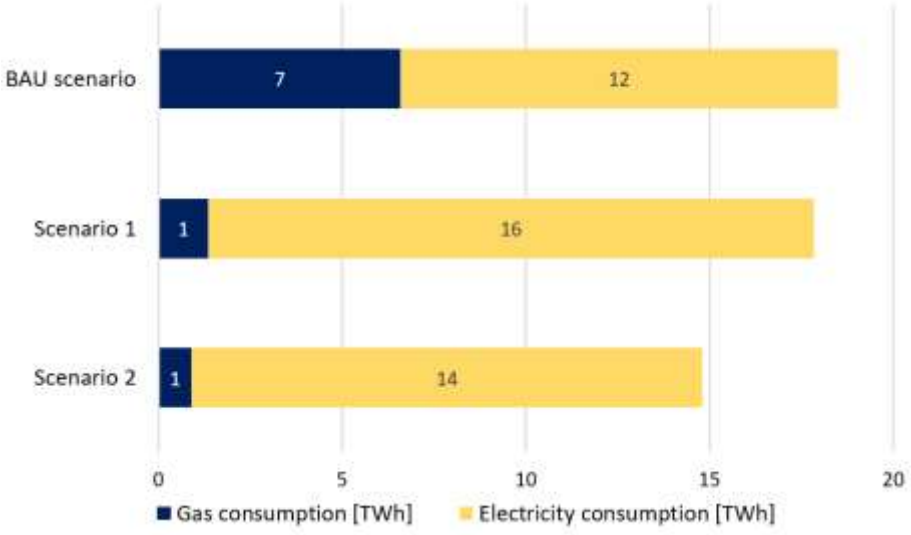

Figure 5.11: Energy consumption by energy source for the three scenarios over 25 years.

5.5.3 Electricity peak

Figure 5.12 shows the annual electric peak demands for the whole site (thermal plant and existing buildings + Faubourgs) at each phase of the scenarios. The Business As Usual scenario requires the lowest peak demand among the three scenarios (107 MW) because it relies on gas for most of the heating needs. The highest peak demand, on the other hand, occurs in the Electrification scenario. The installation of the electric steam boiler in the third year generates a significant increase in the electric peak demand. The peak demand increases even more during the following three years as the Faubourgs buildings and data center are gradually completed. As a result, the peak electric demand in year 8 is equal to 154 MW, and it persists for the whole period between the eighth year and the 25th.

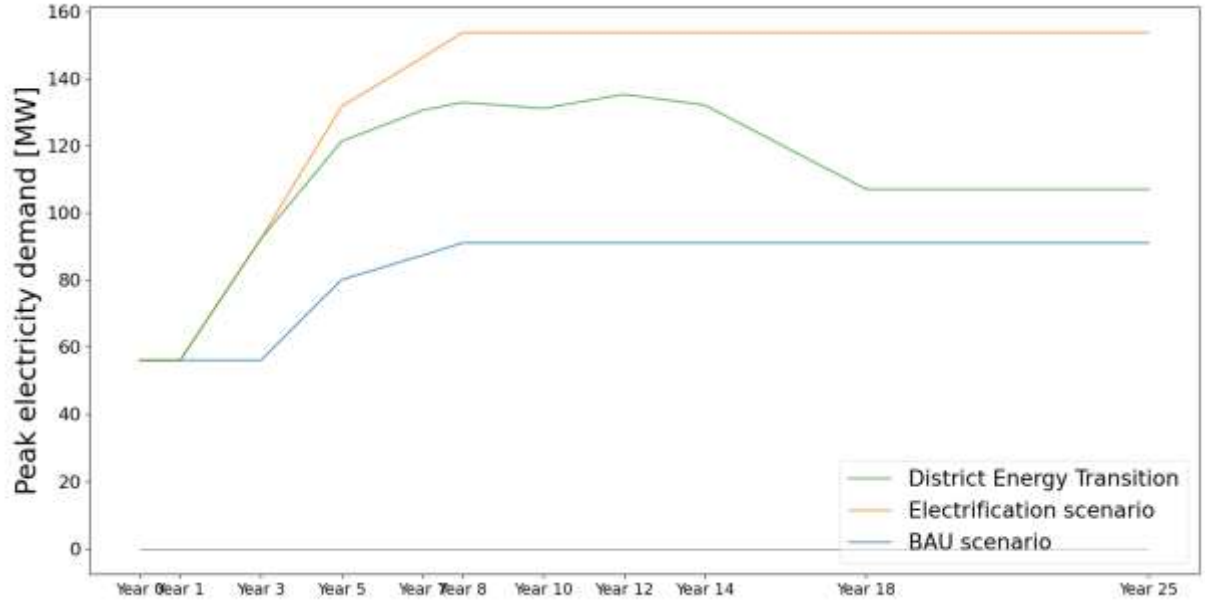

Figure 5.12: Peak electricity demand over the years for the whole site.

On the other hand, the District Energy Transition scenario presents the same electric demand peak for the first three years, as both scenarios assume the same actions on the existing thermal plant (heat pump and electric boiler). The peak demand for the following years is lower than for the Electrification scenario due to several reasons. First, for the years three through eight, the thermal loads for the Faubourgs buildings are fully fulfilled by networks with efficient heat pumps, resulting in lower electricity demand for heating and cooling. Later, as the existing buildings are retrofitted and converted to hot water heating and cold water cooling in the following years, the

heat pump recovers much more heat between the networks, operating with an increased combined COP. The more thermal loads are covered by the heat pump, the less are the electric boiler and chiller used; thus, the lower the electric demand. The electric peak reaches 135 MW in year 12, but decreases drastically after to 107 MW in the 18th year due to higher use of efficient heat pumps.

5.5.4 GHG emissions

CO_2 emissions related to energy use for the BAU scenario are estimated to be 1208 kt $CO_{2,\,eq}$ over 25 years. The most significant contribution to GHG emissions comes from the buildings connected to the steam network, as they account for the largest share of heat demand covered by gas-fired boilers. On the other hand, CO_2 emissions for the "electrification" scenario equal 277 kt $CO_{2,\,eq}$, 77% less than the BAU scenario. Lastly, the emissions produced during 25 years for the "district energy transition" scenario are estimated to be 189 kt $CO_{2,\,eq}$, 84% less than the BAU scenario.

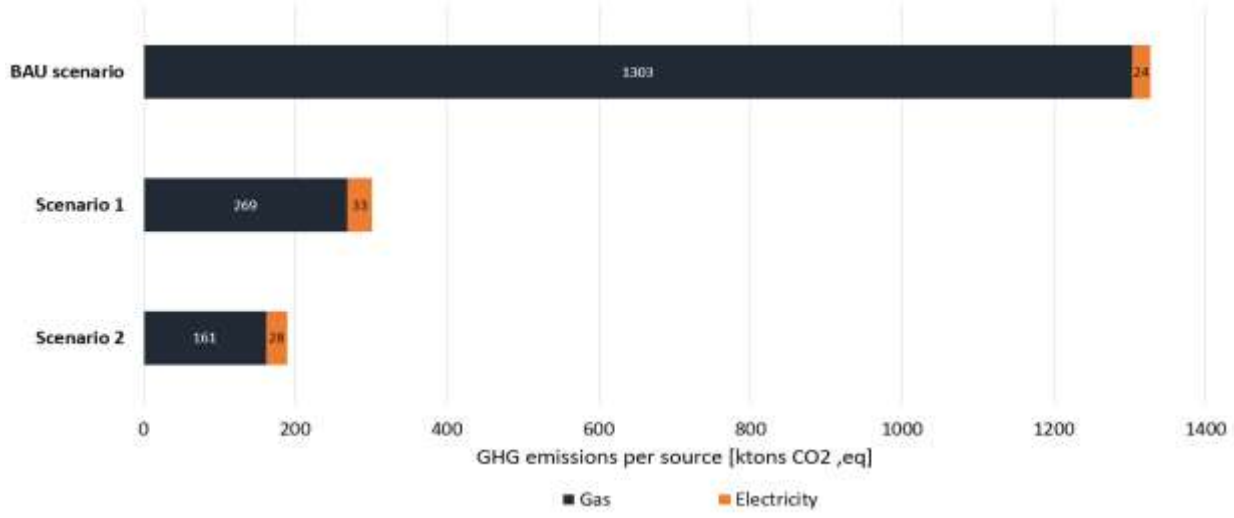

Figure 5.13: GHG emissions comparison over 20 years between the three scenarios.

Figure 5.14 shows the variation of emissions at each phase of the three scenarios. The most dramatic reduction in CO_2 emissions is in the third year, when the electric steam boiler replaces the gas-fired steam boiler 82% of the time. The completion of new Faubourgs buildings increased the emissions by 15% for the BAU scenario and by 9% for the electrification scenario. However, the emissions were reduced by 35% in the District Energy Transition scenario, as the completed Faubourgs buildings were connected to the networks instead of using a conventional energy system. The continuous reduction in CO_2 emissions in the District Energy Transition scenario is due to a lower load ensured by the steam network at each phase and, thus, a lower gas consumption.

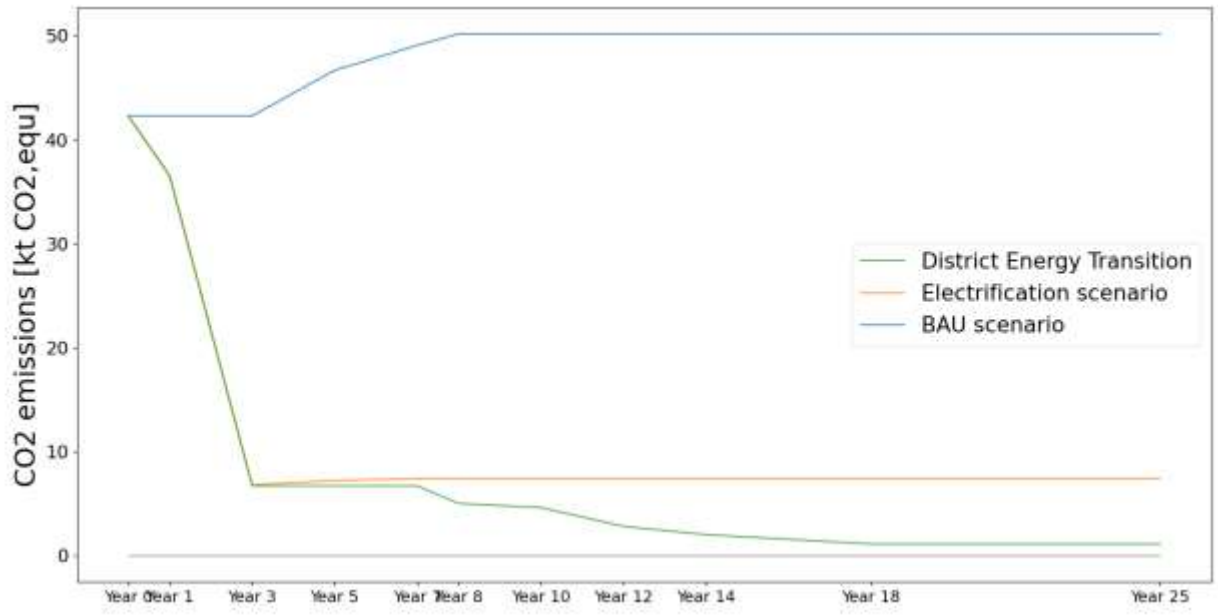

Figure 5.14: GHG emissions comparison at each phase between the three scenarios.

5.6 Conclusion

This chapter discussed three potential future scenarios for a growing neighborhood in Montréal. The study found that if no actions are taken to mitigate the use of natural gas in energy systems, the released GHG emissions can reach 1.2 million tonnes of $CO_{2,\,equ}$, released into the environment (BAU scenario) by 2047. Partial electrification of the existing thermal plant combined with full electrification of the new buildings can reduce these emissions by 77% (Electrification scenario). The last scenario relies on integrating the new buildings into the existing district energy system, combined with the electrification of the thermal plant and conversion of existing buildings from steam to hot water heating. This District energy Transition scenario maximizes the synergies between heat and cold demands and the use of efficient heat pumps. It results in reducing the GHG emissions by 84 %, going slightly further than the Electrification scenario.

Although both scenarios are successful in terms of reducing GHG emissions, the Electrification scenario results in a very large electrical peak demand for the thermal plant and the individual energy systems of the new buildings. The electric peak is increased from 91 MW in the BAU scenario to 154 MW (70% increase), required for 17 years out of 25. On the other hand, the peak electric demand for the District Energy Transition scenario reaches 107 MW for years 18 and

beyond, after requiring a higher peak demand (up to 140 MW) for a few years during the transition of existing buildings from steam to hot water heating.

CHAPTER 6 GENERAL DISCUSSION AND CONCLUSION

6.1 Thesis contributions and main results

Previous efforts to decarbonize district energy systems (DES) have focused on modern DES using hot water as the heat carrier fluid. However, the literature on decarbonizing existing steam-based DES or building on the existing networks to transition toward decarbonized cities is scarce. This thesis presents a study that assesses such a *District Energy Transition* scenario and compares it to a *Business as usual* future and to an *Electrification* scenario that considers the existing network and new buildings separately. The study presented here is also original in that it combines modelling the existing and new buildings in EnergyPlus to obtain detailed hourly heating and cooling loads with a TRNSYS model of the networks and the thermal plant.

The buildings included in this study comprise existing buildings already connected to a DES and newly constructed buildings, including a 12 MW data center. The current DES comprises three district networks: a steam-based, a hot-water-based, and a cold-water-based network.

In Chapter 3, the modelling methodology of the existing buildings is addressed. Building archetypes developed by the United States Department of Energy are used to assess the community thermal and electric loads. These archetypes are calibrated with measured data for 2019 provided by Énergir Chauffage et Climatisation Urbaines (ÉCCU), the company operating the existing networks. Further calibration relied on the billed electricity power supplied for some buildings. Archetypes selected and adapted in a previous study are re-simulated using an appropriate weather file to model the newly built area.

The detailed methodology for modelling the existing DES is represented in Chapter 4. The three networks are modelled separately. First, the steam network is modelled by conceptualizing six building blocks comprising the 14 clients of the steam network. Then, the blocks are connected to the thermal plant using steam pipes, condensate pipes, and steam traps. The hot and cold water networks are modelled as two loops consisting of two pipes each, serving one building block comprising the six buildings connected to the hot and cold water networks. In the absence of actual design data, all networks are modelled based on engineering assumptions found in the literature and a simplified layout to obtain a reasonable estimation of thermal losses and dynamic behavior. The DES energy consumption and GHG emissions are calculated for a typical meteorological year.

The GHG emissions are compared to the average annual emissions declared by the company over the past ten years, and the error is as low as 1.5%.

The main focus of this work is to determine decarbonization scenarios for the whole site. Therefore, three future scenarios are considered in Chapter 5. The first scenario consists of the *Business as usual* scenario, where no modernization to the existing DES is performed, and the new buildings are equipped with individual energy systems corresponding to a "non-decarbonized" scenario. The second scenario is the *Electrification* scenario, where the existing network and the new buildings are decarbonized separately. In the existing DES, a heat pump is added to recover waste heat from the cold water network to the hot water network, and a 35 MW electric steam boiler is installed. On the other hand, the new buildings use a fully electric system to provide their thermal demands. The last scenario is the *District Energy Transition* scenario, which considers expanding the existing DES to the new buildings and decarbonizing the urban energy system as a whole. In this scenario, the existing buildings currently connected to the steam network are modernized and converted gradually to hot water heating, and they are also connected to the cold water network. An electric steam boiler is used during the transition phase until all buildings are converted. Heat pumps are used to provide heating and cooling to the hot and cold water networks through recovery between the two networks and by using the Saint-Laurent river as an additional heat source/sink.

Results show that both the *Electrification* and the *District Energy Transition* scenarios achieve very significant reductions in GHG emissions over a 25-year period, respectively of 77% and 84%. The main difference in the energy performance is that the *Electrification* scenario results in a much larger electrical peak demand, which is increased by 70 % over the *Business as usual*, while the *District Energy Transition* scenario only increases the peak electrical demand by 17% after temporarily imposing a higher peak during the gradual energy transition. This confirms that the existing DES in Montréal, while currently representing a major GHG source, can become an asset in transforming the city towards a carbon-free future.

6.2 Limitations and suggestions for future work

This thesis makes no attempt to quantify the economic aspects of different scenarios. The network piping layout and sizing are approximated, and a more detailed design study would be required to perform a techno-economic comparison between the scenarios. Some pipe dimensions used in our

analysis are probably overestimated, and local storage could be used to reduce the peak thermal demands if a detailed study would confirm these sizes.

The transition of existing buildings from steam to hot water is realistic, as shown by the current project in Ottawa [60], but would have significant cost implications. Other measures (e.g. envelope retrofit) could be implemented at the same time, potentially resulting in cost-saving synergies.

The Faubourgs neighborhood study [1] assesses other potential benefits of DES, such as avoiding heat rejection from air-source chillers (reducing urban heat island effects) and limiting distributed air-conditioning systems with GHG-intensive refrigerants. These benefits have not been considered in this study. However, they would contribute to a better assessment of the decarbonization potential of the investigated scenarios, and give a broader picture of their contribution to urban resilience.

REFERENCES

[1] Ecohabitation, “Infrastructure resiliente et carboneutre pour Montréal, arrondissement Ville-Marie, secteur des Faubourgs,” Nov. 2019. [Online]. Available: https://ocpm.qc.ca/sites/ocpm.qc.ca/files/pdf/P109/3.4.3_rapport_reseauthermique_faubourgs_2019vf.pdf

[2] Canada and Environment and Climate Change Canada, *Pan-Canadian framework on clean growth and climate change: canada’s plan to address climate change and grow the economy*. 2016. Accessed: May 29, 2022. [Online]. Available: http://www.deslibris.ca/ID/10065393

[3] Government of Canada, “Homes and buildings,” Feb. 2021.

[4] J. Whitmore and P.-O. Pineau, “The state of energy in Quebec.” HEC Montréal, 2019.

[5] C40, “C40 Cities - A global network of mayors taking urgent action to confront the climate crisis and create a future where everyone can thrive.” https://www.c40.org/ (accessed Jun. 04, 2022).

[6] Ville de Montréal, *Plan climat 2020–2030*. Montréal, QC: Ville de Montréal, 2020. [Online]. Available: https://montreal.ca/articles/plan-climat-montreal-objectif-carboneutralite-dici-2050-7613

[7] L. Riahi, “District energy in cities, unlocking the potential of energy efficiency and renewable energy,” United Nations Environment Programme, 2015.

[8] D. Woodson, J. Giffin, P. Holt, J. Torcov, J. Wauthy, and A. Mogerman, “The Evolution of Low Carbon District Energy and Innovative Solutions at University of British Columbia,” *IDEA MAIN Conf.*, p. 65, Jun. 2018.

[9] Pollution probe, “What Does the Future Hold for Natural Gas?,” Pollution Probe, Toronto, ON, Nov. 2019. [Online]. Available: https://www.pollutionprobe.org/

[10] C. Marguerite, R. Geyer, D. Hangartner, M. Lindahl, and S. V. Pedersen, “Heat Pumps in District Heating and Cooling Systems,” p. 56, Mar. 2019.

[11] G. Schweiger, J. Rantzer, K. Ericsson, and P. Lauenburg, “The potential of power-to-heat in Swedish district heating systems,” *Energy*, vol. 137, pp. 661–669, Oct. 2017, doi: 10.1016/j.energy.2017.02.075.

[12] J. Barco-Burgos, J. C. Bruno, U. Eicker, A. L. Saldaña-Robles, and V. Alcántar-Camarena, “Review on the integration of high-temperature heat pumps in district heating and cooling networks,” *Energy*, vol. 239, p. 122378, Jan. 2022, doi: 10.1016/j.energy.2021.122378.

[13] “District energy guide.” American society of Heating, refrigerating and Air-Conditionning Engineers, 2013.

[14] M. A. Pierce, “Competition and Cooperation: The Growth of District Heating and Cooling, 1882:1917,” *Int. Dist. Heat. Cool. Assoc.*, p. 12.

[15] S. Werner, “International review of district heating and cooling,” *Energy*, vol. 137, pp. 617–631, Oct. 2017, doi: 10.1016/j.energy.2017.04.045.

[16] H. Lund *et al.*, “4th Generation District Heating (4GDH),” *Energy*, vol. 68, pp. 1–11, Apr. 2014, doi: 10.1016/j.energy.2014.02.089.

[17] J. E. Thorsen, O. Gudmundsson, and M. Brand, “Distribution of district heating: 1st generation.” Danfoss District Heating Application Centre, Sep. 19, 2016. Accessed: May 26, 2022. [Online]. Available: https://www.linkedin.com/pulse/distribution-district-heating-1st-generation-oddgeir-gudmundsson/?trk=pulse_spock-articles

[18] S. Werner, “District heating and cooling in Sweden,” *Energy*, vol. 126, pp. 419–429, May 2017, doi: 10.1016/j.energy.2017.03.052.

[19] P. A. Østergaard *et al.*, “The four generations of district cooling - A categorization of the development in district cooling from origin to future prospect,” *Energy*, vol. 253, p. 124098, Aug. 2022, doi: 10.1016/j.energy.2022.124098.

[20] A. McL. Hawks, “The Colorado Automatic Refrigerator System at Denver, Colo.,” *Trans. Am. Soc. Civ. Eng.*, vol. 24, no. 1, pp. 389–392, Jan. 1891, doi: 10.1061/TACEAT.0000790.

[21] B. Dwyer, “A Look Back: Tony Mirabella on TEN’s 40 Years of Growth,” *Ten Co. Inc*, vol. Second Quarter 2003, no. Issue 2, p. 6.

[22] Bernoulli system, “Case-story_district-cooling la defense.pdf.” Bernoulli System AB. [Online]. Available: https://bernoulli.se/wp-content/uploads/2020/06/Case-story_district-cooling.pdf

[23] Low Carbon Design & Research Institute, “District energy systems development roadmap study in APEC economies.” APEC Energy Working Group, Mar. 2015.

[24] Asian Development Bank, “District Cooling in the People’s Republic of China: Status and Development Potential,” Asian Development Bank, Jan. 2017. doi: 10.22617/RPT168582-2.

[25] M. Jangsten, “Gothenburg District Cooling System,” Degree of licentiate of engineering thesis, Chalmers University of Technology, Gothenburg, Sweden, 2020. [Online]. Available: https://www.researchgate.net/publication/340692480_Gothenburg_District_Cooling_System_-_An_evaluation_of_the_system_performance_based_on_operational_data

[26] V. Heffernan, “TORONTO WATERFRONT: Toronto Cools Off Naturally – A Deep Lake Water Cooling System,” *Canadian consulting engineer*. https://www.canadianconsultingengineer.com/features/toronto-waterfront-toronto-cools-off-naturally-a-deep-lake-water-cooling-system/ (accessed May 26, 2022).

[27] J. Sipila, “District cooling in Helsinki – The Most Advanced Cooling Solutions.” Helsigin Energia.

[28] M. Thyholt and A. G. Hestnes, “Heat supply to low-energy buildings in district heating areas,” *Energy Build.*, vol. 40, no. 2, pp. 131–139, Jan. 2008, doi: 10.1016/j.enbuild.2007.01.016.

[29] H. Lund *et al.*, “The status of 4th generation district heating: Research and results,” *Energy*, vol. 164, pp. 147–159, Dec. 2018, doi: 10.1016/j.energy.2018.08.206.

[30] S. Buffa, A. Soppelsa, M. Pipiciello, G. Henze, and R. Fedrizzi, “Fifth-Generation District Heating and Cooling Substations: Demand Response with Artificial Neural Network-Based

Model Predictive Control," *Energies*, vol. 13, no. 17, p. 4339, Aug. 2020, doi: 10.3390/en13174339.

[31] H. Lund *et al.*, "Perspectives on fourth and fifth generation district heating," *Energy*, vol. 227, p. 120520, Jul. 2021, doi: 10.1016/j.energy.2021.120520.

[32] S. Buffa, M. Cozzini, M. D'Antoni, M. Baratieri, and R. Fedrizzi, "5th generation district heating and cooling systems: A review of existing cases in Europe," *Renew. Sustain. Energy Rev.*, vol. 104, pp. 504–522, Apr. 2019, doi: 10.1016/j.rser.2018.12.059.

[33] J. von Rhein, G. P. Henze, N. Long, and Y. Fu, "Development of a topology analysis tool for fifth-generation district heating and cooling networks," *Energy Convers. Manag.*, vol. 196, pp. 705–716, Sep. 2019, doi: 10.1016/j.enconman.2019.05.066.

[34] D. Azhgaliyeva, "Energy Storage and Renewable Energy Deployment: Empirical Evidence from OECD countries," *Energy Procedia*, vol. 158, pp. 3647–3651, Feb. 2019, doi: 10.1016/j.egypro.2019.01.897.

[35] H. Lund and B. V. Mathiesen, "Energy system analysis of 100% renewable energy systems—The case of Denmark in years 2030 and 2050," *Energy*, vol. 34, no. 5, pp. 524–531, May 2009, doi: 10.1016/j.energy.2008.04.003.

[36] B. Sibbitt *et al.*, "The Performance of a High Solar Fraction Seasonal Storage District Heating System – Five Years of Operation," *Energy Procedia*, vol. 30, pp. 856–865, 2012, doi: 10.1016/j.egypro.2012.11.097.

[37] P. A. Østergaard and H. Lund, "A renewable energy system in Frederikshavn using low-temperature geothermal energy for district heating," *Appl. Energy*, vol. 88, no. 2, pp. 479–487, Feb. 2011, doi: 10.1016/j.apenergy.2010.03.018.

[38] R. Ismaen, T. Y. ElMekkawy, S. Pokharel, A. Elomri, and M. Al-Salem, "Solar Technology and District Cooling System in a Hot Climate Regions: Optimal Configuration and Technology Selection," *Energies*, vol. 15, no. 7, p. 2657, Apr. 2022, doi: 10.3390/en15072657.

[39] E. Loewen, "TransformTo Steps: Lake Ontario points to the future of district energy," *TAF*, Apr. 05, 2018. https://taf.ca/low-carbon-solutions-lake-ontario-future-district-energy/ (accessed May 26, 2022).

[40] "Lake source cooling," *Cornell university*, May 10, 2017. https://medium.com/cornell-university/lake-source-cooling-d307913dfc47

[41] Cornell university, "Cooling production home," *Cornell university faculties and campus serevices*. https://fcs.cornell.edu/departments/energy-sustainability/utilities/cooling-home/cooling-production (accessed May 25, 2022).

[42] Celsius, "The river provides indoors cooling," Nov. 19, 2019. http://celsiuscity.eu/the-river-provides-indoors-cooling/

[43] CLUES WP 5, "Seawater heating system." University College London. [Online]. Available: https://www.ucl.ac.uk/clues/sites/clues/files/hague.pdf

[44] MBS Modern Building Services, "River Thames is heat source for apartment development," Nov. 01, 2013. https://modbs.co.uk/news/fullstory.php/aid/12563/River_Thames_is_heat_source__for_apa

rtment_development.html#:~:text=Down%20at%20Kingston%20upon%20Thames,has%20been%20finding%20out%20more.

[45] A. Lyden, "Viability of river source heat pumps for district heating," Master of Science thesis, University of Strathclyde engineering, 2015.

[46] A. David, B. V. Mathiesen, H. Averfalk, S. Werner, and H. Lund, "Heat Roadmap Europe: Large-Scale Electric Heat Pumps in District Heating Systems," *Energies*, vol. 10, no. 4, p. 578, Apr. 2017, doi: 10.3390/en10040578.

[47] Celsius, "Free cooling from water," 2019. https://celsiuscity.eu/free-cooling-from-water/ (accessed May 28, 2022).

[48] E. Falk, "Heat recovery from district cooling," Master of Science thesis, Faculty of Engineering | Lund University, Lund, Sweden, 2019. [Online]. Available: http://lup.lub.lu.se/student-papers/record/9006790

[49] I. G. Moghaddam, M. Saniei, and E. Mashhour, "A comprehensive model for self-scheduling an energy hub to supply cooling, heating and electrical demands of a building," *Energy*, vol. 94, pp. 157–170, Jan. 2016, doi: 10.1016/j.energy.2015.10.137.

[50] H. Ahmadisedigh and L. Gosselin, "Combined heating and cooling networks with waste heat recovery based on energy hub concept," *Appl. Energy*, vol. 253, p. 113495, Nov. 2019, doi: 10.1016/j.apenergy.2019.113495.

[51] O. Hyde-Keller, "Brown launches three-year, $24 million project to boost thermal efficiency," Nov. 28, 2017. https://www.brown.edu/news/2017-11-28/thermal#:~:text=Conversion%20from%20steam%20to%20hot,in%20the%20central%20heating%20plant (accessed May 29, 2022).

[52] J. Ewin, "Strategically transitioning from steam to hot water," presented at the IDEA 2019, The Energy For More Resilient Cities, Pittsburgh, PA, Aug. 21, 2017. [Online]. Available: https://www.districtenergy.org/idea2019/viewdocument/strategically-transitioning-from-st

[53] I. Oliker, "How Modern Hot Water Systems Can Lower Campus Energy Use." Joseph technology Corp., Jul. 31, 2019. Accessed: May 13, 2022. [Online]. Available: https://www.hpac.com/heating/article/20929899/how-modern-hot-water-systems-can-lower-campus-energy-use

[54] "Hot water district energy system," *UBC's energy and water infrastructure*. https://energy.ubc.ca/ubcs-utility-infrastructure/district-energy-hot-water/#:~:text=Academic%20District%20Energy%20System%20(ADES)&text=The%20ADES%20Steam%20to%20Hot,hot%20water%20district%20energy%20system (accessed May 29, 2022).

[55] J. Kearney, A. Dell, D. Ellis, and P. Kantor, "Stanford energy system innovations: Steam to Hot Water in 33 Months," 2015. [Online]. Available: http://www.urecon.com/documents/pdfs/white_papers/SESI.pdf

[56] C. Moyer, M. Bove, and J. Morejohn, "Converting UC Davis District Steam to a Carbon-Neutral Hot Water System," presented at the International district energy association annual meeting, Jun. 27, 2018. [Online]. Available:

https://www.districtenergy.org/HigherLogic/System/DownloadDocumentFile.ashx?DocumentFileKey=f641e3a1-963a-0529-0a7a-f4fa1c7acc62&forceDialog=0

[57] J. Stagner, “Global District Energy Climate Award 2013 - Stanford University,” 2013.

[58] University of Rocherster, “Current status report on conversion to hot water,” presented at the IDEA campus energy conference, Mar. 08, 2018.

[59] J. Kearney, B. Sewak, and F. Ahmed, “Stanford energy system innovations (SESI) Program: Steam to Hot water conversion.” Stanford University.

[60] L.-M. Desjardins, “Modernisation du réseau thermique urbain d’Ottawa,” presented at the Webinar of the Réseau Énergie et Bâtiments, Montréal, QC, Apr. 20, 2022.

[61] C. C. Davila, “Urban building energy modeling,” Phd dissertation, Massachusetts Institute of Technology, 2017. doi: 10.1201/9780429402296-21.

[62] W. Li *et al.*, “Modeling urban building energy use: A review of modeling approaches and procedures,” *Energy*, vol. 141, pp. 2445–2457, Dec. 2017, doi: 10.1016/j.energy.2017.11.071.

[63] C. F. Reinhart and C. Cerezo Davila, “Urban building energy modeling – A review of a nascent field,” *Build. Environ.*, vol. 97, pp. 196–202, Feb. 2016, doi: 10.1016/j.buildenv.2015.12.001.

[64] R. Mohammadiziazi, S. Copeland, and M. M. Bilec, “Urban building energy model: Database development, validation, and application for commercial building stock,” *Energy Build.*, vol. 248, p. 111175, Oct. 2021, doi: 10.1016/j.enbuild.2021.111175.

[65] L. Frayssinet, L. Merlier, F. Kuznik, J.-L. Hubert, M. Milliez, and J.-J. Roux, “Modeling the heating and cooling energy demand of urban buildings at city scale,” *Renew. Sustain. Energy Rev.*, vol. 81, pp. 2318–2327, Jan. 2018, doi: 10.1016/j.rser.2017.06.040.

[66] Q. Zhang, “Residential energy consumption in China and its comparison with Japan, Canada, and USA,” *Energy Build.*, vol. 36, no. 12, pp. 1217–1225, Dec. 2004, doi: 10.1016/j.enbuild.2003.08.002.

[67] R. Nesbakken, “Price sensitivity of residential energy consumption in Norway,” *Energy Econ.*, vol. 21, no. 6, p. 23, 1999, doi: https://doi.org/10.1016/S0140-9883(99)00022-5.

[68] Y. Shimoda, T. Fujii, T. Morikawa, and M. Mizuno, “Residential end-use energy simulation at city scale,” *Build. Environ.*, vol. 39, no. 8, pp. 959–967, Aug. 2004, doi: 10.1016/j.buildenv.2004.01.020.

[69] Y. Chen, T. Hong, and M. A. Piette, “Automatic generation and simulation of urban building energy models based on city datasets for city-scale building retrofit analysis,” *Appl. Energy*, vol. 205, pp. 323–335, Nov. 2017, doi: 10.1016/j.apenergy.2017.07.128.

[70] É. Mata, A. Sasic Kalagasidis, and F. Johnsson, “Building stock aggregation through archetype buildings: France, Germany, Spain and the UK,” *Build. Environ.*, vol. 81, pp. 270–282, Nov. 2014, doi: 10.1016/j.buildenv.2014.06.013.

[71] C. Petersdorff, T. Boermans, and J. Harnisch, “Mitigation of CO2 emissions from the EU-15 building stock: beyond the EU Directive on the Energy Performance of Buildings,” *Env. Sci Pollut Res Int*, Sep. 2006, doi: 10.1065/espr2005.12.289. PMID: 17067030.

[72] European commission, “Guidelines accompanying Commission Delegated Regulation (EU),” p. 28, 2012.

[73] I. Theodoridou, A. M. Papadopoulos, and M. Hegger, “A typological classification of the Greek residential building stock,” *Energy Build.*, vol. 43, no. 10, pp. 2779–2787, Oct. 2011, doi: 10.1016/j.enbuild.2011.06.036.

[74] T. Loga, N. Diefenbach, B. Stein, and R. Born, “TABULA - Scientific Report Germany: Further Development of the National Residential Building Typology,” 2012, doi: 10.13140/RG.2.2.16035.17445.

[75] M. Deru *et al.*, “U.S. Department of Energy Commercial Reference Building Models of the National Building Stock,” NREL/TP-5500-46861, 1009264, Feb. 2011. doi: 10.2172/1009264.

[76] Office of energy efficiency and renewable energy, “Commercial reference buildings.” https://www.energy.gov/eere/buildings/commercial-reference-buildings (accessed Jun. 20, 2020).

[77] Office of energy efficiency and renewable energy, “Prototype building models,” *Building energy codes program*. https://www.energycodes.gov/prototype-building-models (accessed Jun. 20, 2020).

[78] International code council, *International energy conservation code*. 2011.

[79] CanmetENERGY, “Building Technology Assessment Platform (BTAP),” 2019. https://github.com/canmet-energy/btap

[80] S. Stephen, “High-performance commercial building systems,” LBNL--53538, 821762, Jan. 2003. doi: 10.2172/821762.

[81] E. Fabrizio and V. Monetti, “Methodologies and Advancements in the Calibration of Building Energy Models,” *Energies*, vol. 8, no. 4, pp. 2548–2574, Mar. 2015, doi: 10.3390/en8042548.

[82] D. Coakley, “A review of methods to match building energy simulation models to measured data,” *Renew. Sustain. Energy Rev.*, p. 21, 2014.

[83] A. Chong, Y. Gu, and H. Jia, “Calibrating building energy simulation models: A review of the basics to guide future work,” *Energy Build.*, vol. 253, p. 111533, Dec. 2021, doi: 10.1016/j.enbuild.2021.111533.

[84] T. Yang, Y. Pan, J. Mao, Y. Wang, and Z. Huang, “An automated optimization method for calibrating building energy simulation models with measured data: Orientation and a case study,” *Appl. Energy*, vol. 179, pp. 1220–1231, Oct. 2016, doi: 10.1016/j.apenergy.2016.07.084.

[85] ASHRAE, “Measurement of Energy and Demand Savings,” p. 170, 2002.

[86] Place Bonaventure, “History of Place Bonaventure,” *About us*. http://placebonaventure.com/en/about-us/history/ (accessed Sep. 20, 2020).

[87] Le 1000 de la Gauchetière, “History: Then and Now,” *Le 1000*. https://www.le1000.com/en/le1000/history (accessed Oct. 24, 2020).

[88] Sunlife building, “About us: Enduring Majesty,” *MTL 1918 Sunlife building*, Sep. 23, 2020. https://www.sunlifebuilding.ca/about-us/

[89] MACH group, “Place Victoria.” https://www.groupemach.com/en/property/53-place-victoria.html

[90] MACH group, “1060 Robert-Bourassa.” https://www.groupemach.com/en/property/29-1060_robert-bourassa.html

[91] Petra group, “1100 René-Bourassa.” http://www.groupepetra.com/eng/properties/view?id=15

[92] ÉCCU, “Our clients,” *Énergir urban heating and cooling*. http://energirccu.com/en/they-put-their-trust-in-us (accessed Oct. 20, 2020).

[93] Ville de Montréal, “Unités d’évaluation foncière,” *Données ouvertes*. https://donnees.montreal.ca/ville-de-montreal/unites-evaluation-fonciere (accessed Oct. 20, 2020).

[94] Map Developers, “Distance Calculator tool,” *Distance finder*. https://www.mapdevelopers.com/distance_finder.php (accessed Oct. 20, 2020).

[95] Emporis, “Buildings,” *Emporis*. https://www.emporis.com/buildings (accessed Oct. 20, 2020).

[96] M.-A. Pouliot, “Hydro-Québec is poised to attract data centers,” *Hydro-Québec Strategic Plan 2016-2020*, Jun. 08, 2016. http://news.hydroquebec.com/en/press-releases/1045/hydro-quebec-is-poised-to-attract-data-centres/

[97] M.-A. Pouliot, “Montréal the Best Place in the World to Set up a Data Center,” *Press release*, Jun. 04, 2019. http://news.hydroquebec.com/en/press-releases/1503/montreal-the-best-place-in-the-world-to-set-up-a-data-center/

[98] American Society of Heating, Refrigeration and Air-conditioning Engineers, “Climatic data for building design standards,” *ASHRAE Stand. Proj. Comm.*, p. 193, Jul. 2020.

[99] M. Kottek, J. Grieser, C. Beck, B. Rudolf, and F. Rubel, “World Map of the Köppen-Geiger climate classification updated,” *Meteorol. Z.*, vol. 15, no. 3, pp. 259–263, Jul. 2006, doi: 10.1127/0941-2948/2006/0130.

[100] Simeb, “Fichiers météo pour le Québec,” *Données météo*. https://www.simeb.ca:8443/index_fr.jsp (accessed Jan. 19, 2021).

[101] D. J. Brayshaw, “The Importance of Weather and Climate to Energy Systems.pdf.” American meteorological society BAMS, Jun. 22, 2020.

[102] Engineering Climate Services Unit, “CWEC_FMCCE_v_2020,” *Engineering Climate Datasets*. https://climate.weather.gc.ca/prods_servs/engineering_e.html (accessed Jan. 19, 2021).

[103] ASHRAE, “Standard for the Design of High-Performance Green Buildings,” 2014.

[104] EnergyPlus engineering reference, “The Reference to EnergyPlus Calculations,” 2013.

[105] K. Gowri, D. Winiarski, and R. Jarnagin, “Infiltration modeling guidelines for commercial building energy analysis.” Pacific northwest national laboratory, 2009.

[106] Natural Resources Canada, “Commercial/Intitutional sector - Quebec,” *Comprehensive Energy Use Database*. https://oee.nrcan.gc.ca/corporate/statistics/neud/dpa/menus/trends/comprehensive/trends_com_qc.cfm

[107] B. Palm and S. Sawalha, “Energy Usage Prediction Model Comparing Indoor Vs. Outdoor Ice rinks,” p. 49.

[108] R. and A.-C. E. American Society of Heating, *2014 ASHRAE handbook: refrigeration.* Atlanta, GA: ASHRAE, 2014.

[109] Lindo systems, “LINGO 19.0 - Optimization Modeling Software for Linear, Nonlinear, and Integer Programming,” *Lindo systems inc.* https://www.lindo.com/index.php/products/lingo-and-optimization-modeling

[110] L. Leroy, “Modelling neighborhood-scale energy scenarios,” Master of Science thesis, Polytechnique Montréal, Montréal, QC, 2020.

[111] Ed. Éditeur officiel du Québec, “Règlements sur l’économie de l’énergie dans les nouveaux bâtiments.” 2019.

[112] American Society of Heating Refrigerating and Air-Conditioning Engineers, “Chapter 33: Pipe Sizing.” ASHRAE Inc., 1997.

[113] H. Wilson, “Pressure Drop in Pipe Fittings and Valves: A Discussion of the Equivalent Length (Le/D), Resistance Coefficient (K) and Valve Flow Coefficient (Cv) Methods,” *AioFlo 1.09: Pipe Sizing and Flow Calculation Software*, Oct. 2012. https://www.katmarsoftware.com/articles/pipe-fitting-pressure-drop.htm

[114] ASME Code for Pressure Piping, B31, “Power Piping.” The American Society of Mechanical Engineers, 2018.

[115] ECCU, “Sustainable development,” *Energir urban heating and cooling*. http://www.energirccu.com/en/sustainable-development

[116] TEQ, “Facteurs d’émission et de conversion.” Transition Énergétique Québec, 2019.

[117] MELCC, “Registre des émissions de gaz à effet de serre,” 2022. https://www.environnement.gouv.qc.ca/changements/ges/registre/index.htm (accessed Mar. 23, 2022).

[118] C. Leroy, J. Tamasuaskas, and D. Giguère, “Heat Pump Pre-Screening Tool for New Commercial and Institutional Buildings,” p. 9, 2017.

[119] B. B. Bafrouei, “Assessing the energy flexibility potential of residential Photovoltaic panel with battery systems in cold climate,” p. 173.

[120] Ministère de l’Environnement and et de la Lutte contre les changements climatiques, “Suivi hydrologique de différentes stations hydrométriques,” *Expertise hydrique et barrages*, 2022. https://www.cehq.gouv.qc.ca/suivihydro/graphique.asp?NoStation=001003 (accessed Apr. 10, 2022).

[121] Ecohabitation, “Infrastructure de production et de distribution énergétique, projet Louvain Est, Ahuntsic-Cartierville, Montréal” Opportunity study, Dec. 2021.

APPENDIX A SPECIFICATIONS OF THE SAINT-LAURENT RIVER POTENTIAL

The Saint Laurent River can significantly decarbonize the city of Montréal as it encompasses significant heating and cooling capacity. Depending on the network's thermal requirements, the heat pump uses the river's water as a heat source or a heat sink. The significant flow rate of the river allows the use of a greater volume of water, lowering the temperature difference between the HP's inlet and outlet water source temperature, thus, having a minimal effect on the flora and fauna of the river. According to the experts who worked on the Louvain-Est project [121], the river's water temperature can reach a minimum value of 4 ℃, and the water's temperature at the outlet of the HP can not go less than the freezing temperature (0 ℃).

Two datasets are required for the evaluation of the thermal capacity of the river: the deep river water temperature all year long and the mass flow rates. As no information regarding the deep water temperature is available, the river's temperature was supposed to be between -1.5 ℃ and 25 ℃ and the water exiting the HP towards the river was considered at 0.5 ℃ in winter.

The daily flow rate was obtained from the center of hydrologic expertise in Québec [120]. The available information included the daily measured volume flow rate of the river and the maximum and minimum flow rate estimates for each day according to historic data from 1970 to 2012. The graph also shows the estimated daily median temperature of the river's water.

The temperature difference between the water entering and leaving the HP is given by Equation (7).

$$\Delta T = \frac{P_{th}}{\dot{m} * Cp} \tag{7}$$

Where P_{th} represents the maximum cooling and heating power.

$\dot{m}$ represents the river's volumetric flow rate

Cp represents the specific heat capacity of water

The maximum thermal load required from the river is 75 MW, required in heating from the 18th year and forward. The river's volume flow rate $\dot{m}$ is considered equal to the minimum flow rate in a year (5500 m^3/s) to assess the worst-case scenario.

$$\Delta T = \frac{P_{th}}{\dot{m} * Cp} = \frac{75000000\ W}{5500\frac{m^3}{s} * 1000\frac{kg}{s} * 4186\frac{J}{kg℃}} = 0.003\ ℃$$

The maximum river's water temperature variation is determined to be 0.003℃. Moreover, in order to provide 1 GW of thermal energy – enough for all Montréal – will only vary the river's temperature by 0.04 ℃.

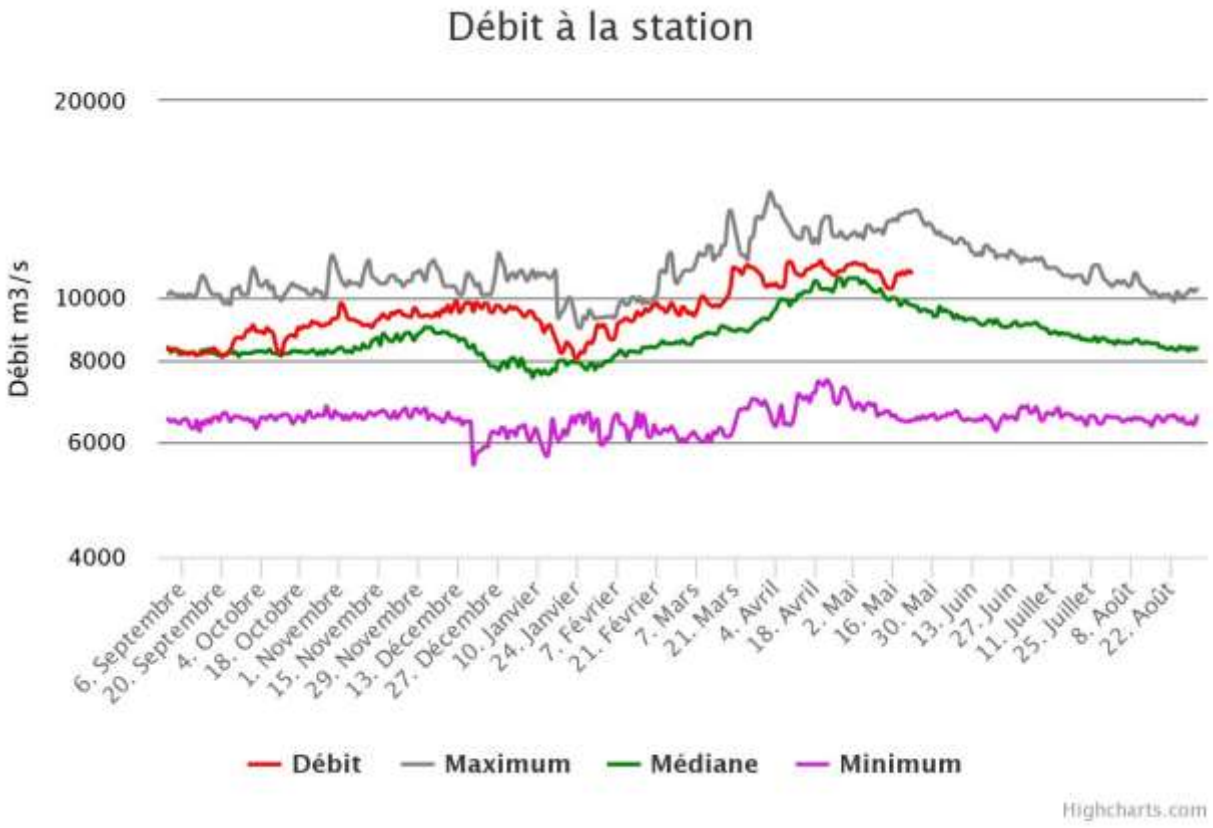

Figure 6.1: Saint Laurent River daily temperature (photo retrieved on the 18th of May 2022).